The fixed-scale transformation approach to fractal growth

A. Erzan

Department of Physics, Faculty of Science and Letters, Istanbul Technical University, Maslak, Istanbul, Turkey

L. Pietronero

Dipartimento di Fisica, Universitá di Roma "La Sapienza," I-00185 Roma, Italy

A. Vespignani

Instituut-Lorentz, University of Leiden, 2300 RA, Leiden, The Netherlands

Irreversible fractal-growth models like diffusion-limited aggregation (DLA) and the dielectric breakdown model (DBM) have confronted us with theoretical problems of a new type for which standard concepts like field theory and renormalization group do not seem to be suitable. The fixed-scale transformation (FST) is a theoretical scheme of a novel type that can deal with such problems in a reasonably systematic way. The main idea is to focus on the irreversible dynamics at a given scale and to compute accurately the nearest-neighbor correlations at this scale by suitable lattice path integrals. The next basic step is to identify the scale-invariant dynamics that refers to coarse-grained variables of arbitrary scale. The use of scale-invariant growth rules allows us to generalize these correlations to coarse-grained cells of any size and therefore to compute the fractal dimension. The basic point is to split the long-time limit ($t \to \infty$) for the dynamical process at a given scale that produces the asymptotically frozen structure, from the large-scale limit ($r \to \infty$) which defines the scale-invariant dynamics. In addition, by working at a fixed scale with respect to dynamical evolution, it is possible to include the fluctuations of boundary conditions and to reach a remarkable level of accuracy for a real-space method. This new framework is able to explain the self-organized critical nature and the origin of fractal structures in irreversible-fractal-growth models. It also provides a rather systematic procedure for the analytical calculation of the fractal dimension and other critical exponents. The FST method can be naturally extended to a variety of equilibrium and nonequilibrium models that generate fractal structures.

CONTENTS

I. Introduction: Physics of Fractals 546
II. Properties of Fractal-Growth Models 547
  A. The basic models: Diffusion-limited aggregation and dielectric breakdown model 547
  B. The fractal dimension 550
  C. Essential features of the problem 553
  D. Why usual methods are problematic 554
III. The Fixed-Scale Transformation Strategy and its Basic Ideas 554
IV. Basic Concepts 557
  A. Pair-correlation configurations and the fractal dimension 558
    1. Characterization of fractal structures with a fine-graining procedure 558
    2. Void distribution 559
  B. The fixed-scale transformation 561
  C. Fixed-scale transformation application to the Eden model 564
  D. Fluctuations of boundary conditions 564
  E. Empty configurations: The extended fixed-scale transformation 566
  F. Asymptotic scale-invariant dynamics 567
V. Applications of Fixed-Scale Transformation to Hamiltonian Equilibrium Problems 567
  A. Critical fluctuations and fractal growth 567
  B. The percolating cluster 568
    1. Fixed-scale transformation application to the percolation problem 568
    2. Alternative connectivity conditions 570
    3. Percolation on the triangular lattice 572
    4. Topological properties: Backbone and chemical distance 572
  C. Ising and Potts clusters 573
  D. Polymers and lattice animals 573
  E. Summary of the fixed-scale transformation results for Hamiltonian problems 574
VI. Application to Simple Dynamical Problems 574
  A. Directed percolation 574
  B. Invasion percolation 576
  C. Sandpile models (self-organized criticality) 578
VII. Fixed-Scale Transformation for Diffusion-Limited Aggregation and Dielectric Breakdown Model 578
  A. Renormalization of the dynamics for diffusion-limited aggregation and the dielectric breakdown model 579
    1. Space of growth rules 579
    2. Asymptotic structure of the dynamics 580
    3. Parametrization of the growth rules 582
    4. Scale-invariant screening and noise-reduction parameters 583
    5. Renormalization group for the noise-reduction parameter 583
  B. Fixed-scale transformation for diffusion-limited aggregation and dielectric breakdown model with the standard growth rules 586
    1. Simplest method for computing the fractal dimension of diffusion-limited aggregation and dielectric breakdown model 586
    2. Empty configurations 587
    3. Multifractal properties of the growth probability 588

 0034-6861/95/67(3)/545(60)/$16.00

C. Diffusion-limited aggregation and dielectric breakdown model in three dimensions 588
D. Fixed-scale transformation for diffusion-limited aggregation and dielectric breakdown model with renormalized growth rules 589
E. Topological properties: Backbone 589
VIII. Fractal-Growth Phenomena 590
A. Cluster-cluster aggregation model 590
B. Analytical calculation of cluster-cluster aggregation fractal dimension with the fixed-scale transformation approach 591
C. Born model for fracture 593
D. Levy flight clusters 594
IX. Relationship to Path Integrals and Other Methods of Dynamical Critical Phenomena 595
A. Dynamical critical phenomena and fractal growth 595
B. Path-integral approaches to fractal growth 595
C. Towards gross variables: The stationarity condition and the hierarchical ansatz 596
D. The fixed-scale transformation as a Markovian process 597
1. Equilibrium models 598
2. Non-Markovian processes 599
E. The fixed-scale transformation and scale-invariant dynamics 600
X. Conclusions 601
Acknowledgments 601
References 602

I. INTRODUCTION: PHYSICS OF FRACTALS

Fractal geometry provides a new perspective of nature and allows us to consider irregularities as intrinsic entities (Mandelbrot, 1982; Pietronero and Tosatti, 1986; Stanley and Ostrowsky, 1986; Feder, 1988; Vicsek, 1992). The property of self-similarity implies irregularities at all scales, and for this reason it cannot be described within the framework of the usual analytical methods. The broader framework of fractal geometry provides a quantitative mathematical description of systems with self-similar properties, and it enables us to include in the scientific problematic a vast class of new phenomena in various fields of science. At the level of phenomenological description, the fields in which this concept has the largest impact are disordered systems, critical phenomena, aggregation phenomena, nonlinear dynamics and turbulence, the development of spatiotemporal intermittencies and $1/f$ noise, self-organized critical systems, and various others including the large-scale structure of the universe. This last case is a good example of the importance of having a broader mathematical framework even for the phenomenological description of experimental data. Galaxy distributions are usually analyzed with statistical tools that imply *a priori* homogeneity at large scale. The reanalysis of the same data with no *a priori* assumptions leads us instead to conclude that no intrinsic average density can be identified in these systems and that fractal correlations extend up to the present observational limits (Coleman and Pietronero, 1992). This shows the importance of the broader conceptual framework of fractal geometry for systems with large fluctuations, even at the stage of data analysis. Similar examples of phenomenological analysis or modeling can be found in various other fields. The structure of velocity field in fully developed turbulence, for example, can be described phenomenologically by a simple model of multifractal cascade (Benzi *et al.*, 1984; Paladin and Vulpiani, 1987). This interesting observation, however, does not explain how scaling behavior actually arises from the Navier-Stokes equation. This brings us to the basic problem of trying to go beyond the level of a phenomenological description and to address the basic question: *Why nature makes fractals?*

In more specific terms, this question can be rephrased as three points: (1) How are patterns generated? (2) How does this happen at all scales? and (3) How does one assign statistical weights to these patterns? In practice, one cannot try to address this question for all fractal problems separately. One would like, instead, to develop first some general concepts by studying in detail a particular phenomenon and then trying to extend those concepts to other cases. This is the scheme for the formulation of a theory of fractal growth that consists therefore of two stages: (a) define a model that contains the essential physical ingredients for fractal growth; (b) develop the theoretical concepts necessary to understand this model and to compute its properties analytically.

The first part of this program was accomplished a few years ago with the introduction of the model of diffusion-limited aggregation (DLA; Witten and Sander, 1981) and the dielectric breakdown model (DBM; Niemeyer *et al.*, 1984). These models have a direct relation with several phenomena like dendritic growth, dielectric breakdown, and viscous fingering, and they are considered prototypical fractal-growth models in a more general perspective, too. Extensive computer simulations have been performed on these models, and they show a self-organized behavior leading to fractal structures.

In relation to these models, the above set of questions may be rephrased as follows.

(1) How does DLA make fractals? How is spatial symmetry spontaneously broken, and how are holes of all scales left behind as the pattern grows? What distinguishes this set of growth rules from, say, the Eden model, which leads instead to compact structures?

(2) How can we compute the fractal dimension analytically and understand the self-organized nature of this process? This is a non-Hamiltonian system whose dynamics is intrinsically irreversible, so that we have no *a priori* way in which to assign a statistical weight to the density fluctuations.

Before we try to address these questions for DLA and the DBM, it should be noted that in physics there is a rich domain of scale-invariant phenomena, namely, second-order phase transitions, for which the renormalization-group (RG) theory (Wilson and Kogut, 1974; Amit, 1978) provides a comprehensive understanding of the scale invariance and critical behavior. This is actually one of the reasons for the increasing interest in fractals among physicists. A characteristic of usual criti-

cal phenomena is that they occur at the critical point of equilibrium phase transitions. In retrospect, we can now see that the usual theoretical framework of the RG refers to the self-similar properties that occur exactly at the equilibrium point and, in practice, are rarely observed unless one looks for them specifically. The fractal structures that are instead common in nature, like clouds, trees, mountains, lightnings, galaxies, etc., arise instead from a more common situation in which they represent the attractor of an irreversible dynamical process that leads spontaneously to complex scale-invariant structures without the need for the fine-tuning of any parameter. It is curious that among all the scale-invariant structures that one can observe, those that were first studied in detail and fully understood are the most hidden ones. It is reasonable to conjecture that in the future the scale invariance of critical phenomena will represent just a small class of cases, which had, however, an enormous intellectual impact, within the broader framework of mostly self-organized structures. The great theoretical challenge is then to find a general theory for both critical and self-organized scale invariance.

There have been several attempts to generalize the RG theory for irreversible fractal growth and DLA in particular. Field-theoretical approaches (Parisi and Zhang, 1985; Peliti, 1985; Shapir and Zhang, 1986) lead to effective Lagrangians that, however, correspond to an unrenormalizable strong-coupling theory without upper critical dimension and therefore cannot be treated with standard methods. Field-theoretic methods have instead been successful for the surface profile of the 2D Eden model (Kardar *et al.*, 1986). This problem is, however, very different from that of the fractal dimension of DLA, and it can be mapped into an effective equilibrium problem.

For the real-space renormalization group (RSRG), the crucial problem is that, in irreversible growth, the asymptotic fractal structure can only be defined when the growing interface is infinitely far away. This can never be achieved by integrating over degrees of freedom inside a given box (Burkhardt and van Leeuwen, 1982). Furthermore, in the interesting Nagatani (1987a, 1987b) approach (see also Wang *et al.*, 1989a, 1989b), it is not possible to distinguish between fractal and nonfractal structures or to understand the self-organized nature of the process. Another theoretical approach to DLA has been developed recently by Halsey *et al.* (Halsey and Leibig, 1992; Halsey, 1994). The method is based on the competition between DLA branches and seems very interesting but specific to this model.

One can also look at the formation of fractal patterns from the standpoint of systems of partial differential equations. In this way one is able to determine, for any set of parameter values, if a certain type of fluctuation will be attenuated or, on the contrary, if it will grow. However, one is not able to assign *a priori* weights to fluctuations that may occur around a given solution. So we are once more frustrated: not having a measure over our space of "shapes," we are unable to compute the expectation values and correlation functions, and thus unable to compute things like the fractal dimension.

Over the past few years we have developed a novel theoretical method, the fixed-scale transformation (FST), to deal with irreversible fractal growth by focusing explicitly on the irreversible dynamics. The method is defined in real space; it is based on two steps that we illustrate here for DLA, but which can be easily generalized to many other systems.

(1) *Correlations in the "frozen" structure.* For a given dynamics (growth rules), one should be able to define the correlation properties corresponding to the final structure generated by this process. This structure is frozen in the sense that it will not continue to be modified by further growth. This corresponds to an asymptotic time limit ($t \to \infty$) with respect to the growth dynamics. The correlation properties of the structure are characterized by an intersection set perpendicular to the growth direction. The FST is defined by the dynamical evolution, in the growth direction, of the short-range correlation properties of this intersection. This construction refers to the asymptotic final structure, and, in order to compute the FST matrix elements, one must consider *lattice path integrals* defined by the growth rules. The calculation of these path integrals can be improved in a systematic way; in addition, by working at a fixed scale, it is possible to include the effect of the fluctuations of the boundary conditions. In this way one can achieve a remarkable level of accuracy and systematicity for a real-space method. From the FST fixed point, one obtains the correlation properties between pairs of sites. In order to extend these results to long-range correlations, the basic idea is to reinterpret these "sites" as coarse-grained block variables. This requires the identification of the dynamics (growth rules) that refers to coarse-grained cells. If a scale-invariant asymptotic dynamics can be identified, its use in the FST allows us to characterize the correlation properties between pairs of coarse-grained variables of any size. From these one can finally obtain the asymptotic correlation properties and compute the fractal dimension analytically.

(2) *Scale-invariant dynamics.* This problem consists in the identification of the effective growth rules for coarse-grained variables at the asymptotic scale. In practice, one must consider a renormalization scheme for the growth probabilities. It is easy to derive general symmetry properties of the scale-invariant dynamics. For example, probabilities defined per "site" evolve into "bond"-type upon renormalization. In addition, the FST scheme allows us to identify the crucial element for generating fractal structures in the persistence of screening effects at the asymptotic scale. A study of the scale transformation of noise reduction shows the existence of an *attractive fixed point* that allows us to understand the self-organized nature of the growth process. In addition, screening effects also remain strong at the asymptotic scale, and the scale-invariant growth rules turn out to be

rather close to the small scale.

This separation between long-time and large-scale limits is crucial for the description of irreversible fractal growth, and it is the basic point of the FST method. In the usual theoretical methods of statistical mechanics, the time limit is usually eliminated in view of ergodicity. In this respect the FST corresponds to a novel theoretical framework that can be easily extended to all those problems in which a frozen fractal structure is generated by a dynamical process. In this review we shall consider several examples corresponding to both irreversible and equilibrium dynamics.

In Sec. II we describe the properties of the prototypical fractal-growth models DLA and DBM. In Sec. III we focus on the essential concepts of the FST approach, while in Sec. IV we present a detailed description of the method. In Sec. V we show how fractal structures generated by equilibrium problems can also be studied by this method. In Sec. VI we apply the FST to simple dynamical systems. In Sec. VII we study the problem of the renormalization of the dynamics of DLA/DBM, and we show the detailed application of the FST to these models. In Sec. VIII the method is extended and applied to other fractal growth phenomena like cluster-cluster aggregation. In Sec. IX we discuss the relations of the FST methods with usual path integrals and field-theory approaches. Finally, in Sec. X, we summarize the situation and discuss possible developments.

II. PROPERTIES OF FRACTAL-GROWTH MODELS

A. The basic models: Diffusion-limited aggregation and dielectric breakdown model

In nature there are very many examples of structures that show fractal properties (Mandelbrot, 1982). The idea is to concentrate on some specific case with the hope that theoretical concepts eventually developed for that case could then be modified and applied to other situations. This is, for example, what has happened for the critical properties of second-order phase transitions. For this class of problems, a key role was played by the Ising model that was crucial to the development of the ideas that led to the renormalization group (Amit, 1978; Burkhardt and van Leeuwen, 1982). These ideas could be extended to virtually any other model.

For fractals, the first growth model based on a well-defined physical process was diffusion-limited aggregation (DLA; Witten and Sander, 1981). This was generalized by the dielectric breakdown model (DBM; Niemeyer *et al.*, 1984), which also clarifies the mathematical nature of the phenomenon. This model is based on an iterative stochastic process in which the growth probability is modulated by the electric field around the structure as given by the solution of the Laplace equation with appropriate boundary conditions. These models can explain the origin of fractal structures in a variety of processes like dielectric breakdown, dendritic growth, and viscous fingers in fluids (Vicsek, 1992). In addition, there are various other problems in which fractal patterns arise from solutions of time-dependent differential equations with fixed or moving boundary conditions. Often these are studied using discretized models like cellular automata, discrete maps on lattices, or models of self-organized criticality (SOC; Bak *et al.*, 1987, 1988) that lead to spatial and temporal intermittency. It seems reasonable that the understanding of problems like DLA and DBM is a necessary step in order to progress in this whole area. For these reasons they are considered to be the prototypical fractal-growth models, analogous to the Ising model for phase transitions. They have been studied extensively through numerical simulations, and in this section we briefly summarize their main properties.

DLA was first defined on a two-dimensional square lattice. Given a central (seed) particle, new particles are added one by one from a faraway region (a random point of a large circle). A new particle performs a random walk, and when it touches a site nearest to the initial seed, it stops and becomes part of the aggregate. Then a new random-walking particle is added that stops when it touches a site that is nearest to the aggregate, and so on. If a particle never touches the aggregate, it is eliminated when it reaches a certain (large) distance from it. The process can be easily generalized to any space dimension, and it can also be defined without a lattice (off-lattice) by assuming that particles have a certain size and by allowing them to make steps of a given length in any direction. A particle stops when it touches another particle that belongs to the aggregate (Meakin, 1988; Meakin and Tolman, 1989). The iteration of such a simple dynamical process leads spontaneously to highly complex fractal structures like that shown in Fig. 1 in which the colors refer to the times at which particles were added to the aggregate.

DBM can be defined by considering a square lattice in which the central point represents an electrode with potential $\phi=0$, while the second electrode with $\phi=1$ consists of a circle at infinity as shown in Fig. 2. The bonds on which breakdown has already occurred (black) constitute the pattern at a given time that is considered equipotential. The local field around this structure is defined by the Laplace equation

$$\nabla^2\phi=0 \tag{2.1}$$

with the boundary conditions of constant potential on the grown structure ($\phi=0$) and a different value of the potential ($\phi=1$) at infinity (faraway circle). The growth probability p_j for each bond (j) at the perimeter of the structure is then related to the local field in the following way:

$$p_j=\frac{|\nabla\phi_j|^\eta}{\sum_j|\nabla\phi_j|^\eta}\ , \tag{2.2}$$

where η is a parameter that modulates the randomness of

the process. After a bond is added, the grown structure changes and so does the boundary condition for the new probability distribution. A new bond is then added, and so on.

For $\eta=1$, there is a close connection between DLA and DBM, in view of the fact that a diffusion equation with sources and sinks is identical to the DBM equations. In this respect the DLA growth process represents a Monte Carlo realization of the probability distribution defined by the DBM (Pietronero and Wiesmann, 1984). To be precise, in order for the two processes to be exactly the same, in DLA one should let the particle reach the aggregate and then add to it the last-visited empty site. For $\eta=0$, the effect of the Laplace equation is suppressed, and one recovers one version of the Eden model that leads to compact structures (Eden, 1961). In this respect the DBM is particularly interesting from a theoretical standpoint, because it generates a family of models that range continuously from compact to fractal structures. Apart from generalizing the DLA growth process, the DBM illustrates the underlying mathematical properties in relation to partial differential equations like the Laplace equation. This connection is quite surprising, because usually a Laplace equation produces

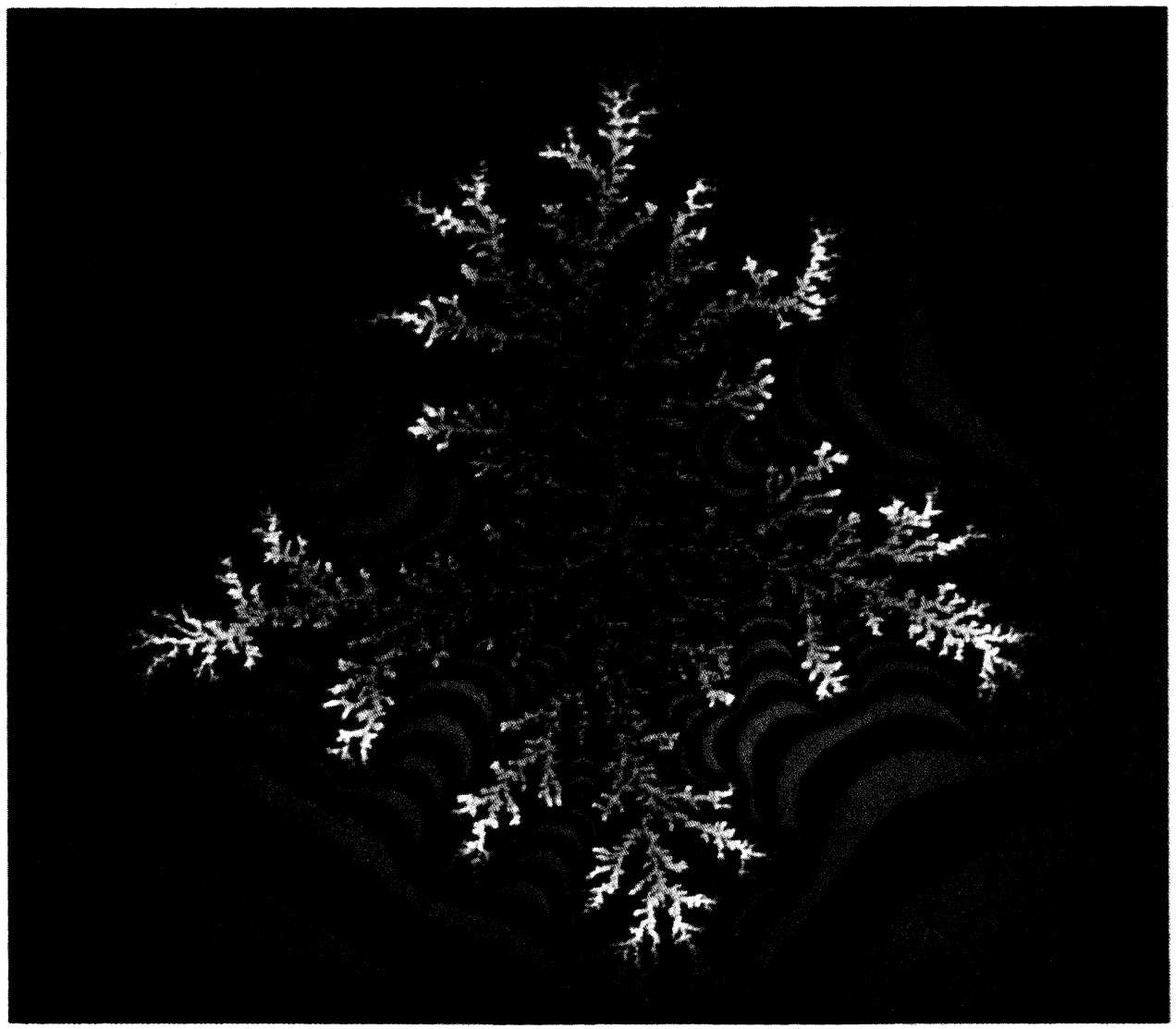

FIG. 1. DLA/DBM cluster (off-lattice) with radial boundary conditions. The colors of the structure refer to the aggregation time of each particle. Note the screening effect: late (red) particles cease modifying the inner blue portion, which therefore can be considered asymptotic. Only for this "frozen" part can fractal properties be properly defined. The contours around the structure represent equipotential lines for the Laplacian field. A pair of black and white stripes corresponds to a change by a factor of 10 of the potential (courtesy of C. J. G. Evertsz and B. B. Mandelbrot).

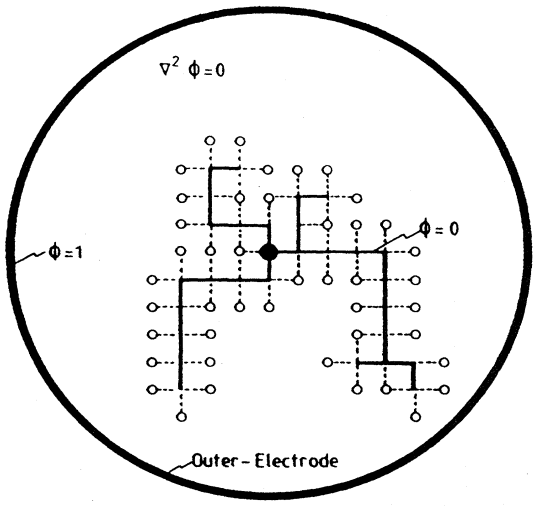

FIG. 2. Iterative mathematical nature of the DBM. The growth process corresponds to an irreversible dynamical process with long-range correlations in both space and time. No statistical weight can be assigned to a given configuration without taking into account its entire history. In the circle is a schematic of the DBM. The central point represents one of the electrodes ($\phi=0$), while the other electrode is given by a circle at large distance ($\phi=1$). The discharge pattern (black dots and bonds) is equipotential with the central electrode ($\phi=0$). The dashed bonds represent the candidates for the next growth processes, and their relative growth probabilities are proportional to the potential gradient (local field).

smooth solutions: the potential at a given point is the average of the potentials of the neighboring points. Here we see instead that a stochastic growth scheme (see Fig. 2) in which probabilities are defined by Laplace equations spontaneously drives the growth boundaries into a highly irregular fractal shape. This is a deep mathematical point essential for the understanding of this type of fractal.

The previous discussion refers to radial geometry that leads to structures of the type shown in Fig. 1. One can also define the growth process starting from a base line and proceeding towards a faraway line with a different potential. Three examples of this type for different values of η are shown in Fig. 3. Since, in practice, the length of the base line is finite and one uses periodic boundary conditions, topologically the growth occurs on the surface of a cylinder (Evertsz, 1989, 1990). For this geometry the initial stage of growth (scaling regime) shows the developments of larger and larger correlations and a corresponding decay of density along the H axis. When correlations reach the size of the basis (b), the density remains constant and one enters the "steady-state regime" in which fractal properties can be determined by a box-counting method.

The two processes (radial and cylindrical) give rise to basically similar structures; however, we shall see that there are small but persistent differences among the structures, and the conclusion that the differences are due just to finite-size effects is not obvious. The cylinder geometry offers conceptual advantages for a theoretical discussion because it defines a unique growth direction and it allows the independent variation of basis and height, which, in radial geometry, are linked intrinsically.

B. The fractal dimension

The most characteristic feature of these models is that they are intrinsically critical and give rise spontaneously to fractal structures. We shall see, however, that, as soon as one tries to make this statement more precise and quantitative, a number of problems appear, some of which are still open.

In order to discuss fractal dimension, one should make clear that this is a property that refers to the frozen part

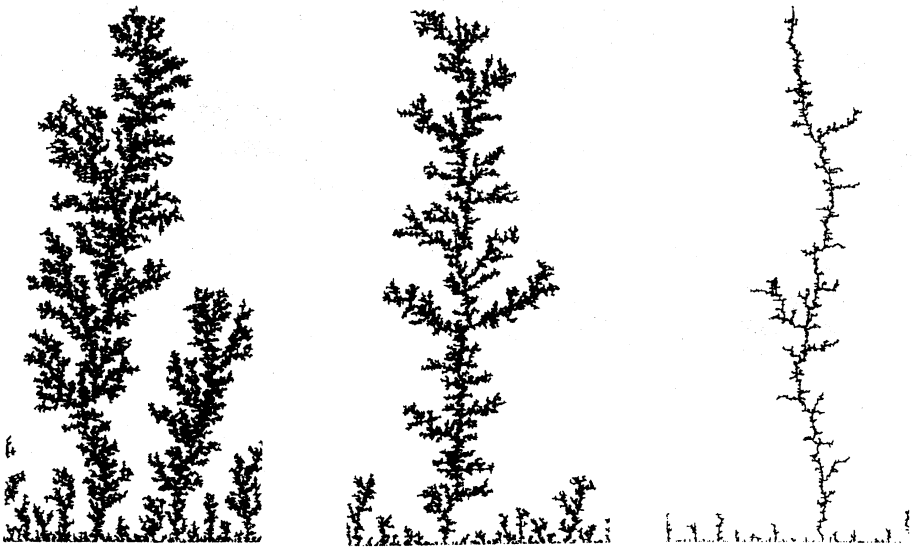

FIG. 3. DBM clusters grown in a cylinder geometry with circumference $L=256$ and height $H=3L$. The cluster on the left corresponds to $\eta=0.75$; the one in the center, to $\eta=1$ (equivalent to DLA); and the one on the right, to $\eta=4$ (courtesy of C. J. G. Evertsz).

of the structure, namely, the zone that is fixed, asymptotically and that will not be modified by further growth. For Fig. 1, for example, this zone consists essentially of the blue parts, because one can see that the last particles added (red) did not penetrate further into this zone. For the cylinder case, the frozen zone consists of the entire structure somewhat below the growing profile.

This discussion is important in clarifying the problem of the lattice anisotropy effect that has been much debated in the literature (Meakin, 1988). For the radial growth, if the growth process is defined on a square lattice, one observes at small scales a reasonably circular shape, while at larger scales the structure observed is cross shaped, as shown in Fig. 4(a). If one measures fractal dimension in a global sense by the mass-length ratio (gyration radius), one observes that, until the shape is about circular, $D \simeq 1.70$, while for larger sizes and noncircular shapes this value apparently drops to about $D \simeq 1.5$ for the largest sizes ($N \simeq 10^6$). This result has given rise to much discussion abut the effect of lattice anisotropy on the asymptotic value of fractal dimension.

In order to clarify this point, one must distinguish between the effect of lattice anisotropy on the velocity of the growing interface that determines the overall profile and the local fractal features that should only be measured in the frozen region within the growing interface. If the profile is not circular and one defines the fractal dimension in a global way, these two effects are mixed and the result is spurious. This implies that for noncircular shapes, one should use only local probes to define fractal dimension. Therefore the result $D \simeq 1.5$ obtained from a global gyration-radius analysis should not be considered a correct determination of fractal dimension.

This discussion makes it clear that the *overall* shape of the growing interface and the *structure* produced by the growth process are two different problems. From a recent analysis (Arneodo *et al.*, 1989), one can actually conjecture that the average growing interface of DLA may be governed by the same equations as the interface of the deterministic Saffman-Taylor problem that produces compact structures instead. The fractal aspect of the problem corresponds, instead, to the asymptotic properties of the structure that is left behind once the growing interface goes to infinity. Therefore it is only in this sense that we shall discuss fractal properties in the following.

For two-dimensional DLA, the various methods for defining fractal dimension give the following results.

(a) *Radial geometry* (the data are from various authors reviewed by Meakin and Tolman, 1989): (i) Off-lattice (mass-radius relation): $D=1.715$ ($N \simeq 10^6$). (ii) Square lattice (circular shape; small sizes): $D=1.71$. (iii) Density-density correlation: $D=1.66/1.68$. (iv) Box counting (generalized to the qth moment): $D(q=0)=1.61$; $D(q=1)=1.65$; $D(q=2)=1.65$. (v) Box counting (wavelet analysis): $D(-15<q<15)=1.60$.

(b) *Cylinder geometry* (from Evertsz, 1989, 1990; Piccioni, 1995): (i) Box counting (scaling regime): $D=1.68$. (ii) Box counting (intersection of steady-state regime): $D=1.65$. If DLA were to produce a simple fractal structure with universal properties, all these values should coincide. To some degree they do, because the fluctuations in the observed values of D are of the order of 5%, and it is conceivable that they are due to finite-size effects. However, these data are derived from accurate and rather large simulations, and it is also possible that radial and cylinder geometries lead to different corrections to scaling. In fact, recent large-scale simulations (Mandelbrot, 1992; Mandelbrot *et al.*, 1995) suggest a scenario in which radial DLA presents scaling corrections that are related to the nonequilibrium dynamical aspects of the phenomenon. These scaling corrections have a counterpart in the dynamical drift that drives the structure to an increasingly multiarmed shape. The numerical rate of this drift can be measured quantitatively with a lacunarity effect specific to DLA grown in circular geometry. It is worth observing that the value of the fractal dimension measured for circular crosscut is the same as that obtained for intersection sets of clusters grown in cylindrical geometry ($D \simeq 0.65$). Moreover, the value obtained does not depend upon the measurement technique. This seems to suggest that the question of

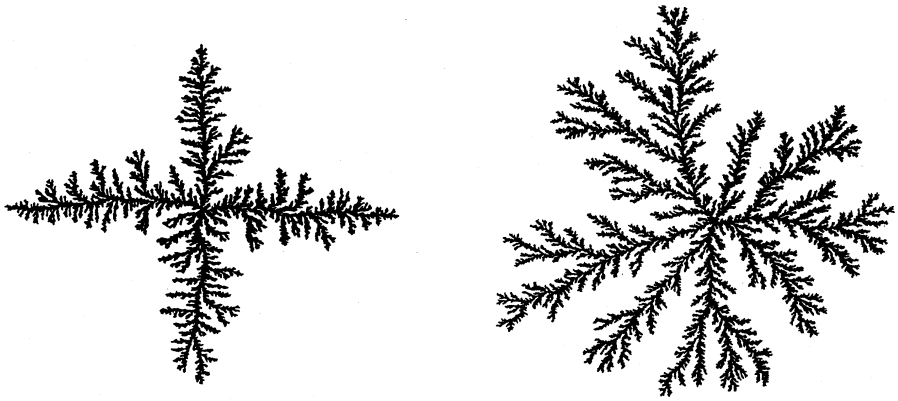

(a) (b)

FIG. 4. Large DLA clusters ($N \simeq 10^6$) for radial geometry on a square lattice (a) and off-lattice (b).

universality of DLA is best addressed on the crosscut. In fact, this is the only set that possesses an important geometric characteristic that is independent of the growth boundary conditions: it is always transverse to the growth direction. Therefore it is possible that measurements on this set take into account only the intrinsic growth dynamics of the phenomenon, leaving apart the effects induced by the geometry of the boundary conditions. In addition, the fact that cylindrical DLA does not present deviations from self-similarity is probably due to the fact that the cylinder size is defined externally and does not depend upon the growth process itself (Piccioni, 1995).

For the DBM, the value of D as a function of the parameter η varies continuously from $D(\eta=0)=2$ (Eden limit) to $D=1$ for large values of η [Fig. 5(b)]. Whether this limit is reached in a smooth way for $\eta\to\infty$ or above a finite critical value η_c remains an open question.

Until now we have discussed growth in only a two-dimensional embedding space ($d=2$). Simulations have actually been performed up to $d=8$ (Meakin and Tolman, 1989), and the results are shown in Fig. 5(a). These data are compared with the dimension of the self-repelling polymer that is an equilibrium problem of standard nature with an upper critical dimension $d_c=4$. In this respect, one can say that DLA does not show an upper critical dimension. This can also be understood from the fact that the long-range coupling due to the Laplace equation is always relevant in any dimension.

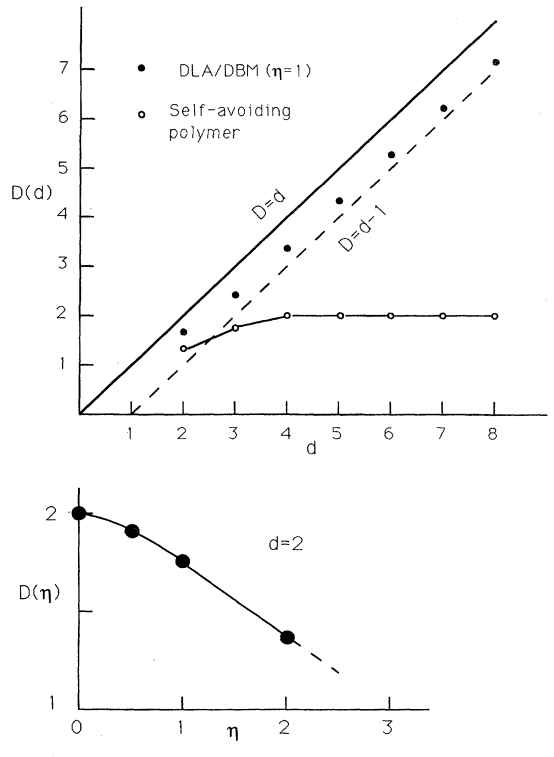

FIG. 5. Initial label: (a) Fractal dimension of DLA clusters as a function of the dimension of the embedding Euclidean space. Note the absence of an upper critical dimension as shown instead by the exponents of the self-avoiding walk. (b) Fractal dimension for DBM clusters in two dimensions as a function of the parameter η.

For large values of d, there is evidence that the limiting behavior $D=d-1$ is approached from above. This can be understood from a simple argument due to Ball and Witten (1984). For a cluster of dimension D, the number of particles N is related to the radius R by

$$N\simeq R^D . \tag{2.3}$$

The growing interface is characterized by N' points,

$$N'\simeq\frac{dN}{dR}\simeq R^{D-1} . \tag{2.4}$$

In order for growth to occur, the incoming random walk should have a nonzero probability of hitting the interface. The points visited by a random walk have a dimension $d_w=2$. The condition of growth corresponds therefore to the condition that the intersection dimension d_I between the random walk and the interface be positive.

This leads to

$$d_I=d_w+(D-1)-d\geq 0 \tag{2.5}$$

and therefore

$$D\geq d-1 . \tag{2.6}$$

In addition to the determination of the fractal dimension of the original DLA and DBM models, there have been many other studies that have also considered different properties of the original models or variations and generalizations of these models. The main results are the following.

(a) *Noise reduction.* In the noise-reduction generalization of the DLA and DBM growth rules, a bond is grown only after having been hit by S particles (Kertesz and Vicsek, 1986; Nittman and Stanley, 1986). A counter is raised by 1 each time a particle hits the respective bond. When a counter reaches the value S, the corresponding bond is occupied and the new perimeter bonds near this one start with a counter equal to zero. The effect of this procedure is a systematic reduction of the noise. In fact, the introduction of the parameter S corresponds to averaging over several realizations of the same stochastic process. This reduces the fluctuations and introduces, through the counters, a memory effect. For a finite value of S, the branches acquire a finite thickness, while for $S\to\infty$, screening is suppressed and the structure becomes compact.

Initially, the effect of the noise-reduction parameter was studied mainly with respect to the overall shape of the cluster or with respect to the anisotropy problem in a square lattice (Eckmann *et al.*, 1989, 1990). This led to the conjecture that a large value of S might accelerate the approach to the asymptotic behavior with respect to these properties. In relation to the fractal properties, the

situation is instead the following (Moukarzel, 1992): (i) The asymptotic value of the fractal dimension D does not change for any finite value of S. (ii) Since for $S>1$ the branches acquire a certain thickness ξ, there is a crossover from a compact structure for $R \leq \xi$ to a fractal structure for $R \gg \xi$.

Therefore the intrinsic fractal properties are universal with respect to the value of S. However, for a large value of S, these properties develop only above a certain size.

(b) *Anisotropy and self-affinity.* A simple inspection of the structures generated by DLA and the DBM makes evident that these structures are connected in the growth direction, but not connected in the perpendicular direction. This gives rise to different correlation properties in the two directions (Meakin and Tolman, 1989). Detailed studies for the cylinder geometry show, in addition, that the nature of the clusters may be self-affine (Evertsz, 1989, 1990). Of course, in such a case, it is also possible to define a fractal dimension, but its meaning is not as general as in the case of isotropic scaling. These effects are a warning (Mandelbrot, 1992; Mandelbrot *et al.*, 1995) that the structure has fractal properties, but not of the simplest type. This may actually be a possible reason for the discrepancies observed in the value of D as a function of geometry and method of analysis.

(c) *Multifractality.* This is a generalization of the concept of fractal in which one considers the possibility that a continuum distribution of different singularities may be present instead of a single type as in the case of a simple fractal (Paladin and Vulpiani, 1987). This extension, however, does not cover other possible complications like self-affinity. Multifractals arise naturally in self-similar distributions even as given from a simple multiplicative process. Clearly, the growth probability in DLA and the DBM is a distribution with some sort of self-similar properties, so it was natural to expect multifractal behavior. It seems, however, that, even if multifractals appear to describe some features of this probability distribution, they do not provide a complete description, nor is it evident what may be the advantage in looking at the problem from this perspective. In particular, the portion of the spectrum corresponding to positive values of the q moment appears to be relatively well behaved. On the other hand, various pathologies have been observed for negative values of q, and the situation is at the moment rather controversial (Coniglio *et al.*, 1986; Bohr *et al.*, 1988; Blumenfeld and Aharony, 1989; Mandelbrot and Evertsz, 1990; Schwarzer *et al.*, 1990; Marsili and Pietronero, 1991).

A particularly relevant point of the multifractal spectrum is the exponent $\alpha_{\min}$ corresponding to the strongest singularity. On the basis of simple scaling arguments, it is possible to conjecture a relation between $\alpha_{\min}$ and the fractal dimension D of the entire cluster (Turkevich and Scher, 1985),

$$D = 1 + \alpha_{\min} . \tag{2.7}$$

This relation appears to be in good agreement with numerical results on DLA.

(d) *Multiscaling.* It has been conjectured that the local fractal dimension for a large but finite cluster might vary continuously from the bulk value to a lower value when approaching the interface. The situation in this respect is not yet conclusive (Coniglio and Zannetti, 1990; Ossadnik, 1992).

C. Essential features of the problem

Here we provide a short description of the crucial elements that should be addressed when formulating a theoretical scheme.

(a) *Irreversible dynamical process.* In Fig. 2 we showed schematically the mathematical nature of the growth process. It consists of the iteration of an irreversible stochastic process with long-range couplings in both space and time. It is not possible to assign a statistical weight to a configuration without considering explicitly its dynamical evolution, i.e., its complete history. This implies that the dynamical effects should be explicitly considered. The discrete structure of the process appears to be an essential element, and it is not clear how to define a continuum limit for such a process.

(b) *Self-organized criticality.* The system evolves spontaneously towards a fractal structure without the fine-tuning of any parameter. In this respect the asymptotic structure is an attractor for the dynamics. This situation is basically different from the usual equilibrium critical phenomena in which the fixed point is repulsive and the fine-tuning of a critical parameter is necessary.

(c) *Screening and freezing.* The screening effects due to the Laplace equation appear to be essential to generate empty regions that will never be filled asymptotically and will lead to the fractal structure. For this reason the fractal properties become well defined only in those regions of the structure that are asymptotically frozen, namely, that will not continue to be modified by further growth because they are completely screened.

(d) *Universality.* These growth processes show well-defined universal fractal properties with respect to a number of possible variations: lattice topology, site or bond growth, presence or absence of a diagonal bond, different initial configurations, and, in general, all small-scale modifications of the process.

For the DBM, fractal dimension depends explicitly on the parameter η, and it is not universal in this respect. The fractal properties appear to be relatively universal with respect to radial or cylinder growth geometry. However, as we have discussed, this point requires a more detailed clarification because small but persistent discrepancies are present.

The situation is different for the morphological properties that refer to the overall shape of the structure. These are much less universal than the local fractal properties and are strongly modified by the lattice topology and various other small-scale modifications. This reduced degree of universality with respect to critical phenomena

should be considered an interesting point, because, after all, the fractal structures one observes in nature are quite various.

D. Why usual methods are problematic

The fact that these growth models produce structures with self-similar properties raised the expectation that our understanding of them could be achieved by following the ideas developed for critical phenomena. There are, however, important differences between these two classes of problems, and the application of renormalization-group (RG) ideas to fractal growth turned out to be rather problematic. The main reasons for this situation are the following.

(a) *Field theory framework.* The usual starting point in a field-theory formulation of these problems is the diffusive free field. This means that one looks at the problem essentially as a random walk plus some interactions. In this way it is possible to formally write down the action of a field theory for DLA (Parisi and Zhang, 1985; Peliti, 1985). However, from this point it is impossible to proceed in a constructive way, because the coupling that characterizes the interactions diverges with length scale in any dimension and it leads to a hopeless strong-interaction problem. This implies that there is no length scale in any dimension and it leads to a hopeless strong-interaction problem. This implies that there is no upper critical dimension and that the theory is unrenormalizable. In addition, if one were to consider a generalization to the DBM with $\eta \neq 1$, this would lead to a noncluster aggregation, is not even conceivable from a field-theory point of view. As with other problems of this type, it is possible to improve the situation through lattice regularization. In this way one treats the interaction exactly, and the perturbation theory is defined by an appropriate sum of lattice path integrals. We shall see that the fixed-scale transformation operates exactly along these lines.

(b) *Real-space renormalization group.* The standard real-space renormalization group (RSRG) leads to conceptual problems for fractal growth. For the RSRG, one usually considers a box and integrates over the internal degrees of freedom in order to define the renormalized variables. If the variables correspond to the asymptotic occupation of the sites, this approach will not work for irreversible fractal growth. In fact, in DLA and the DBM, the asymptotic occupation of a given portion of space can only be defined when the growing interface goes to infinity. Therefore one must also take into account faraway external processes. For these reasons, the attempts to describe DLA using the usual RSRG approach, by integrating over the internal degrees of freedom (Gould *et al.*, 1983), give rise to basic problems. A more detailed discussion of these can be found in Pietronero *et al.* (1988b). This criticism does not apply to Nagatani's (1987a, 1987b) RG approach, also elaborated upon by Wang *et al.* (1989a, 1989b), which refers only to growth probabilities and not to the asymptotic occupation of the sites. However, these methods are also problematic because the relation to fractal dimension is via phenomenological relations like Eq. (2.7), and the renormalization of the growth probabilities does not capture, in our opinion, the essential dynamics of the process and its self-organized nature (see Sec. VII). Because of these reasons, they cannot distinguish between fractal and nonfractal structures, in the sense that they cannot show, for instance, that the Eden model (DBM with $\eta=0$) leads to compact structures.

(c) *Mean-field and Flory-type approaches.* There have been various attempts to define mean-field or Flory-type approaches for DLA (Muthukumar, 1983; Honda *et al.*, 1986). The situation is, in this respect, rather confusing. As we have seen, one of the main problems is in identifying the relevant fields; in addition, the proper definition of a continuum limit is not trivial. Roughly speaking, one can consider the mean-field limit as the one in which fluctuations have been eliminated from the problem. There are various ways to eliminate fluctuations; and in all the cases, this has the effect of destroying fractal properties, leading to a compact object. The most sensible mean-field approach seems to lead only to the relation $D=d$; this does not appear terribly interesting and can be easily derived in several ways. On the other hand, this situation can be understood in the following way. If we consider that the generation of a fractal structure corresponds to the appearance of anomalous dimensions at the critical point, this corresponds in some sense to a nontrivial η exponent in critical phenomena (Amit, 1978). Mean-field as well as Flory-like methods can deal with exponents that correspond to the approach to the critical point but not with the anomalous dimensions, because they always imply that $\eta=0$. It seems therefore that fractal properties appear only as deviations from mean-field behavior. In this respect it should be noted that the claimed mean-field expressions that lead to nontrivial values of D have been derived with *ad hoc* assumptions whose meaning is not clear (Muthukmar, 1983; Honda *et al.*, 1986).

III. THE FIXED-SCALE TRANSFORMATION STRATEGY AND ITS BASIC IDEAS

From a theoretical standpoint, the problem of irreversible fractal growth consists in the calculation of the correlation function $G(r_1,r_2,t)$ which refers to the probability of occupation of the points r_1 and r_2 after a total time t for the growth process (Fig. 6). This time is defined by the total number of particles or bonds added to the structure. Actually, the fractal properties become well defined only asymptotically with respect to the two following limits.

(a) *Asymptotic time limit* ($t \to \infty$). This means that one should consider regions of the system that are very far from the growing interface and that will not continue to be modified by further growth (freezing condition).

(b) *Large scale limit* ($r \to \infty$). This implies that one

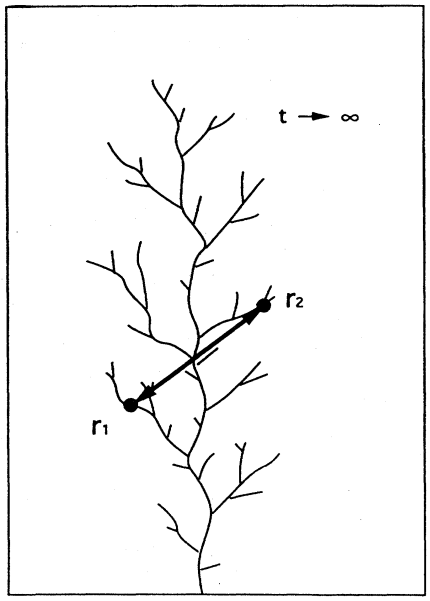

FIG. 6. The fractal exponent is related to the asymptotic correlations of the points of the structure once the growing interface is infinitely far away ($t \to \infty$; "frozen structure").

should consider scales at which eventual scale-invariant properties become well defined.

For a fractal structure, one would expect the following behavior:

$$\lim_{|r_1-r_2|\to\infty} \lim_{t\to\infty} G(r_1,r_2;t)=g(r_1-r_2)\sim|r_1-r_2|^{-(d-D)} , \tag{3.1}$$

where D is the fractal dimension and d is the embedding Euclidean dimension.

Following the usual theoretical approaches, one would attempt to consider these two limits together. However, those approaches were developed for equilibrium problems, in which the time evolution is replaced by the sum over the static configurations, and one has, in practice, only the large scale limit. This is, then, performed by renormalization schemes of various types. For the reasons presented in Sec. II, the problem posed by Eq. (3.1) does not seem treatable with the usual methods.

Given this situation, we have tried to formulate a theoretical framework of a novel type, the fixed-scale transformation, that focuses explicitly on irreversible dynamical evolution. The FST method has been improved and clarified in the past few years, and it is now able to treat in a rather systematic way the class of problems of irreversible fractal growth as well as several others.

The basic point of the FST method is to treat *separately* the two limits $t \to \infty$ and $r \to \infty$. For the asymptotic time limit, it is very important to describe accurately the convergence of the asymptotic structure. We shall see in Sec. IV that this convergence is crucial in order to understand whether the structure is fractal or compact. In this way we can compute the nearest-neighbor correlations between pairs of sites as given by the appropriate lattice path integrals, shown schematically in Fig. 7. The large-scale limit ($r \to \infty$) is then performed by interpreting our "sites" as coarse-grained cells of a generic size. This can be done if one is able to identify scale-invariant dynamics (growth rules) for our problem. The use of scale-invariant dynamics in the FST implies that the resulting nearest-neighbor correlation refers to coarse-grained cells of any size, and from these one can then obtain the fractal dimension.

Let us first consider the problem of the asymptotic time limit. We start by defining the nearest-neighbor (NN) pair correlations at the minimal scale. Consider, for example, the original DBM growth rules. In order to define the NN correlations, we must consider a pair of sites and study the possible configurations of this pair that occur in the asymptotic structure generated by the growth process. We are interested in conditional probabilities, so one site of each pair will certainly be occupied (black). This leads to only two possibilities: a configuration of type 1 with an occupied (black) and an empty (white) site [see (a) in Fig. 7], and a configuration of type 2 with both sites occupied [black; see (b) in Fig. 7]. The probabilities for the occurrence of these

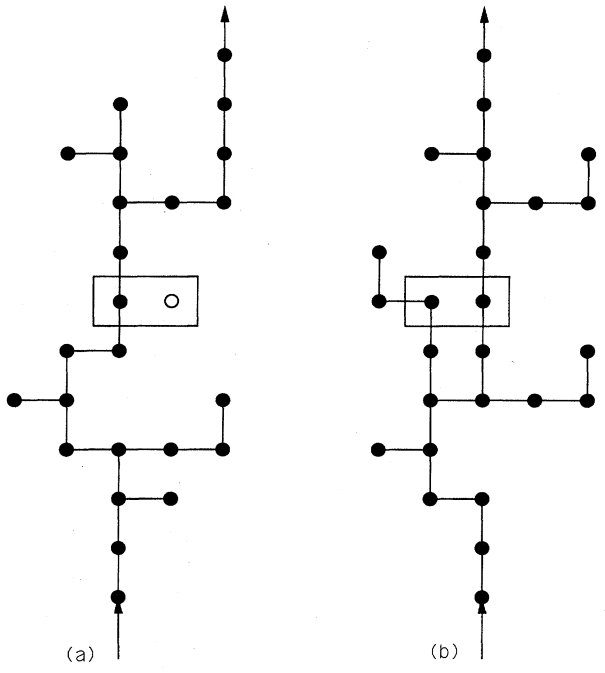

FIG. 7. Schematic for the computation of the pair correlation induced by growth processes. Given an occupied site, we ask for the occupation probability of the nearest-neighbor one. This should be done by evaluating the weight of all the growth processes that do or do not lead to the occupation of this site.

configurations are defined as C_1 and C_2, respectively. In practice, instead of following the scheme illustrated in Fig. 7, it is more convenient to consider the conditional probabilities between pairs of sites. In order to compute these probabilities, one must consider the probability $M_{i,j}$ $(i,j=1,2)$ that a pair configuration of type i will be followed, in the growth direction (k), by a pair configuration of type j (Fig. 8). This leads to a transfer-matrix problem whose vector **C** contains the probabilities for the different pair configurations.

The matrix elements $M_{i,j}$ can be computed by *lattice path integrals* over the possible growth processes that correspond to the configurations i and j. How to do this in practice will be discussed in Secs. IV and VIII. Note that the configurations considered should correspond to the asymptotic (frozen) structure. This implies that the lattice path integrals should be extended until the growing interface is far enough away from these configurations, so that they can be considered asymptotic (long-time limit).

In order to make this calculation quantitatively accurate, it is important to consider also the possible environments (boundary conditions) outside the growing column defined by the dashed lines in Fig. 8. This implies that the matrix elements $M_{i,j}$ should be replaced by weighted averages (see Sec. IV), in which a parameter λ_n characterizes the various possible boundary conditions and $P(\lambda_n)$ is the corresponding probability that will depend on **C**. This leads to a more complex nonlinear transformation whose fixed point can be determined analytically using suitable truncation schemes (see Sec. IV).

Strictly speaking, the FST scheme we have been discussing allows for the computation of NN pair correlations at the minimal scale only. However, were it possible to interpret out "sites" as coarse-grained cells and to use *growth rules* that are *scale invariant,* as shown in the bottom of Fig. 8, then the fixed-point probabilities (C_1,C_2) would characterize the correlations between coarse-grained cells of any size. This means that one would obtain exactly the same process with the same probabilities at different scales. This would allow us to perform the large-scale limit $(b\to\infty)$, because long-range correlations would be described by NN pair correlations of large cells, and from these the fractal dimension is computed.

In order to perform the important step corresponding to the large-scale limit, one must be able to control how the growth rules change under a scale transformation (Fig. 9). DLA and the DBM are intrinsically critical in the sense that their dynamics evolves into the scale-invariant one without the tuning of any parameter. Therefore the question of the universality and scale-invariant properties of DLA and the DBM is related to their effective asymptotic dynamics. In addition, the knowledge of this effective dynamics is one of the key points in the understanding of why these models give rise to self-organized fractal structures. This problem is, in general, very complex due to the large number (in princi-

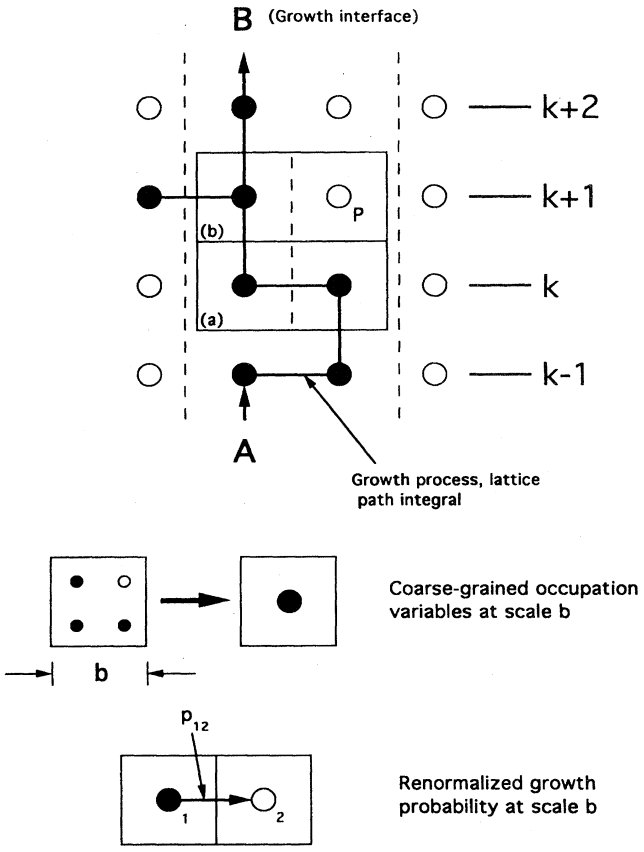

FIG. 8. A crucial concept in the FST method is the nearest-neighbor correlation between cells of a given scale b. One can study this problem by considering the probability that a cell of type i (a) will be followed, in the growth direction (k), by a cell of type j (b). These probabilities are defined by lattice path integrals corresponding to the growth dynamics at a given scale (b). If one uses a scale-invariant growth dynamics, the above correlations can be extended to coarse-grained cells of any size, and the fractal dimension can be computed.

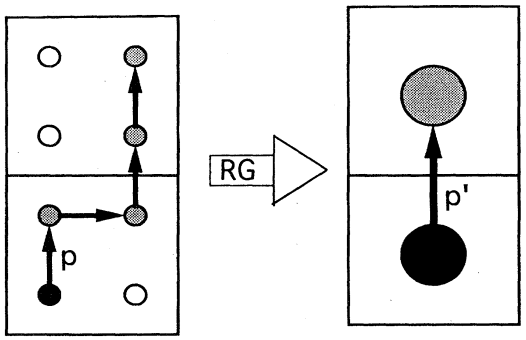

FIG. 9. Simple scheme showing the nature of the renormalization process for the growth rules.

ple, infinite) of parameters that may appear in the dynamics. In practice, however, one can fix a subset of parameters and study their evolution under scale change. This allows us to understand some general symmetry properties that belong to scale-invariant dynamics: (i) growth probabilities should be defined per bond. If one starts with site probabilities, these evolve into bond-type upon scale transformation. (ii) An eventual probability assigned to a diagonal bond disappears under scale change (see Sec. VII.A). Within the complex space of growth rules (Fig. 10), the FST framework points, however, to the essential concepts: Fractals can be generated only if screening persists in the scale-invariant regime (Sec. IV). Note that the presence of screening due to the Laplace equation in the original growth rules does not guarantee that a similar effect persists for coarse-grained variables (Fig. 9). In fact, if one studies the growth rules for a coarse-grained cell, a problem of noise reduction naturally appears. The larger the cell, the larger will be the number of particles (bonds) necessary to span it. Naively, therefore, one could expect that, asymptotically, the effective noise-reduction parameter S diverges. This would eliminate screening effects and lead to a compact structure. Therefore the key feature of the asymptotic growth rules is the identification of the *fixed-point noise-reduction parameter.*

In Sec. VII we discuss a renormalization scheme for the noise-reduction parameter S that allows us to address the problem of the large-scale limit ($r \to \infty$). The main result is that the fixed-point noise-reduction parameter turns out to be of order unity ($S^* = 2.4$) with an *attractive fixed point.* These results clarify therefore the *self-organized critical* nature of DLA patterns, in contrast, for example, to percolation, in which the fixed point p_c is repulsive. This is due to the fact that, under scale change, noise is automatically generated by the dynamics of the system, as discussed in detail in Sec. VII. In addition, the fact that the value of S^* is close to 1 shows that *screening* is *asymptotically preserved* and that the minimal-scale growth rules are already rather close to the asymptotic ones.

In order to illustrate the basic philosophy of the FST method, it is particularly simple and instructive to consider its application to the percolating cluster interpreted as a fractal-growth process (Pietronero and Stella, 1990). The first step is to define the scale-invariant dynamics. This can easily be done by a renormalization procedure like the one shown in Fig. 9.

As we shall see in Sec. V.B, the scale-invariant growth probability is defined by the (nonuniversal) critical parameter $p_c = 0.5$. From a FST standpoint, this corresponds to the scale-invariant dynamics. One can then proceed to define the fixed point with respect to dynamical evolution. From the fixed point of this new transformation, fractal dimension is finally obtained. The detailed implementation of this scheme will be discussed later (Sec. IV).

In the present example, one determines p_c by a simple renormalization method. The usual way to compute the exponents would be by differentiating this expression at the fixed point. The FST works in a different way because it allows us to compute the *universal* fractal dimension D directly from the *nonuniversal* value of the critical parameter p_c. For fractal structures corresponding to usual critical phenomena, we have, therefore, the following conceptual scheme.

$$\left.\begin{array}{c} p_c, T_c \\ \text{Value of the nonuniversal} \\ \text{critical parameter} \end{array}\right\} \Longrightarrow \text{FST} \Longrightarrow \left\{\begin{array}{l} D \text{ (fractal dimension)} \\ \text{Universal critical} \\ \text{exponent} \end{array}\right.$$

This scheme is particularly suitable for irreversible fractal growth because it allows us to treat problems that are impossible within the usual RG methods.

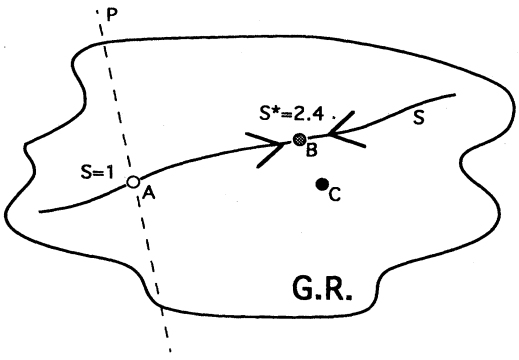

FIG. 10. Schematic showing the space of growth rules (G.R.). Point A corresponds to the original DLA/DBM growth rules. Under an ideal renormalization, this point would flow to point C, which represents the "exact" scale-invariant growth rules. Our scheme consists in renormalizing the growth rules along the line defined by the noise-reduction parameter S. The idea is that the fixed point obtained in this way (point B) is a good approximation to the "exact" one (point C). Line P corresponds to a generalization of the growth rules that goes outside the correct basin of attraction.

IV. BASIC CONCEPTS

In this section we describe in detail the formulation of the fixed-scale transformation method. Our discussion does not refer to the application to a particular model, and we shall be as general as possible. However, one should keep in mind that the FST method has been formulated for irreversible-Laplacian-growth models, and some concepts can be better established referring to them. Here we shall focus mainly on the way to evaluate

the asymptotic NN pair-correlation functions with a suitable lattice path integral corresponding to the irreversible-growth process. This provides a general framework for calculating the fractal dimension and the anomalous exponents once the scale-invariant growth rule of the model is known.

A. Pair-correlation configurations and the fractal dimension

1. Characterization of fractal structures with a fine-graining procedure

When considering a fractal structure, it is convenient to focus on a lower-dimensional subset. For a fractal structure of dimension D embedded in two dimensions, a convenient choice is the intersection set with a line perpendicular to the growth direction [see Fig. 11(a)]. The basic result for the intersection of fractal structure is the additivity of codimensions (Mandelbrot, 1974). Specifically, by using the definition of fractal dimension, we can prove that the intersection set is also a fractal and that its dimension is $D'=D-1$. For homogeneous self-similar structures, the intersection can be done in any direction. In the case of structure generated by a growth process, for reasons that will become clear in the following, the intersection must be perpendicular to the growth direction. We can analyze the set of points generated by the intersection using a procedure called box covering. A box is characterized by a black dot if it contains some points belonging to the structure. Conversely, a box is characterized by a white dot if it does not contain any point of the structure. Note that in Fig. 11 we do not consider the two-dimensional nature of the cells. However, in the sense of the renormalized growth process, the cells should be squares. First, we consider a box of the size of our maximum length scale along the intersection [Fig. 11(b)]. This box contains the whole set of points; so it is black. We then divide this box into two subboxes, considering length scales half of the previous length. As this subdivision process continues [Fig. 11(b)], white boxes begin to appear, corresponding to regions in which there is no part of the structure. Then the process of subdivision continues only for the occupied boxes. Clearly, voids (empty boxes) are generated at all scales if the structure is fractal. This way of describing the intersection set can be thought of as, a "lattice-gas" description, with "occupied" and "empty" sites (Erzan, 1992). In fact, we can associate each box of size l with a lattice-gas variable defined as

$$n_i(l)\equiv\begin{cases}1 & \text{(occupied)}\\ 0 & \text{(empty)}\,.\end{cases} \tag{4.1}$$

Clearly, one can obtain the fractal dimension D by the scale-invariant statistics of this lattice gas. To look at the scale-invariant statistics of this set, we focus on the elementary process by which a black (occupied) box is divided into two, as observed in Fig. 12. We start by defining the NN pair-correlation configurations along the intersection. For the intersection set of Fig. 11, we must consider all the possible configurations of site pairs generated by the growth process, and thus the two following probabilities: (i) a configuration of type 1 with an occupied (black) site and an empty (white) site; and (ii) a configuration of type 2 with both sites occupied (black).

The probabilities of occurrence of these configurations are then defined by C_1 and C_2, respectively, with the normalization requirement $C_1+C_2=1$. These probabilities, strictly speaking, characterize only the NN transverse correlation at a given scale. However, where it is possible to interpret our sites as coarse-grained cells and use

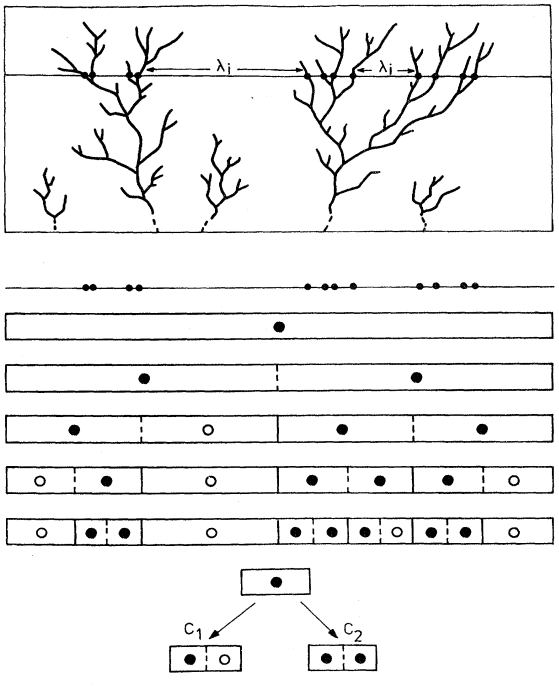

FIG. 11. Definition of the intersection set in the case of the two-dimensional DLA; in the lower part we show a schematic of the process of box covering for the set of points given by the intersection of the fractal structure with a line.

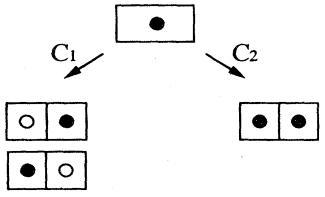

FIG. 12. Elementary process of fine graining for a box that contains some elements of the set. These configurations also define the nearest-neighbors sites pair-correlation function.

the scale-invariant dynamics, the resulting scale-invariant C_i would then characterize correlation between cells of any size. In such a situation our pairs of cells of variable sizes correspond to the generators of the box-covering process of the intersection set, whose scale-invariant probabilities of fragmentation are given by the same C_i. In this case, it is easy to show that, in the asymptotic limit, the number of occupied boxes at scale $l/2$ can be related to the number at scale l. In fact, the average number of black sub-boxes that appear at the next level of fine graining from a black box is

$$\langle n \rangle = \sum_i n_i C_i = C_1 + 2C_2 \tag{4.2}$$

and then

$$N(l/2) = N(l)\langle n \rangle \ . \tag{4.3}$$

This means that for each iteration of the fine-graining process the number of occupied boxes increases on average by a factor $\langle n \rangle$. It is easy, therefore, to show that the (box-counting) fractal dimension of the intersection set is

$$D' = \frac{\ln\langle n \rangle}{\ln 2} \tag{4.4}$$

and that the fractal dimension of our original structure is directly related to the value C_1, C_2 by

$$D \equiv D' + 1 = 1 + \frac{\ln(C_1 + 2C_2)}{\ln 2} \ . \tag{4.5}$$

The problem of the calculation of the fractal dimension is then shifted to the calculation of the asymptotic distribution $\{C_i\}$. Fixed-scale transformation will provide a systematic way to evaluate the C_i's considering the generators of the fragmentation process as the basic diagrams of the dynamics of the system.

Finally, it is important to note that all the previous definitions and formulas can be extended to more complex fragmentation processes or intersections, as in the case of the intersection for fractal structure embedded in three dimensions (Vespignani and Pietronero, 1991).

2. Void distribution

A complete description of the intersection set defined in the previous section also requires a characterization of the empty segments of Fig. 11. These correspond to the voids between adjacent branches of the fractal structure. It is convenient to introduce $P(\lambda)$, defined as the conditional probability that a given occupied box on the intersection will be neighbored on the right by a void of size λ. Here we derive an explicit relation between the distribution C_1, C_2 of the elementary diagrams of the fine-graining process and the distribution $P(\lambda)$. The connection between C_i and $P(\lambda)$ can be made exact only by assuming that the C_i correspond to the generators of a noncorrelated fine-graining process.

In principle, however, it is also possible to generalize the method to a fragmentation process that depends on the environment (Siebesma *et al.*, 1990).

The exact result for uncorrelated fragmentation is given in an iterative form (Tremblay and Siebesma, 1989):

$$P(\lambda=0) = \frac{C_2}{(1+\frac{1}{2}C_1)(C_2+\frac{1}{2}C_1)} \ , \tag{4.6a}$$

$$P(\lambda=2l+1) = \frac{1}{2(1-C_2)} P(\lambda=l) \ , \tag{4.6b}$$

$$P(\lambda=2l) = \frac{1}{4(1+C_2)} P(\lambda=l) + \frac{(1-C_2)^2}{4(1+C_2)} P(\lambda=l-1) \ . \tag{4.6c}$$

In order to derive Eqs. (4.6), it is necessary to introduce a minimal length scale b defined by the size of the finest structures we intend to describe. Note that this does not really introduce a cutoff, because b drops out of the final expressions. Given the structure of the set used, it is convenient to define lengths as

$$\lambda_n = 2^n b \quad (n = 0, 1, 2, \ldots) \ , \tag{4.7}$$

where the largest value of n is given by the upper cutoff length in the system. Looking at Fig. 11, one may be tempted to consider separately each stage of the fine-graining process and see how many void segments of given length appear at each step. To do so would be incorrect because, if in the end several white segments of different sizes are adjacent, they would be computed as several different λ's, while, indeed, they correspond to a single void whose size is of the order of the largest among these segments. Therefore, in order to compute the void distribution, it is necessary to consider all possible correlations between the various steps of the fine-graining procedure. In this respect it is convenient to start at the finest level and consider a coarse-graining process. In Fig. 11, this corresponds to starting from the lowest level of fine graining in which a black box is of linear size b and going up level by level.

By going up a single level, one can see that each black box of size b is grouped together with another black or white box of size b to form a black box of length $2b$ at the next level of coarse graining. This process of pairing can involve with equal probability 1/2 the box to the right or the left of the considered one, as shown in Fig. 13. The probability is the same because the segments defined by the process of coarse graining are independent with respect to the occupied points of the structure. These processes lead to pairs of adjacent cells that correspond to a configuration of type 1 or type 2. In the following we shall refer to these processes as "left" or "right boxing" (Fig. 13).

We begin by calculating $P(\lambda=0)$, namely, the probability that an occupied box of size b will be neighbored at the right by another occupied box. With probability 1/2, the first boxing process will occur on the right side. In

this case one need only to require that the resulting boxing configuration be of type 2. This will be equal to the conditional probability of having a cell of type 2 given a black site, i.e., $C_2/(C_2+\frac{1}{2}C_1)$. If the first boxing is instead on the left, we must consider the next level of coarse graining. If this second boxing process occurs on the right, we must require the configuration to be of type 2 [with probability $C_2/(C_2+\frac{1}{2}C_1)$]. In addition, we must require the left side of the right pair of this boxing configuration to be a black box. This produces, therefore, a multiplicative factor $(C_2+\frac{1}{2}C_1)$. On the contrary, if the second boxing is on the left, we must go on the next level of coarse graining, and so on. At the end of this process, one obtains a probability tree of type

$r:\frac{1}{2}C_2/(C_2+\frac{1}{2}C_1)$

$r:\frac{1}{2}\dfrac{C_2}{(C_2+\frac{1}{2}C_1)}\cdot(\frac{1}{2}C_1+C_2)$

$l:\frac{1}{2}$

$r:\frac{1}{2}\dfrac{C_2}{(C_2+\frac{1}{2}C_1)}\cdot(\frac{1}{2}C_1+C_2)^2$

$l:\frac{1}{2}$

$l:\frac{1}{2}$

(4.8)

where we identify l or r as the left or right boxing, respectively. Summing up all the terms of the probability tree, we obtain the series

$$P(\lambda=0)=\frac{1}{2}\frac{C_2}{\frac{1}{2}(C_1+C_2)}\sum_n\left[\frac{1}{2}\left[C_2+\frac{1}{2}C_1\right]\right]^n$$
$$=\frac{C_2}{(1+\frac{1}{2}C_1)(C_2+\frac{1}{2}C_1)}\,, \tag{4.9}$$

which corresponds to Eq. (4.6a).

Let us now focus on the recursive relation (4.6b). We consider the probability $P(\lambda=(2l+1)b)$ that corresponds to the conditional probability that a given occupied box of size b will be neighbored on the right by a void of size $\lambda=(2l+1)b$. This situation is depicted in Fig. 14. Suppose that the first boxing process for the given structure occurs on the right side. The boxing configuration at this level of coarse graining is shown in Fig. 14(a). The boxing configuration is given in this case by an occupied box of size $2b$, neighbored by l empty boxes of size $2b$. The probability of this boxing configuration is then $P(\lambda'=l)$, where λ' means that the voids are measured on the length scale $2b$. In addition, we must require that the left pair of the boxing configuration have the right site empty, conditional to the other site's being occupied, and that the left side of the right pair be occupied. This produces, therefore, the multiplicative factor $\frac{1}{2}C_1/(C_2+\frac{1}{2}C_1)$ and $\frac{1}{2}C_1+C_2$, respectively. When the first boxing is instead left, the resulting boxing configuration will be as that shown in Fig. 14(b). The probability of this boxing configuration is again $P(\lambda'=l)$, with a multiplicative factor $\frac{1}{2}C_1$ given by the condition that the right pair have the left site empty and the right site be occupied. Considering that each boxing process will occur with probability $\frac{1}{2}$, we have

$$P(\lambda=2l+1)=\frac{1-C_2}{2}P(\lambda'=l)\,. \tag{4.10}$$

From the scale invariance of the distribution, we have $P(\lambda=l)=P(\lambda'=l)$, recovering Eq. (4.6b).

We can now pursue the same approach to calculate the recursive relation (4.6c) for $P(\lambda=2l)$. If the first boxing occurs on the right side, the boxing configuration with cell of size $2b$ will be as that depicted in Fig. 15(a). The distance between the left and the right pair is of $l-1$ empty boxes of size $2b$. The probability of this boxing configuration is $P(\lambda'=l-1)$ multiplied by the factor rising from the condition on the right and left pair, i.e., $\frac{1}{4}C_1^2/(C_2+\frac{1}{2}C_1)$. If the first boxing occurs instead on the left side, the boxing configuration will be formed by l empty boxes of size $2b$ with probability $P(\lambda'=l)$. See Fig. 15(b). In addition, we have the multiplicative factor $\frac{1}{2}C_1$ given by the requirement on the fine structure of the right pair. Summing up the two boxing processes, we obtain

$$P(\lambda=2l)=\frac{(1-C_2)}{4}P(\lambda'=l)$$
$$+\frac{(1-C_2)^2}{4(1+C_2)}P(\lambda'=l-1)\,, \tag{4.11}$$

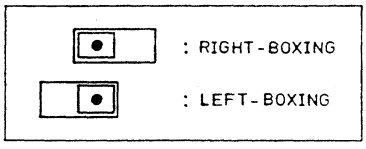

FIG. 13. Association of a second box to a given black box, which can happen on either left or right with equal probability.

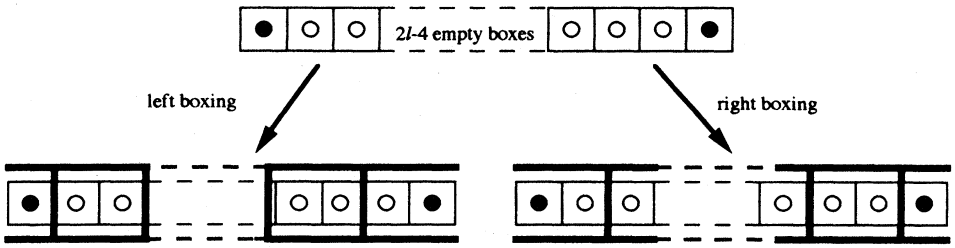

FIG. 14. Boxing processes involved in the calculation of the conditional probabilities that a given occupied box of size b will be neighbored at the right by a void of size $\lambda=(2l+1)b$.

and, using the scale invariance of the $P(\lambda)$, we recover Eq. (4.6c).

With these recursive relations, one can compute $P(\lambda)$ for any λ, obtaining the complete void distribution as a function of the C_1,C_2 of the basic diagrams used in the characterization of the intersection set. It is easy to check that the integrated void distribution has the expected behavior for a fractal structure (Mandelbrot, 1982)

$$P(\lambda \geq \Lambda)=F\Lambda^{-D'} , \tag{4.12}$$

where F is the lacunarity and D' is the fractal dimension of the intersection set.

B. The fixed-scale transformation

We have seen that both the fractal dimension D and the void distribution of a given fractal structure can be related to the distribution $\{C_i\}$ of the configurations of the NN pair-correlation function (i.e., the generators of the fine-graining process for the intersection set), provided that these hold for boxes of arbitrary sites. The basic problem is to compute the pair correlations induced by the growth processes corresponding to the considered model. Let us first consider the problem at the minimal scale. Considering a pair of sites under the condition that one of the two sites be part of the structure, we ask for the probability that the neighboring site will also be part of the structure. In practice, we should consider all the growth processes that pass through the first site (Fig. 7), analyze their statistical weight, and sum the probabilities of those paths that also occupy the second point. This would lead to

$$C_2=\frac{\sum_{\{\alpha\}} W'_\alpha}{\sum_{\{\alpha\}} W_\alpha} , \tag{4.13}$$

where the index α runs over all possible growth processes of lattice path integrals, and the primed sum in the numerator is restricted only to those paths that lead to the occupation of both sites, as the one in Fig. 7(b).

In the form of Eq. (4.13), the calculation can only be performed numerically. However, one can look at this problem in terms of a transfer matrix from a pair configuration i to a pair configuration j along the growth direction. Essentially, this is the fixed-scale transformation, which can be thought of as a master equation for the $\{C_i\}$ under translation. Using the translational invariance of the structure, we search for the fixed point of this master equation. In this way the C_i can be seen as the probability of the basic diagrams of the dynamics of the system, and the fixed-scale transformation matrix elements $(M_{i,j})$ are the conditional probabilities that, in the asymptotic structures, a configuration of type i will be followed by a configuration of type j in the growth direction. Therefore we can write in full generality the fixed-scale transformation as an iterative equation of type:

$$\{C_i^{k+1}\}=\{M_{i,j}\}\{C_i^k\} , \tag{4.14}$$

where k denotes the order of iteration, corresponding to the height of the intersection.

Let us now focus on the case of a structure defined in a two-dimensional space. In this case the intersection set is characterized by two configurations of site pairs and the respective occurrence probabilities C_1,C_2. The fixed-scale transformation is then

$$\begin{bmatrix} C_1^{k+1} \\ C_2^{k+1} \end{bmatrix} = \begin{bmatrix} M_{1,1} & M_{2,1} \\ M_{1,2} & M_{2,2} \end{bmatrix} \begin{bmatrix} C_1^k \\ C_2^k \end{bmatrix} . \tag{4.15}$$

Clearly the asymptotic invariant distribution $\{C_i^*\}$ will be given by the fixed point of the FST. Using the relations $\sum_j M_{i,j}=1$ and $\sum_i C_i=1$, we find the fixed-point solutions to be

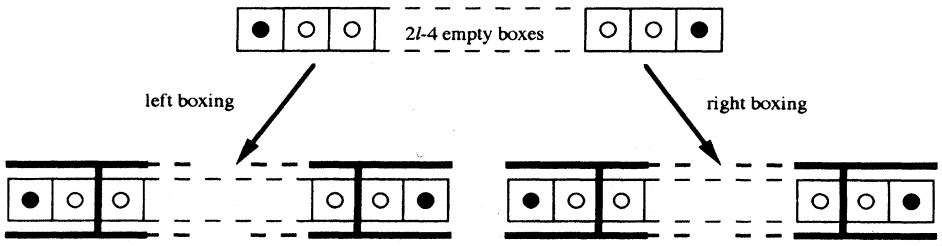

FIG. 15. Boxing processes involved in the calculation of the conditional probabilities that a given occupied box of size b will be neighbored at the right by a void of size $\lambda=(2l)b$.

$$C_1^* = \left[1+\frac{M_{1,2}}{M_{2,1}}\right]^{-1}, \tag{4.16}$$

and, in terms of the matrix elements, $\langle n \rangle$ becomes

$$\langle n \rangle = \frac{2M_{1,2}+M_{2,1}}{M_{1,2}+M_{2,1}} . \tag{4.17}$$

The above relation in combination with Eqs. (4.4) and (4.5) allows one to compute the fractal dimension D of the structure. In the more complete treatment of Sec. IV.E, the matrix elements $M_{i,j}$ will be nonlinear functions of the distribution C_i. In this case the determination of the fixed-point distribution is more complex and often requires the introduction of approximate schemes of calculation.

Our definition of the matrix elements makes the FST a sort of transfer matrix for the probability of occurrence C_1, C_2 of the elementary configurations. However, it is important to note in this respect that the fractal dimension (the critical exponent) is calculated from the eigenvector (with eigenvalue equal to 1) and not from the eigenvalue of the iterative transformation (Erzan and Pietronero, 1991). In fact, we do not use the transformation of the density under scale change, nor do we extract from it the eigenvalue λ from which $D'=\ln\lambda/\ln b$. In our case, we write instead a fixed-scale recursive relation whose fixed point is directly the average conditional density $\langle n \rangle$ from which we can find $D'=\ln\langle n \rangle/\ln b$. Comparing this relation with the previous one, we have $\langle n \rangle=\lambda$. The FST can then be thought of as the fixed-point equation for the eigenvalue itself; to actually find the scaling exponents D, we must use the fixed-point solutions directly. It is important to note that the FST is defined at a given scale; however, if one has scale-invariant matrix elements, the resulting value of $\langle n \rangle$ will be the same at all scales and therefore can be related to the fractal dimension D'. In order to have such a situation, one should use scale-invariant dynamics in the calculation of the matrix elements, which is not necessarily the microscopic one, and it must be found using different methods.

From the previous discussion, the dynamics of the system turns out to be the essential point of the FST approach, and it is contained in the matrix elements

$$M_{i,j} = \text{prob}(i \rightarrow j) , \tag{4.18}$$

which define the conditional probability of having a cell of type i followed by a cell of type j on the line adjacent to it. The matrix elements can be defined by the lattice path integrals corresponding to the various growth processes. The basic point of this approach is that it is now possible to assign a statistical weight for both reversible and irreversible dynamical processes. It should be noted that for irreversible dynamical problems, this whole construction refers to the "frozen structure," which has already grown to its asymptotic state and for which no further evolution will occur. This implies that the lattice path integrals should be extended until the growing interface is far enough away from the starting configurations, so that they can be considered asymptotic (large time limit).

In order to calculate explicitly the matrix elements, we have developed a diagrammatic graphical method. We start with a configuration of type j and consider a "growth" column above it. A nontrivial problem is the choice of lateral boundary conditions for the column. The two simplest choices are "closed" and "open" boundary conditions. "Closed" means adopting periodic boundary conditions. This implies that our structure will immediately be followed by a similar structure. On the contrary, "open" means infinite period, in the sense that no other structure will be present. We must then consider all the graphs linking the occupied sites in the initial cell to the sites of the next cell in the column. By the order of graph we mean the number of bonds occupied by the path, excluding the trivial starting one on top of the cell. We must also enforce the connectivity of the column; therefore each path consists of a connected sequence of bonds. The matrix elements are evaluated by summing up the weight of each graph of a given order that leads from a configuration of type i to a configuration of type j. In this sense the calculation of the matrix elements corresponds to a lattice path integral defined by the growth process.

It is very simple to assign the weight of each path, following the dynamical evolution inside the growth column. Consider, for example, Fig. 16 where the starting cell is of type 1. We cannot consider growth in the initial cell because it is conditionally "frozen." Therefore we have only two possible paths, indicated by the arrows of the corresponding growth process. The probabilities of the relevant growth processes are indicated by $p_{i,j}$, where the first index, i, refers to the growth bond and the second one, j, refers to the order of graph to which it will give rise. Clearly, the probabilities of the growth processes are normalized inside the column. At second order, the resulting graphs are five, generated from the two

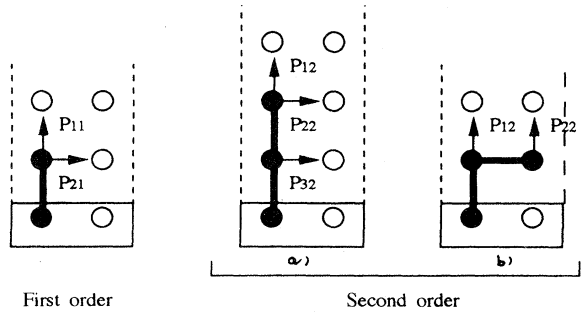

FIG. 16. Graphical evaluation of the matrix elements $M_{1,j}$ at firt and second order. We consider all the growth processes that define the probability for the next cell to be of type 1 or 2. The first site on top of the initial cell will be necessarily occupied, and it is already included in the starting configuration.

first-order graphs a,b of Fig. 16. Each of them has a weight given by the product of the probability of the first-order path and the probability of the growth process that leads to the corresponding second-order path. We can now evaluate the matrix elements at the first two orders. At first order, only the process $p_{2,1}$ will lead to the occupation of both sites in the cell on top of the starting one; therefore $M_{1,2}^{(I)}=p_{2,1}$. At second order, all the paths generated from the growth process $p_{2,1}$ belong to the matrix element $M_{1,2}$. In addition, the first-order path a of Fig. 16 can generate a double occupation in the first growth cell with probability $p_{3,2}$. We then have at first and second order

$$M_{1,2}^{(I)}=p_{2,1}\ , \tag{4.19a}$$

$$M_{1,2}^{(II)}=p_{2,1}+(1-p_{2,1})p_{3,2}\ , \tag{4.19b}$$

$$M_{1,1}^{(II)}=1-M_{1,2}^{(II)}\ . \tag{4.19c}$$

We can repeat all the previous steps starting with a cell of type 2 (Fig. 17), and we obtain

$$M_{2,2}^{(I)}=p_{2,1}+p_{3,1}\ , \tag{4.20a}$$

$$M_{2,2}^{(II)}=p_{2,1}+p_{3,1}+(1-p_{3,1}-p_{2,1})(p_{3,2}+p_{4,2})\ , \tag{4.20b}$$

$$M_{2,1}^{(II)}=1-M_{2,2}^{II}\ . \tag{4.20c}$$

Clearly, the values of the growth probabilities $p_{i,j}$ necessary to define the matrix elements are defined through the growth rules of the model considered and depend upon the graph order, the boundary conditions, and the type of starting configuration.

Apart from the problem of boundary conditions, it should be noted that this graphical expansion for the matrix elements implies the following approximations schemes. First, we do not consider growth outside the column above the initial cell. Such growth should be included, though, if one is considering processes up to very high order. Second, our definition of the growth probabilities implies that some growth will certainly occur above our initial configurations, for example, the trivial starting one. This implication is not strictly true, because, in principle, all sites above the initial cell may remain asymptotically empty because growth may occur mainly outside the column. In a following section (IV.E), we generalize the FST to include this effect and show that it gives rise to higher-order corrections because the environment can be properly described in terms of boundary conditions.

The asymptotic matrix elements are those evaluated at the infinite order:

$$M_{i,j}=\lim_{n\to\infty} M_{i,j}^{(n)}\ ; \tag{4.21}$$

but, in practice, the series [Eqs. (4.18) and (4.19)] can be truncated when the probability of occupation of site 2 in Fig. 16 or 17 is virtually negligible. This is called the freezing condition. In fact, if there is a screening effect in the dynamical process, the higher-order terms of the series will correspond to configurations in which site 2 of Fig. 16 is strongly screened by growth that has occurred at other sites. Such a fact is crucial, because it allows for the rapid convergence of the series of $M_{i,2}$ to a value smaller than 1. This is a key point in the formation of fractal structures. In fact, a convergence of the $M_{i,2}$ to a number smaller than 1 would imply that

$$M_{1,1}=1-M_{1,2}>0 \tag{4.22}$$

asymptotically. Therefore there is a finite probability that growth will leave sites empty even asymptotically, and, for the scale invariance of the problem, *holes of all scales will be generated.* The FST then states a precise condition for distinguishing between compact and fractal structures. Given the growth rule of a model, it is possible, by looking at the FST matrix elements, to decide whether it will give rise to a fractal structure. In this sense the FST illuminates the key point for the generation of fractal structures as the *screening effect* of the growth dynamics of the model.

In the case of Hamiltonian or equilibrium problems like Ising clusters and percolation, the previous discussion regarding the practical evaluation of matrix elements must be slightly changed. In fact, these problems are not naturally defined from a dynamical standpoint. We can follow two possible routes. The first is to define some dynamical description of the critical clusters (Pietronero and Stella, 1990; Erzan and Pietronero, 1990). The second is to obtain the matrix elements with

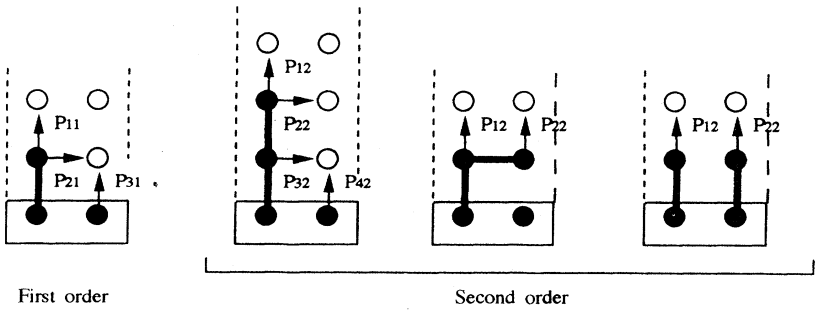

FIG. 17. Graphical evaluation of the matrix elements $M_{2,j}$ at first and second order. In this case, too, the first site on top of the initial cell is already included in the starting configuration.

a purely geometric approach based on the equilibrium properties of the model (Pietronero and Stella, 1990; Erzan, 1992; Di Stasio *et al.*, 1994). In this last case each connected configuration is characterized by its equilibrium statistical weight.

C. Fixed-scale transformation application to the Eden model

In this section we apply the FST to the Eden model. This application shows how the FST allows us to distinguish between compact and fractal structures through the analysis of the convergence of the matrix elements. The Eden model (Eden, 1961) is a growth model in which every perimeter site has the same probability of growing. This model, although it has interesting scaling behavior for the surface, leads to compact clusters, namely, those with dimension $D=d$. In this case the growth dynamic does not have screening properties; i.e., each growth process is equiprobable, and the series that define the FST matrix elements are slowly converging.

Let us now show the calculation of the matrix element $M_{1,1}$. Using the graphical expansion defined in the previous section, we must consider the diagram depicted in Fig. 18 and look at the probability that site 2 of the figure will not be occupied during the growth process. At first order, the probability of this occurring is 1/2, while at second order it is 2/3. It is easy to show that at each order two new possible sites of growth are added and then at nth order the probability is $n/(n+1)$.

We obtain therefore an upper limit for the matrix element,

$$M_{1,1}^{\text{Eden}} \leq \prod_{n=1}^{N} \frac{n}{n+1} = \frac{1}{2}\frac{2}{3}\frac{3}{4}\cdots\frac{N-2}{N-1}\frac{N-1}{N} = \frac{1}{N} . \tag{4.23}$$

One can see, therefore, that the matrix element $M_{1,1}$ converges to zero and $M_{1,2}$ to 1 for $N\to\infty$, but only as a power law. This clearly occurs also for the matrix elements $M_{2,1}$ and $M_{2,2}$. As a function of the order of the process considered, the fractal dimension therefore has the behavior

$$[2-D_{\text{Eden}}^{(N)}] \leq O\left[\frac{1}{\log N}\right] , \tag{4.24}$$

and we recover the exact Eden limit $D=2$ at infinite order.

The Eden model reaches its dynamical equilibrium very slowly because of the lack of screening in the growth rules. This implies that one must consider growth processes up to infinity. This fundamental point is impossible to implement in RSRG attempts where the growth is allowed only within the considered cell, and this is the main reason for the failure of this kind of approach.

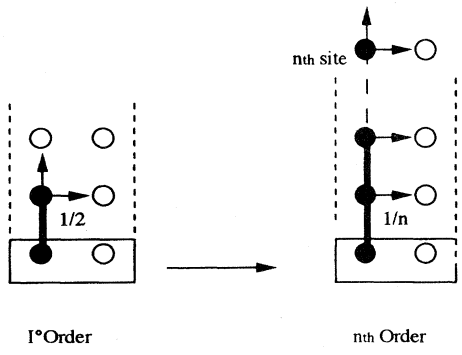

FIG. 18. Schematic of the growth process considered for the analysis of the Eden limit and the calculation of Eq. (4.22).

D. Fluctuations of boundary conditions

One of the key elements of the FST approach is the explicit inclusion of boundary conditions in the evaluation of matrix elements. This is possible mainly because the method works at a fixed scale. For nonlocal growth rules, in fact, the growth of a structure will be very different if it is isolated or surrounded by other points of the structure. This is reflected in a strong dependence on the boundary conditions of the elementary growth process probabilities in the graphical expansion of Sec. IV.B. This is a new type of problem that is usually neglected in the RSRG method, because it would be extremely difficult to include these effects for a cell containing several sites.

Here we show how that FST can include the fluctuations of boundary conditions self-consistently using the void distribution of Sec. IV.A. For the graphical method, we characterize with different boundary conditions the different environments in which growth takes place. We specify these different environments by the size λ between the growing structure being considered and the next branch which can influence it. Clearly, the distribution for each of these situations is $P(\lambda)$, as given by Eq. (4.6). In order to compute explicitly the matrix elements, each void-gulf of size λ must correspond to boundary conditions of period λ. With respect to the use of the distribution $P(\lambda)$ in defining the boundary conditions, there is an additional fact to consider. Our basic configurations of the graphic expansion correspond to pairs of sites of which at least one is black, so at the higher level of coarse graining they correspond necessarily to a black site. To this site we can directly apply the above void distribution. However, if we ask for the probability that a pair of sites will be followed at distance λ by a black site (boundary condition of period λ), the answer is slightly more complicated. In fact, with probability $P(\lambda)$, the pair will be followed by another pair in which at least one of the two sites is black. So if we consider the probability that the site occupied will be that

closer to the considered pair, we shall require the extra condition that the pair configuration be of type 2 or type 1, but with the occupied site on the left. Therefore the additional factor is $(C_2+\frac{1}{2}C_1)$ and the correct distribution of boundary conditions to be used in our calculation of matrix elements is

$$P'(\lambda)=P(\lambda)(C_2+\tfrac{1}{2}C_1)\ . \tag{4.25}$$

This discussion implies that the probability distribution for the size of voids defines the probability distribution for having a certain boundary condition in the elementary growth process. This means that the generic matrix element $M_{i,j}$ should be interpreted as the convolution over all possible boundary conditions around the growth column,

$$M_{i,j}=\sum_n P'(\lambda_n)M_i,j(\lambda_n)\ . \tag{4.26}$$

In this way we define an effective average dynamics with respect to the fluctuations of boundary conditions. An alternative way would be to define the C_i for each boundary condition and average at the end, obtaining a self-consistent equation. We prefer to use the simplest version [Eq. (4.26)], because this effect is already a small correction and the results of the various methods are usually very close.

It is important to note that $P'(\lambda_n)$ is a function of C_1, C_2; therefore the iterative transformation becomes nonlinear,

$$\begin{bmatrix}C_1\\C_2\end{bmatrix}=\sum_n P'(\lambda_n,C_1,C_2)\begin{bmatrix}M_{1,1}(\lambda_n) & M_{2,1}(\lambda_n)\\ M_{1,2}(\lambda_n) & M_{2,2}(\lambda_n)\end{bmatrix}\begin{bmatrix}C_1\\C_2\end{bmatrix}\ . \tag{4.27}$$

The corresponding fixed-point solution will be the following nonlinear equation of infinite order for C_1:

$$C_1^*=\left[1+\frac{\sum_n P'(\lambda_n,C_1^*,C_2^*)M_{1,2}(\lambda_n)}{\sum_u P'(\lambda_n,C_1^*,C_2^*)M_{2,1}(\lambda_n)}\right]^{-1}\ . \tag{4.28}$$

In practice, the calculation of the series in Eq. (4.27) would be rather laborious, because it would imply recomputing all the matrix elements for each value of λ that was included in the series. The simplest nontrivial method for including the boundary-condition fluctuations consists in assuming that the matrix elements will not be too sensitive to the distance of the next branch unless it is very close. In this sense we can consider mainly two different types of matrix elements. The first type is evaluated with "closed" boundary conditions (one cell period) for which the next branch is very close. The second type of matrix elements is instead calculated with open boundary conditions (infinite period). This means that all the intermediate matrix elements are considered essentially identical to the second type. We have then only two possibilities; and by calling $M_{i,j}^{\rm cl}$ and $M_{i,j}^{\rm op}$ the matrix elements corresponding to closed and open boundary conditions, we obtain

$$M_{i,j}=P'(\lambda=0)M_{i,j}^{\rm cl}+\sum_{n\neq 0} P'(\lambda_n)M_{i,j}^{\rm op}\ . \tag{4.29}$$

Using Eq. (4.24), we obtain

$$P'(\lambda=0)=\frac{C_2}{(1+\frac{1}{2}C_1)}\ ; \tag{4.30}$$

and from the normalization condition, we have

$$\sum_{n\neq 0} P'(\lambda_n)=1-P'(\lambda=0)\ , \tag{4.31}$$

which finally gives

$$M_{i,j}=\left[\frac{2C_2}{2+C_1}\right]M_{i,j}^{\rm cl}+\left[\frac{3C_1}{2+C_1}\right]M_{i,j}^{\rm op}\ . \tag{4.32}$$

In this scheme of calculation, the fixed-point equation is drastically simplified, because from infinite order it becomes just of second order. Actually, it is also possible to write down explicitly the fixed-point solution that reads

$$C_1^*=\frac{M_{1,2}^{\rm cl}+M_{2,1}^{\rm cl}-\frac{3}{2}M_{2,1}^{\rm op}-[(\frac{3}{2}M_{2,1}^{\rm op}-M_{1,2}^{\rm cl}-2M_{2,1}^{\rm cl})^2+-4M_{2,1}^{\rm cl}A\,]^{1/2}}{2A}\ , \tag{4.33a}$$

$$A=M_{1,2}^{\rm cl}+M_{2,1}^{\rm cl}-\tfrac{3}{2}(M_{1,2}^{\rm op}+M_{2,1}^{\rm op})\ . \tag{4.33b}$$

Our approximation is based on the fact that the convergence of the series that defines the matrix elements is generally rather fast; so one has to include only a few orders in the calculation. This scheme of calculus, called open-closed, gives very good results in all two-dimensional problems and could be improved by the introduction of intermediate boundary conditions. In three-dimensional problems, the approximation clearly becomes too "simple," because the higher coordination of the lattice introduces more sides on which boundary conditions may be imposed. This calls for the introduction of different and refined schemes of calculus (Vespignani and Pietronero, 1991) in order to obtain reliable results.

The possibility of including fluctuations of boundary conditions in the FST method allows us to reach an accuracy in results beyond that which is usually possible with real-space methods. Finally, developing schemes of increasing complexity, we can test the convergence of the theoretical results in a systematic way.

E. Empty configurations: The extended fixed-scale transformation

The starting point of the FST method is the configurations and the related probabilities of occurrence that define the NN pair-correlation function. This configuration implies that at least one of the sub-boxes must be occupied (conditional correlation). However, in the dynamical process a given pair of sites can be followed in the growth direction by a pair of empty sites. So, while a pair of empty sites cannot appear in the configurations characterizing the NN correlation, it can appear in the dynamical processes that define the FST transfer matrix, as shown in Fig. 19. Here we show in detail an extended scheme of calculation that allows us to include this effect in the FST, generalizing the approach of the previous sections.

Let us focus on the two-dimensional case of the previous sections, where the intersection is done with a line. We must include in the transformation the empty configuration with the corresponding probability C_3. The new FST can be formally written as

$$\begin{bmatrix} C_1^{k+1} \\ C_2^{k+1} \\ C_3^{k+1} \end{bmatrix} = \begin{bmatrix} M_{1,1} & \cdots & M_{3,1} \\ \vdots & \cdots & \vdots \\ M_{1,3} & \cdots & M_{3,3} \end{bmatrix} \begin{bmatrix} C_1^{k} \\ C_2^{k} \\ C_3^{k} \end{bmatrix} . \tag{4.34}$$

Therefore we must introduce the matrix elements $M_{1,3}$, $M_{2,3}$, and $M_{3,i}$, which represent the conditional probabilities for generating a configuration of type 3 starting from one of type 1 and 2 and vice versa. The graphical expansion presented in Sec. IV.B clearly excludes the possibilities of having such configurations. In fact, we consider only the paths and the corresponding growth process that occur in the column above the starting cell, and the growth probabilities are normalized within this column. This clearly eliminates paths like those shown in Fig. 19.

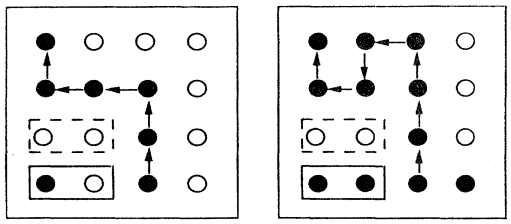

FIG. 19. Completely empty configurations generated by the dynamical process corresponding to the fixed-scale transformation. These two examples show how such a situation can occur.

In practice, to include these situations, we must consider columns of growth with a basis of at least four sites. The basis consists of two or more equal cells, and one of these is considered the cell of type i from which the probabilities $M_{i,j}$ are defined. In this way we enlarge the space of growth, providing more degrees of freedom for the possible growth paths that can now generate empty configurations.

This poses a technical problem, because it is clear that, in order to achieve a sufficient degree of convergence with a basis of four sites or more, one should consider many more elementary growth processes and growth paths than in the case of only two starting sites. In principle, we have to go up to orders comparable to those of the two starting sites. For example, if we use a four-sites basis, we will compute the matrix elements up to the eighth order; that means an average of four growth processes per pair of starting sites, corresponding to a third order, including the trivial one, in the two-sites calculations.

Having obtained the matrix elements of the extended iterative transformation, we can compute the fixed point and therefore the asymptotic distribution. However, once having introduced the empty configurations in the dynamics, we cannot consider them anymore directly related to those of the conditional correlation function. Therefore the conditional correlation is characterized by the distribution $\{\tilde{C}_i\}$, corresponding to the probabilities of having a configuration of type 1 or 2 conditional to the fact that it must have at least one site occupied,

$$\tilde{C}_1 = \lim_{c \to c^*} \frac{C_1^*}{C_1^* + C_2^*} , \tag{4.35a}$$

$$\tilde{C}_2 = \lim_{c \to c^*} \frac{C_2^*}{C_1^* + C_2^*} . \tag{4.35b}$$

For example, let us consider the simplest way to compute the probability that a nonempty configuration will evolve into an empty one. This simplest way is to consider the growth process on two adjacent columns (four-sites basis) normalizing the probability of the growth paths on the union of these two. The two starting configurations at the basis of the two columns are taken to be equal so that the calculation corresponds to the standard scheme with closed boundary condition. Note that, in principle, one could also consider different situations by considering all the possible configurations of two cells and defining a probability distribution for these combinations.

Using this closed-boundary-conditions scheme, we exclude the possibility that an empty cell will generate an occupied one during the dynamical evolution, and we then have definitely that $M_{3,1}=M_{3,2}=0$ and $M_{3,3}=1$. Using these matrix elements, we obtain a transition matrix where the only "relevant" state is given by C_3 (Vespignani and Pietronero, 1990). This implies that the fixed point is

$$\mathbf{C}^*=(C_1^*,C_2^*,C_3^*)=(0,0,1)\ . \tag{4.36}$$

This result may appear, at first, inconsistent, but it is perfectly reasonable. In fact, the density of a fractal structure is asymptotically zero; so if we let the occupied configurations compete with the empty one, the last one will necessarily prevail. However, this is not the point we want to address, because we are interested in the correlation properties of fractal structure, and these are given by the *relative weight* of the nonempty configurations. For the closed-boundary-condition scheme, the FST has constant matrix elements and can be solved exactly. In fact, since we know the fixed point $C^*=(0,0,1)$ for a probability matrix, we can write in full generality

$$\mathbf{C}=\mathbf{h}_0+k_e\mathbf{h}_e+k_n\mathbf{h}_n\ , \tag{4.37}$$

where $\mathbf{h}_0=(0,0,1)$ and $\mathbf{h}_e$ is the effective eigenvector with largest eigenvalue λ_e.

From this it is easy to study the effect of the iteration process. In our definition $\lambda_e>\lambda_n$, and therefore after a certain number of iterations, the contribution of $\mathbf{h}_n$ is negligible with respect to $\mathbf{h}_e$. This implies that $\mathbf{h}_e$ corresponds to the effective direction along which the iterative transformation approaches the fixed point. Then the limiting processes given by Eqs. (4.35) can be properly evaluated,

$$\tilde{C}_1=\frac{h_{e,1}}{h_{e,2}+h_{e,1}}\ , \tag{4.38a}$$

$$\tilde{C}_2=\frac{h_{e,2}}{h_{e,2}+h_{e,1}}\ , \tag{4.38b}$$

where $h_{e,i}$ is the ith component of the eigenvector. Therefore, in the closed-boundary-condition scheme, we can find analytically the probabilities of the fine-graining process generators as a proper combination of components of the eigenvectors with larger eigenvalue (Vespignani and Pietronero, 1990). It is important to note that this result is general and that the fractal dimension is extracted as in the standard scheme from the eigenvectors and not from the eigenvalues of the FST.

We can now extend our treatment of the empty configurations to the open-closed approximations. In the open-closed approximations, the FST becomes a nonlinear transformation whose matrix elements are given by Eq. (4.29), where the $M_{i,j}^{\mathrm{cl}}$ are the matrix elements for closed boundary conditions in which we now include the effect of the empty configuration. The terms $M_{i,j}^{\mathrm{op}}$ are the matrix elements computed with open boundary conditions. They are not affected by the empty configurations, and therefore they remain the same as in the usual calculation. In this case, the fixed point is also $\mathbf{C}^*=(0,0,1)$. However, it is not possible to linearize the system around the fixed point; so we have to compute the asymptotic values of $\tilde{C}_1$ and $\tilde{C}_2$ by process of numerical iteration.

The FST extended scheme has been applied to DLA and the DBM in two dimensions, and the effect of the inclusion of empty configurations for the calculation of fractal dimension is of the order of 1%. This confirms the arguments that empty configurations play, in general, a minor role. It is important to note, however, that this effect can be studied in a quantitative way within the FST framework, showing that the method can be systematically extended to study higher-order effects up to a desired level.

F. Asymptotic scale-invariant dynamics

We have seen that correlation properties calculated with the FST can be related to asymptotic properties and fractal dimension only by using scale-invariant dynamics. For usual critical phenomena, like percolation or Ising-type models, the problem of the asymptotic growth rule is relatively simple. Let us consider the case of the bond percolation model. The scale-invariant growth rule can be easily found through a renormalization procedure. The asymptotic scale-invariant growth probabilities will be given by the fixed point of the renormalization equation of the critical parameters (see Sec. V.B).

The percolation fixed point is repulsive. This means that self-similarity in the thermodynamic limit is ensured only at p_c, and the problem is therefore not *self-critical.* This discussion can be extended to all usual critical phenomena in which the critical parameters are well known. For this reason we shall begin to apply, in the next section, the FST to Hamiltonian equilibrium problems like percolation and Ising or Potts clusters. For Laplacian fractal growth models, the identification of the scale-invariant growth rule is appreciably more complex. We show in Sec. VII how to address this question for DLA and the DBM by deriving some general results about asymptotic dynamics.

V. APPLICATIONS OF FIXED-SCALE TRANSFORMATION TO HAMILTONIAN EQUILIBRIUM PROBLEMS

A. Critical fluctuations and fractal growth

In this section we begin to show specific applications of the FST method. We start with the fractal properties of clusters generated by critical fluctuation of equilibrium problems like percolation, Ising, Potts, polymer statistics, etc. Most of the properties of these models are well known, so they represent an important test for the FST method. Actually, we shall also be able to compute some exponents that were never before computed with standard methods.

The problems discussed in this section represent, therefore, the common area between the FST and the usual theoretical methods. In addition, they are interesting as relatively simple examples in which the FST approach can be implemented in a systematic way.

For these equilibrium properties, the FST allows us to compute the fractal dimension of the clusters generated

exactly at the critical point. This method cannot be used to compute the exponents that characterize the approach to the critical point for which the renormalization group is unavoidable. On the other hand, the FST method can naturally be applied to irreversible-growth models like DLA and similar ones for which the RG is instead problematic.

The basic strategy will be to turn an equilibrium problem into a dynamical fractal-growth process. One has then to identify the scale-invariant dynamics. This consists in determining the scale-invariant form of the Hamiltonian and then finding the value of the nonuniversal critical parameters. For example, for percolation, the scale-invariant dynamics is given by the critical probability p_c, while for Ising, by the critical temperature T_c. From these nonuniversal critical parameters, the FST method allows us to compute directly the universal exponent that characterizes the fractal dimension of the critical clusters. The accuracy will be of the order of that by which the nonuniversal parameters are known. If these are known exactly, an accuracy of the order of 1% for the fractal dimension can be easily achieved.

B. The percolating cluster

Percolation on a lattice consists of assigning an occupation probability p to each bond (or site) and studying the resulting structure as a function of p (Stauffer, 1985). Below a critical probability p_c, one observes isolated clusters of connected bonds (or sites); above p_c, an infinite continuous network of bonds (or sites) develops; while exactly at p_c, one has a critical behavior characterized by one infinite connected cluster, the percolating cluster, and many other finite clusters. The value of p_c can be easily found through a renormalization procedure like the one shown in Fig. 20, in which occupied bonds are denoted by a thick line and empty bonds by a thin line. Considering a configuration of five bonds, we see that it renormalizes into an occupied bond if it is vertically connected. Otherwise it renormalizes into an empty bond (Fig. 20). The renormalization transformation for the bond occupation probability p can be easily computed as

$$p' = 2p^2(1-p)^3 + 8p^2(1-p)^2 + 5p^4(1-p) + p^5 . \qquad (5.1)$$

From this relation one can see immediately that scale invariance is only guaranteed by the nontrivial fixed point $p_c = 0.5$. In this case this result is even exact, but this should be considered as fortuitous. One can also see that this fixed point is repulsive. This means that if we start with $p < 0.5$ at the microscopic scale and look at larger and larger boxes, the occupation probability for these boxes will go to zero. This implies the existence of a p-dependent characteristic length above which no scale-invariant growth rule exists. In practice, this means that only finite clusters can be formed. The opposite will happen if $p > 0.5$. In such a case, above a characteristic length scale, the invariant growth rule will correspond to the occupation of all the coarse-grained bonds, leading therefore to a compact structure. Therefore this problem is *not self-critical* and, in order to get a fractal structure, it needs the fine-tuning of the critical parameter p_c. The fractal properties can be properly defined for the percolating cluster, and this will be the object of our studies. In two dimensions the exact value of the fractal dimension of the percolating cluster $D = 91/48 = 1.8958\ldots$ has been derived by conformal mapping methods (den Nijs, 1979, 1983).

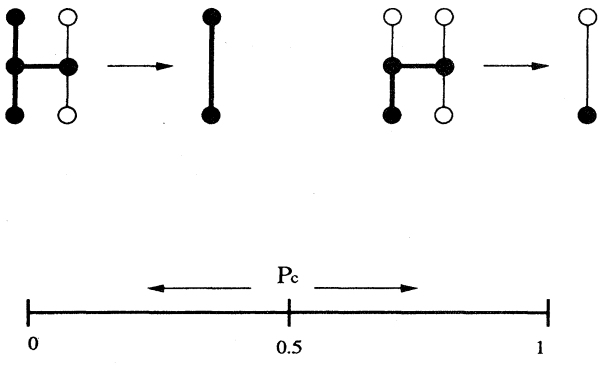

FIG. 20. Renormalization procedure for studying the scale-invariant growth process for percolation. In (a) the connected structure renormalizes into a connected bond, while in (b) the structure is not connected and renormalizes into an empty bond. In the case of percolation, the scale-invariant growth process is characterized by the repulsive fixed point p_c, which is the nonuniversal critical value of the percolation probability.

1. Fixed-scale transformation application to the percolation problem

In order to apply the FST to the percolation problem, it is most convenient to define a dynamic growth process that generates the percolating cluster. This can be achieved by the following process (Vicsek, 1992). Given a starting configuration of sites (even a single one) connected by occupied bonds, one considers all the bonds of the perimeter of this structure. For each bond a stochastic process takes place (only once); with probability p, the bond becomes part of the structure, while with probability $(1-p)$ it will be empty forever. It is easy to see that a cluster generated by this dynamic process has the same statistical weight as in the percolation process (Vicsek, 1992). One should note, however, that even for $p = p_c$ it is not obvious that this process will generate the infinite percolating cluster. There is, in fact, a finite probability (strictly equal to 1, for $p \leq p_c$) that this growth process will generate a finite cluster. Since the fractal dimension is well defined only for the infinite cluster, we must complement this growth process with a condition of *connectivity* in order to make sure that we are actually dealing with the infinite cluster. In the following, we shall consider two different ways of implementing this connectivity condition.

Once the percolation problem has been cast in the form of a dynamical process, the first problem is the identification of the scale-invariant dynamics. From the discussion of the general structure of scale-invariant growth dynamics of Sec. VII, we can see that we should consider the bond version of the model. Site percolation would, in fact, evolve into bond percolation under scale transformation. The scale-invariant dynamics corresponds to the value of the occupation probability that is the same at any level of coarse graining. This can be determined using the simple renormalization scheme previously discussed. In general, however, one should identify the correct symmetry of the scale-invariant dynamics and fix the value of p_c by any method, even a numerical one.

If the value of p_c is known only approximately, the same accuracy will be reflected in the value of D. Note that this is a completely different perspective from that of the RG methods. There the universal exponents are, in fact, defined by the derivative of the RG transformation at the nonuniversal fixed point p_c. In the FST, one starts from the value of p_c and finds the exponents via the fixed point of the iteration that corresponds to the dynamical evolution at the same scale. Since p_c corresponds to the scale-invariant dynamics, the FST fixed point applies to any scale and, therefore, one can relate it to the fractal dimension.

We have seen in Sec. IV.B that the FST is defined via the matrix elements $M_{i,j}$ that give the probability that a configuration of type i will be followed, in the growth direction, by a configuration of type j. For growth in two dimensions (as in the present case), there are only two configurations ($i,j=1,2$). Type 1 corresponds to a pair of sites in which one is occupied (black) and the other is empty (white), while type 2 corresponds to both sites being occupied (black). Note that since we are going to use scale-invariant dynamics, a "site" refers to a general level of coarse graining and not necessarily to the minimal scale.

In practice, in order to compute $M_{1,2}$, one starts with a frozen configuration of type 1 (enclosed in boxes in Fig. 21) and studies the probability that, asymptotically, the following configuration in the growth direction will have both sites occupied. No growth process is considered within the starting configuration because the matrix elements refer to the conditional probability that, *given* a certain configuration, this will be followed by another configuration.

The case shown in Fig. 21 refers to open configuration with respect to boundary conditions (see Sec. IV.D) in the sense that there is no nearby side branch to the structure being considered. We intend to describe the growth with respect to the infinite (connected) percolating cluster, and the growth probability is considered only within the column above the starting (boxed) configuration. One way to implement the condition of connectivity is to assume *a priori* the existence of an occupied line of points above the occupied site of the starting configuration. This assumption is sometimes used also in numerical simulations of dynamic or epidemic percolation (Vicsek, 1992). Later, we shall implement the connectivity condition with a different method, and the results will be very similar for the two methods.

The first nontrivial growth process considered is shown by the arrow in the top configuration of Fig. 21. This bond will be occupied with a probability $p=0.5$ (we omit

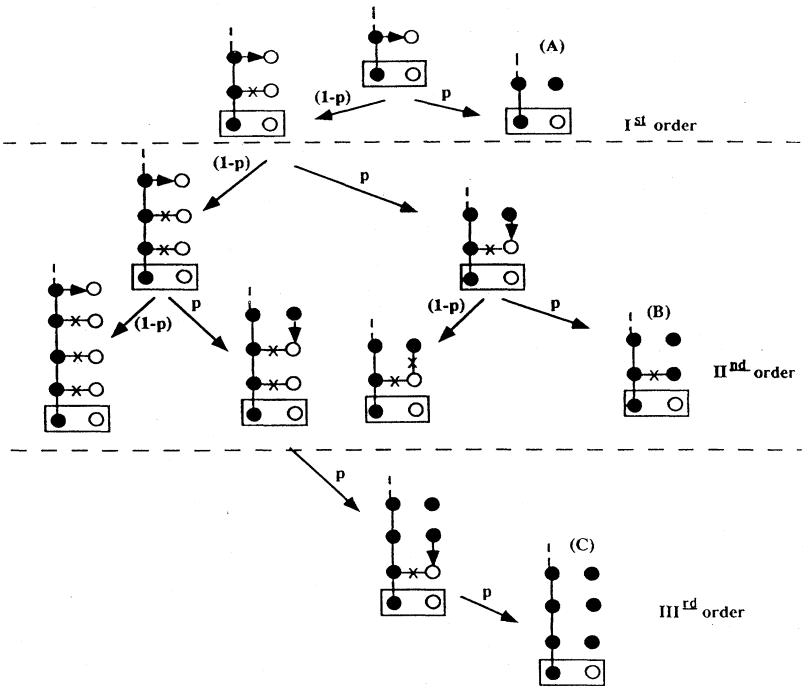

FIG. 21. Scheme of the probability tree for the case of open boundary conditions and on starting configuration of type 1. The connectivity condition is implemented in this case by a pre-existing line of occupied sites above the starting configuration.

the index c for simplicity). This will lead to a configuration of type 2 following the starting one of type 1. In the opposite case, with probability $(1-p)$, the bond does not become occupied, and it will remain empty forever. In this case the bond will be denoted by a cross. The order of the calculation is defined by the number of different arrows that are necessary to reach the initially empty site above the starting configuration. The events that lead to the occupation of this site up to third order are shown in Fig. 21. The corresponding matrix elements are

$$M_{1,2}^{\mathrm{op}}(\mathrm{I})=p=0.5\ , \tag{5.2}$$

$$M_{1,2}^{\mathrm{op}}(\mathrm{II})=p+(1-p)p^2=0.625\ , \tag{5.3}$$

$$M_{1,2}^{\mathrm{op}}(\mathrm{III})=p+(1-p)p^2+(1-p)^2p^3=0.65625\ , \tag{5.4}$$

where the index op refers to the open boundary conditions, and the roman numeral in parentheses refers to the order of the calculation.

In a similar way, one can compute the dynamical evolution conditional to a starting configuration of type 2. The corresponding figure and details can be found in Pietronero and Stella (1990). The matrix elements are, in this case,

$$M_{2,2}^{\mathrm{op}}(\mathrm{I})=p+(1-p)p=0.75\ , \tag{5.5}$$

$$M_{2,2}^{\mathrm{op}}(\mathrm{II})=M_{2,2}^{\mathrm{op}}(\mathrm{I})+(1-p)^2p^2=0.8125\ , \tag{5.6}$$

$$\begin{aligned}M_{2,2}^{\mathrm{op}}(\mathrm{III})&=M_{2,2}^{\mathrm{op}}(\mathrm{II})+(1-p)^3p^3+(1-p)^3p^4\\&\quad+(1-p)^4p^4+(1-p)^4p^5+(1-p)^4p^3\\&=0.849605\ .\end{aligned} \tag{5.7}$$

If we limit our analysis to the case of open boundary conditions, we have all the elements for computing fractal dimension. In this simple case, the fixed point of the FST is given by (see Sec. IV.B)

$$C_1^*=\left[1+\frac{M_{1,2}}{M_{2,1}}\right]^{-1}\ , \tag{5.8}$$

from which one can compute

$$D=1+\frac{\ln\langle n\rangle}{\ln 2}\ , \tag{5.9}$$

where

$$\langle n\rangle=C_1^*+2C_2^*\ . \tag{5.10}$$

In this way we obtain

$$D^{\mathrm{op}}(\mathrm{I})=1.7370\ , \tag{5.11}$$

$$D^{\mathrm{op}}(\mathrm{II})=1.8044\ , \tag{5.12}$$

$$D^{\mathrm{op}}(\mathrm{III})=1.8588\ . \tag{5.13}$$

The third-order result [Eq. (5.13)] is already reasonably close to the exact result $D=91/48=1.8958\ldots$. It should be noted that the results of this scheme, with only open boundary conditions, are strictly *lower bounds* with respect to the exact value. In fact, in this case we have an exact characterization of the scale-invariant dynamics from the value $p_c=0.5$. So the approximations come only from the FST scheme. Therefore, going to higher order in the calculation can only increase the value of the fractal dimension, because it provides new paths for reaching configuration 2. In addition, the use of open boundary conditions also corresponds (in this case) to a lower limit for D, because closed boundary conditions would provide extra paths for reaching configuration 2.

The present scheme with a single type of boundary condition (open) provides an accuracy that is of the order of RSRG schemes. Within the FST we can, however, easily improve the accuracy by considering additional boundary conditions. A very convenient scheme in this respect is the open-closed approximation discussed in Sec. IV.D. In this scheme, one considers in a self-consistent way only two types of boundary conditions, the open one that we have discussed and the closed one in which the considered structure is immediately followed on the right by an extra branch. Actually, for percolation, this is a very good approximation, because boundary conditions of intermediate type would contribute at only very high order.

In order to implement the open-closed scheme, one must therefore also compute the matrix elements for the case of closed boundary conditions. The calculation is similar to the case of open boundary conditions, the only difference being that one must also include the processes in which the type 2 configuration is reached via a path that originates from the extra branch. The effect is therefore to enhance the values of $M_{1,2}$ and $M_{2,2}$ with respect to the corresponding values of the open-boundary-condition situation. The details of the calculation can be found in Pietronero and Stella (1990); here we only report the values of the fractal dimension at various orders,

$$D(\mathrm{I})=1.7370\ , \tag{5.14}$$

$$D(\mathrm{II})=1.8643\ , \tag{5.15}$$

$$D(\mathrm{III})=1.8830\ . \tag{5.16}$$

The value of the most accurate result [D(III)] is now in very good agreement with the exact value, $D=91/48=1.8954$. This shows the importance of the fluctuations of the boundary conditions that, when properly included, can make real-space methods very accurate.

2. Alternative connectivity conditions

We return to the problem of the connectivity condition, which in the previous calculation was ensured by the assumption of a starting line of occupied points. It is actually possible to implement this condition by employing a different method which leads to results that are extremely close to the previous ones. This consists of considering that the starting configuration should be con-

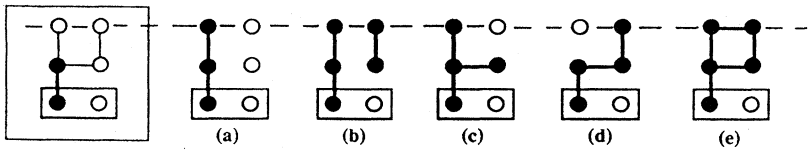

FIG. 22. Calculation of second-order matrix elements with a different connectivity condition. In this case connectivity is guaranteed by the fact that we only consider the connected configurations with their statistical weight. Only cases (c), (d), and (e) contribute to $M^{\rm op}_{1,2}$.

nected to a line at a certain distance; this distance now corresponds to the order of the calculation. For example, Fig. 22 shows the case of open boundary conditions with a starting configuration of type 1. We then consider the possible configurations that connect the starting structure to a dashed line at a distance of two bonds. In this sense the case shown corresponds to a second-order calculation. As one can see in the left-hand structure (boxed) of Fig. 22, the bond above the starting black site must be occupied, otherwise the structure cannot be connected. Therefore we must consider only the three bonds denoted by the three thin lines. This gives a total of eight configurations, but of these we consider only those five that connect the starting structure with the final line. For a configuration with n occupied bonds and n' empty ones, this probability is $p^n(1-p)^{n'}$. Since in our case $p=p_c=0.5$, the statistical weight is the same for all the configurations.

Looking now at the five connected configurations shown in Fig. 22, we can see that the configurations that contribute to the matrix elements $M_{1,2}$ are only (c), (d), and (e). In fact, (a) leaves an empty site above the starting configuration; and (b) leads to two separate clusters, so the two occupied sites on the right-hand side will not be part of the percolating cluster. We have therefore

$$M^{\rm op}_{1,2}({\rm II})=\frac{3}{5}=0.6\ . \tag{5.17}$$

TABLE I. Fractal dimension and critical exponents of structures generated by equilibrium critical phenomena computed with the FST method. The results are compared with the existing simulations or exact estimate values (for the reference of each result, see text).

Model	D exact	D simulation	D FST (best estimate)
Percolation ($d=2$)			
percolating cluster:	91/48=1.8958		1.8914 (test for
square lattice			universality)
triangular lattice			1.8710
backbone		1.647(0.001)	1.60
chemical distance		1.17(0.01)	1.17
Ising and Potts models ($d=2$)			
Clusters:			
$q=2$ (Ising)	187/96=1.9479		1.9570
$q=3$	153/80=1.9125		1.9181
$q=4$	15/8=1.875		1.8841
Droplets:			
$q=2$ (Ising)	15/8=1.875		1.8414
$q=3$	28/15=1.8666		1.7817[a]
$q=4$	15/8=1.875		1.7525[a]
Self-avoiding polymer[b]			
$d=2$	0.75		0.745
$d=3$		0.58(0.01)	0.592
Lattice animals[b]			
$d=2$		0.641(0.001)	0.644

[a]Simplified scheme.
[b]The values reported refer to the exponent $\nu=1/D$.

By repeating this analysis starting with a configuration of type 2, we obtain

$$M^{op}_{2,2}(\mathrm{II})=\frac{12}{16}=0.75\ . \tag{5.18}$$

If we shift the final line to a distance of three bonds from the starting configuration, we can compute the matrix elements up to third order. By performing the same calculations for closed boundary conditions, we obtain, in the open-closed approximation,

$$D(\mathrm{II})=1.8182\ , \tag{5.19}$$

$$D(\mathrm{III})=1.8914\ . \tag{5.20}$$

Note that in this case the order here has a different meaning than in the previous calculation. Nevertheless, the best value [Eq. (5.26)] is quite close to the best value of the previous scheme [Eq. (5.22)], and both are in very good agreement with the exact value.

3. Percolation on the triangular lattice

Previously we computed the fractal dimension of the percolating cluster in two dimensions using as input the topology of the lattice and the value of the bond percolation threshold for the square lattice $p_c=0.5$. Since fractal dimension is expected to be a universal quantity, the application to bond percolation problems with different lattice topologies, and thus different p_c, is an important test of the potential of the method. For the triangular lattice the bond percolation threshold has a value, $p_c=0.34729$, very different from the value for the square lattice. Universality implies that by changing the lattice topology and the associated value of p_c, one should recover the same result for the fractal dimension D. The FST method can also be implemented for the triangular lattice (Pietronero and Stella, 1990), and the results are shown in Table I and Fig. 23.

By comparing these results to those of the square lattice, one can see that, despite the nonuniversal values of p_c being different by more than 30%, the values of D at third order differ by only about 1%. This provides strong support for the FST method in identifying universal exponents using as input the value of the nonuniversal critical parameter p_c and the topology of the lattice.

4. Topological properties: Backbone and chemical distance

In addition to the fractal dimension of the entire percolating cluster, different fractal dimensions have been identified for important topological properties. For example, the chemical distance corresponds to the most direct path (topologically one dimensional) within the percolating cluster. This path appears to be relevant, for example, for the structure of river networks, and its fractal dimension has been determined numerically to be

$$D_{\min}=1.17\pm0.01\ . \tag{5.21}$$

The backbone corresponds instead to the set of sites (or bonds) that are connected by occupied bonds to both edges, by two paths that have no edge in common. Essentially, it consists of those sites through which current would flow were the two edges of the percolating cluster subject to a potential difference. The most accurate numerical determination of the fractal dimension of the backbone gives (Grassberger, 1992)

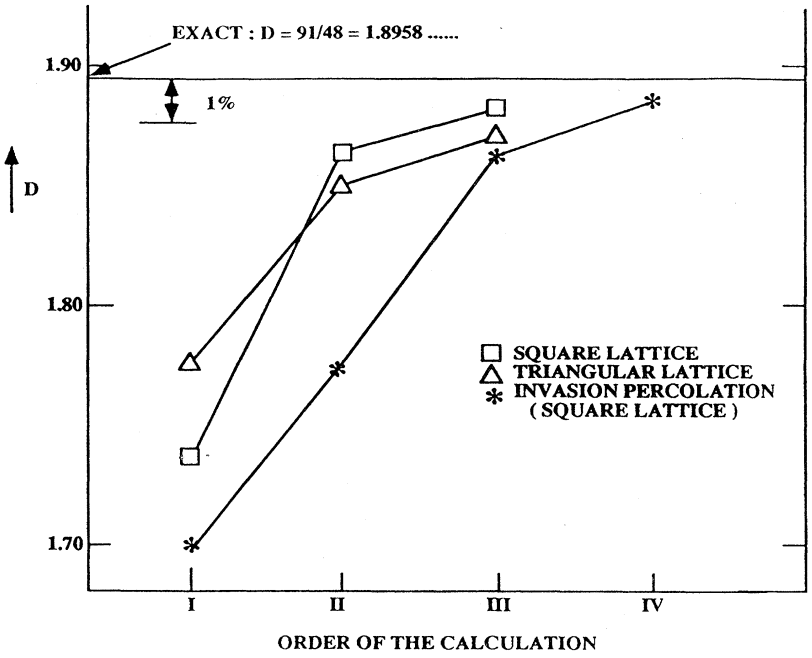

FIG. 23. Values obtained with the FST method for square, triangular, and invasion percolation (Sec. VI) as a function of the order of the calculation. This picture gives some idea about the accuracy and the convergence properties of the method.

$$D_b = 1.647 \pm 0.004 \ , \tag{5.22}$$

and it is in agreement with other studies (Rintoul and Nakanishi, 1992).

Up to now there has been no analytical approach (to our knowledge) for computing the fractal dimensions of the chemical distance and of the backbone. The FST method can also be applied naturally to these topological properties. This can be easily done by considering diagrams like those shown in Fig. 22 (complemented by a few others) but defining the distribution (C_1, C_2) only for those sites or bonds that in these diagrams correspond to the chemical distance or to the backbone, respectively.

For the chemical distance, we obtain (Pietronero and Schneider, 1995; Pietronero *et al.*, 1995)

$$D_c = 1.17 \ , \tag{5.23}$$

while the FST result for the backbone is

$$D_b = 1.60 \ . \tag{5.24}$$

These results are in good agreement with the numerical values and show that these topological problems can be easily approached within the FST scheme.

C. Ising and Potts clusters

The fractal dimension D of the Ising clusters, i.e., the connected clusters of sites with identical spins, has been a controversial issue for a long time. Recently, it was shown (Coniglio, 1989; Duplantier and Saleur, 1989; Stella and Vanderzande, 1989) that the exponents describing Ising clusters at the critical point are those of the $q=1$ Potts model at its tricritical point, with the exact value $D = 187/96 = 1.9479$ in good agreement with numerical estimates. Later, the exact values of the fractal dimension for the Potts clusters with $q=3$ and $q=4$ were also conjectured from conformal mapping arguments (Vanderzande, 1992).

The FST method can be applied to compute the fractal dimensions of Ising and Potts clusters, and the calculation can be extended in a natural way to "droplets" (Coniglio and Klein, 1980; Coniglio and Peruggi, 1982). More details about FST calculations can be found in Erzan and Pietronero (1991).

The first step in the FST scheme is usually the identification of the scale-invariant dynamics. Here we are not using the dynamics directly; rather we are presenting an Ornstein-Zernike-like expansion (Stell, 1987) for the matrix elements of the FST at a generic length scale, where in place of the direct correlation function there appear the correlation functions computed over the NN bonds connecting a site to occupied neighbors. For the scale-invariant statistical properties, we take the bare value of the critical NN coupling (given in essence by the critical temperature), but renormalize the NN correlations by summing over different connecting paths. It can be argued that this procedure takes into account some features of the proliferation one would expect when dealing with coarse-grained variables (Erzan and Pietronero, 1991).

It is important to note that the fractal object in which we are interested is described in terms of a new set of lattice-gas variables whose statistics *are not the same as those of the original spin system,* although determined by it in a way which we shall discuss later. Since we are considering the system at a generic length scale, an "occupied site" in a region at that particular length scale contains a connected part of the cluster of up-spins. Conversely, an "empty site" may contain any number of up-spins which, however, are bounded away from the connected cluster by a number of down-spins. Thus, in this coarse-grained picture, the absence of a bond will signal an "empty" site, on the other hand, and *not* a down-spin, which is important for the correct weighting of the ensuing configurations.

It should be noted that in the present case a configuration of type 1 consists of an occupied site (belonging to the cluster) and an "empty" one in the sense discussed above. We would like to compute the probability $M_{1,2}$ or $M_{2,2}$ that the "empty" site will finally be occupied. Here we take p_k to be the conditional probability for a site to be "up" (belonging to the cluster). It is worth remarking that in this case we have the formation of "empty" sites (absence of bonds) that do not belong to the cluster, but these should not necessarily be considered "down" spins. Therefore the subsequent probability for the occupation of neighbor sites must be computed keeping in mind that these are not down-spins. We can make a simple estimate of p_k, neglecting all but the NN correlations,

$$p_k = \frac{e^{kK_c}}{e^{kK_c} + e^{-kK_c}} \ . \tag{5.25}$$

Here the Ising Hamiltonian is $-H/k_BT = K\sum_{\langle ij \rangle}\sigma_i\sigma_j$, $\sigma_i = \pm 1$, and the Onsager critical point is $K_c = \frac{1}{2}\ln(\sqrt{2}+1)$. In this way we can evaluate the matrix elements (Erzan and Pietronero, 1991) and obtain, by using the lowest-order results,

$$D_{\rm op} = 1.9262 \ . \tag{5.26}$$

One can then include the effect of different boundary conditions (i.e., also closed) and also consider large diagrams in which more correlations can be included, in order to test the convergence of the calculations (Erzan and Pietronero, 1991). It is possible to generalize this approach to the q-state Potts model, in which a cluster refers to a connected configuration of identical spins, and to the case of "droplets." The details of these calculations and the extension to the open-closed scheme can be found in Erzan and Pietronero (1991). Some of the numerical results will be discussed in Sec. V.E.

D. Polymers and lattice animals

There are mainly two different classes of polymers: linear and branched (de Gennes, 1979). In the presence

of a good solvent, the statistics of linear polymers with excluded volume is equivalent to a self-avoiding walk (SAW) on a lattice. If the constituent monomers have three or more functional groups, branched molecules can form, and the statistics of such polymers is more complex and usually described by Lattice Animals (LA) models (Stanley *et al.*, 1982). These systems are seen to have the asymptotic properties of self-similarity when considered at their critical point, i.e., in the limit of infinitely long chains. Within a Grand Canonical context, the self-similarity of the system is automatically guaranteed by fixing the step fugacity k at its critical value k_c. When k is equal to k_c, there is no characteristic cluster size, and we are at the critical point. Here we define as a cluster the connected configurations of monomers. The average end-to-end distance diverges as

$$\xi(k) \sim (k - k_c)^{-\nu} . \tag{5.27}$$

The average number of monomers in a cluster $\langle N \rangle$ can be related to its size ξ by (Vicsek, 1992)

$$\langle N \rangle \sim \xi^{1/\nu} \sim \xi^{D} . \tag{5.28}$$

The application of the FST to these models requires the knowledge of the critical fugacity, and it follows the strategy used in percolation or Ising clusters. As for the percolating cluster, we must ensure the infinite connectivity of the critical configuration; i.e., the starting configuration must be connected to a line at a certain distance, now corresponding to the order of the calculation. Each configuration has a statistical weight given by k_c to the power of the number of bonds in the configuration. The scheme of calculation for LA is more complex than that for the SAW. In this case the configurations may branch or have loops, and the growing site may not be unique. This complication leads to the need for introducing the fluctuations of the boundary conditions and for setting up the full scheme of the FST framework. In order to test the convergence of the method, we performed calculations up to third order (for details, see Di Stasio *et al.*, 1994) that give the results shown in Table I. Again, these results are in very good agreement with numerical simulations (Watts, 1975; Derrida and Stauffer, 1985).

E. Summary of the fixed-scale transformation results for Hamiltonian problems

In this section we have considered the application of the FST to compute the fractal dimension of clusters generated at the critical points of classical Hamiltonian problems. The properties of these models are often well known; so these studies represent an important test for the FST method. The main results are summarized in Table I, and we can see that the accuracy of the FST results is typically of the order of 1 or 2%. This is much better than the usual accuracy of real-space methods. The origin of this systematic improvement can be found in the fact that in the FST, one does not change scale; so the final object of the calculation concentrates essentially on the asymptotic conditional occupation probability of a single point. This allows a detailed treatment of the various configurations, including the self-consistent description of different boundary conditions. This is usually impossible in RSRG, because the object of the calculation is a cell with several sites. In this respect it has recently been shown that the inclusion of different boundary conditions in RSRG gives rise to an appreciable improvement of the results (White and Noack, 1992). This shows that real-space methods can become very accurate if the appropriate scheme is chosen.

As a test of its systematicity, it is important to note that the FST method also has *predictive* power. In our studies of the Ising and Potts clusters (Erzan and Pietronero, 1991), we could easily compute the fractal dimension for Potts clusters in two dimensions for $q=2$, 3, and 4 reported in Table I. At the time of these calculations, there were no analytical or numerical values to use for comparison. After about one year, however, Vanderzande (1992), using conformal mapping arguments, conjectured the exact values for these fractal dimensions, shown in Table I. As one can see, the agreement between the FST results and the (conjectured) exact ones is extremely good even when the FST results were obtained before.

Even though Table I refers to standard Hamiltonian models, several cases—like the backbone and chemical distance for percolation and some of the Potts clusters and droplets—have never been studied with RG methods.

VI. APPLICATION TO SIMPLE DYNAMICAL PROBLEMS

A. Directed percolation

Directed percolation (Kinzel, 1983) is a prototypical model for a wide range of spatially extended dynamical systems like epidemic models and birth-death processes (Grassberger, 1986), contact processes, or interacting particle systems (Schløgel, 1972; Dickman, 1986). It falls into a universality class distinct from ordinary percolation (Kinzel, 1983). At its critical point it can be shown to have the same asymptotic scaling behavior as Reggeon field theory (Grassberger and de la Torre, 1979; Cardy and Sugar, 1980).

Directed percolation (DP) can be defined by considering random graphs consisting of occupied and empty edges embedded in a d-dimensional hypercubic lattice. The order parameter is the probability of encountering spanning paths such that all the nearest-neighbor links belonging to the path are oriented in one of the positive lattice directions. Below a critical concentration p_c of occupied edges, the probability of finding spanning paths goes to zero, with $p_c > p_c^{\text{perc}}$.

This problem can be cast as a dynamical process

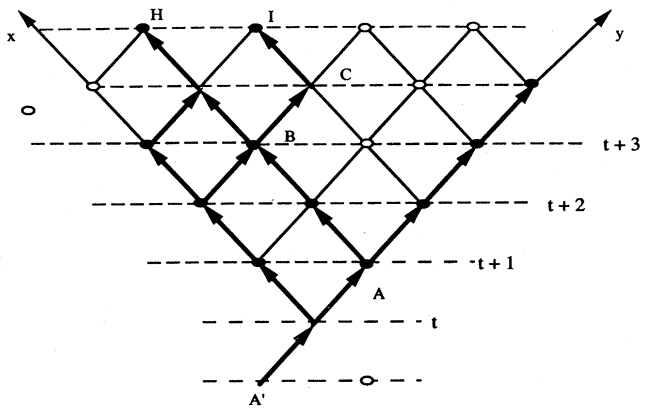

FIG. 24. Part of a connected directed-percolation cluster seen as a dynamical object. Each site may persist to the next time step or disappear. It may also give rise to a new particle at the neighboring site along the positive y direction. At times $t, t+1, \ldots, t+n$, the sets of empty or occupied sites correspond to the successive states of the dynamical system.

(Grassberger, 1986) or stochastic cellular automation (Wolfram, 1983), in $d-1$ dimensions. Each occupied vertex at time t may give rise, at time $t+1$, to at most $2(d-1)$ daughters, each independently with probability p. No spontaneous creation can occur; thus the empty state is the absorbing state. Above a critical threshold p_c, there is a finite probability that the "active" state will be maintained indefinitely.

Of all the examples considered in this review, DP for $d=2$ is the simplest, since the fractal set under consideration consists of the states of a one-dimensional dynamical system. The stationarity condition is simply the requirement that this set remain statistically similar to itself in time (see Fig. 24). (One-dimensional versions of all the other models considered in this review happen to be trivial, in the sense of yielding compact sets.) The FST to the Nth order now connects one state of this one-dimensional dynamical object with another state removed from the first by N time steps (see Figs. 25, 26). This is similar to the framework within which alternative connectivity conditions are implemented in Sec. V.B.

The initial configurations of *type 1* (Fig. 25) may be right or left occupied with equal probability; in each case we first enumerate all nonbranching paths originating in the initial cell and terminating in the corresponding cell at t_{0+N}. These paths are the possible "backbones" whose respective weights are assigned thus: the first link in the backbone is placed with uniform probability in all the different possible positions; then each subsequent step is weighted with $1/v_k$, where v_k is the valence of the vertex encountered at the kth step (Erzan and Pietronero, 1992).

From an examination of Fig. 27, the lowest-order matrix elements $M_{1,2}$ for open and closed boundary conditions are found to be

$$\begin{aligned} M_{1,2}^{\mathrm{op}} &= 1/2p \ , \\ M_{1,2}^{\mathrm{cl}} &= 4/5p - 1/4p^2 \ . \end{aligned} \tag{6.1}$$

Those for an initial cell of *type 2* are

$$\begin{aligned} M_{2,1}^{\mathrm{op}} &= 1-(4/3p-1/3p^2) \ , \\ M_{2,1}^{\mathrm{cl}} &= (1-p)^2 \ . \end{aligned} \tag{6.2}$$

Using the probabilities for encountering open and closed boundary conditions and substituting $p_c=0.644071$ (Baxter and Guttman, 1988; Essam *et al.*, 1988; ben Avraham *et al.*, 1991), we find the fractal dimension D' of the set of active sites of the one-dimensional dynamical system defined above to be

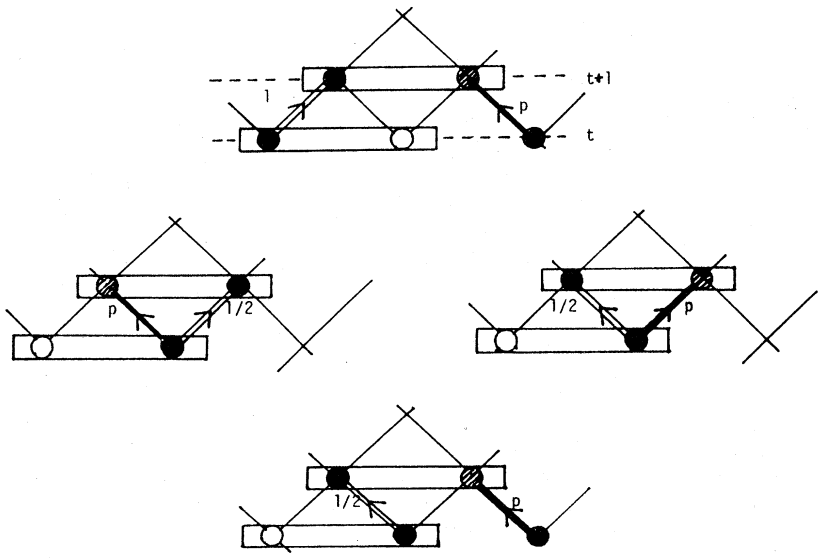

FIG. 25. Graphs, with their respective weights, for the matrix element $M_{1,2}$ of the FST in the lowest order (see text). The backbone is shown as a double bond; the target site is shaded. The graph is further decorated by arrows placed on lines emanating from occupied vertices, each independently, with probability p (and blacking them with probability $1-P$). Vertices at which no bonds terminate are empty, and lines emanating from empty vertices are empty with probability 1.

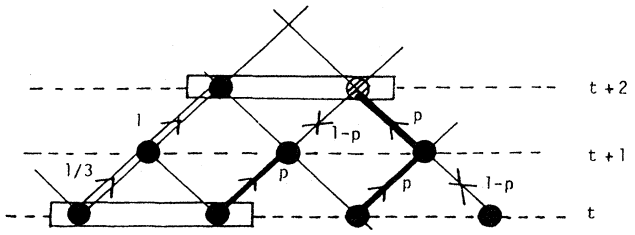

FIG. 26. Graph contributing to $M^{1;1}_{2,2}$. The total probability that the target site will be reached from at least one of the two occupied neighboring sites at t is $p^{(e)}$. Only one of the possible paths is displayed.

$$D'^{(I)}=0.8251\ , \tag{6.3}$$

$$D'^{(II)}=0.7435\ , \tag{6.4}$$

$$D'^{(III)}=0.74655\ , \tag{6.5}$$

for the various orders. For details, see Erzan and Pietronero (1992).

Now recall that D' corresponds to the fractal dimension of transverse sets of occupied points in the DP problem in $d=2$ and is related to the known DP exponents via $D'=1-\beta/\nu_\perp$, where β and $\nu_\perp$ are, respectively, the order-parameter exponent and the exponent for the "transverse" correlation length $\xi_\perp$. The best known series results for these quantities (Baxter and Guttman, 1988; Essam *et al.*, 1988) yield $D'=0.748$.

Directed percolation seen as a birth-death process will be discussed again in Sec. X, within a Fock-space formalism. The matrix elements can then be seen explicitly as sums over directed paths.

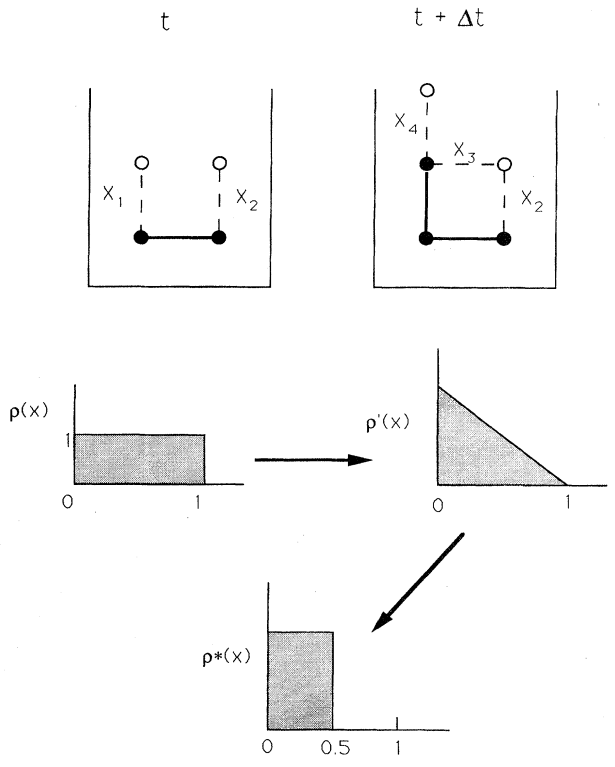

FIG. 27. Example of the *quenched-stochastic* transformation in the case of invasion percolation. In the lower part is shown how the original distribution for variables of the perimeter bonds evolves asymptotically (for details, see text).

B. Invasion percolation

Invasion percolation (IP) was introduced as a dynamical model to simulate the displacement of one fluid by another in a porous medium (Chandler *et al.*, 1982; Wilkinson and Willemsen, 1983; Feder, 1988). The random nature of the rock is mimicked by a quenched random distribution of bond strengths on a lattice (corresponding, say, to channel diameter), ranging uniformly between zero and 1. At any given time, the "front" proceeds one step by picking the channel with the largest diameter among all those immediately available to it, namely, the perimeter bonds. The invasion process is stopped when the fluid reaches the far boundary, or when a spanning invasion pattern is established. The invasion algorithm starting from one occupied site guarantees, as does the DP scheme, that the cluster one obtains is connected, or is the incipient infinite cluster. Once initial conditions (the position of the front at time $t=0$) are specified, the resulting invasion pattern is uniquely determined. Chayes and Chayes (1986) argue that the probability with which a bond is finally occupied or left empty is equal to 1/2, namely, the threshold value for the bond percolation problem in $d=2$, and that therefore the two problems are equivalent. They indeed turn out to have the same fractal dimension, but IP for incompressible fluids falls into a different universality class than percolation (Furnberg *et al.*, 1988). Invasion percolation represents a particularly interesting problem because its dynamics is irreversible and the critical state is self-organized. However, the final cluster is the percolating problem of standard percolation, that is a critical problem of the usual type in which one has to fine-tune the occupation probability to reach criticality.

We saw in Sec. V that it is easy to interpret ordinary percolation into a growth process and treat it with the FST. For IP, the problem is more complex because probability is not assigned per bond, but the growth process is defined by an extremal statistics that involves all the quenched random variables of the perimeter bonds. In order to apply the FST to this problem, it is necessary to define a *stochastic process* that corresponds to the *quenched averages* over all possible realizations of the random variables. We shall see how a deterministic dynamics corresponding to quenched disorder can be mapped into a stochastic one with memory (Pietronero and Schneider, 1990). Consider, for example, the growth

process shown in Fig. 27. At the beginning (left), there are two possible bonds in which growth can take place. With each of these bonds a random variable is associated, denoted X_1 and X_2, respectively. They may take values in the interval [0,1], all values being equally probable. The corresponding probability densities are given by (Fig. 27)

$$\rho_k^{(0)}(x)\equiv 1, \quad x\in(0,1) , \tag{6.6}$$

where the lower index k refers to the site and the upper one in parentheses defines the original flat distribution. Since X_1 and X_2 are assumed to be independent, the probability that $X_1 > X_2$ is given by

$$P(X_1>X_2)=\int_0^1 dx\rho_1^{(0)}(x)\int_0^x dy\rho_2^{(0)}(y)=\frac{1}{2} , \tag{6.7}$$

as required also by symmetry. Let us now assume that growth occurs at the bond with the largest random variable X_i and consider only the two bonds shown in the left part of Fig. 27. If $X_1 > X_2$, we add this bond to the structure, which assumes the configuration on the right of Fig. 27. Note that in some papers growth is defined by the minimum of the X_i. The problem is clearly symmetric, and here we stick to the maximum to be consistent with Pietronero and Schneider (1990).

In the new configuration on the upper right of Fig. 27, two new bonds appear, which are characterized by the random variables X_3 and X_4. We have no information on these bonds; so their probability distribution will be flat. The situation is different for the random variable X_2, because its distribution has already been tested by the growth process and we know that $X_2 < X_1$. This fact includes the information that we have from the growth event itself. The new distribution for X_2 is therefore conditional to the fact that $X_2 < X_1$. This leads to

$$\rho_2^{(1)}(x)=C^{-1}\rho_2^{(0)}(x)\int_0^x dy\rho_1^{(0)}(y) , \tag{6.8}$$

where the normalization constant is

$$C=\int_0^1 dx\rho_2^{(0)}(x)\int_x^1 dy\rho_1^{(0)}(y) . \tag{6.9}$$

Therefore we obtain

$$\rho_2^{(1)}(x)=2(1-x) . \tag{6.10}$$

For the configuration on the right of Fig. 27, we therefore have different distributions for the various independent quenched variables. For X_3 and X_4, we have no information; so they will correspond to the flat initial distribution. For X_2, its distribution is instead conditional to the previous growth event in which this variable was tested, and it is given by Eq. (6.10). We can now assign the growth probabilities for the new configuration on the right of Fig. 27. Let us compute, for example, that X_2 is the maximum of the three quenched variables. We start by computing

$$P(X_2>X_3)=\int_0^1 dx\rho_2^{(1)}(x)\int_0^x dy\rho_3^{(0)}(y)=\frac{1}{3} . \tag{6.11}$$

If this happens, however, the distribution of X_2 becomes conditional also to this event, and we have

$$\tilde{\rho}_2^{(1)}(x)=C^{-1}\rho_2^{(1)}(x)\int_0^x dy\rho_3^{(0)}(y) . \tag{6.12}$$

We can ask for the probability that X_2 will also be larger than X_4 once we know that it is larger than X_3. This is given by

$$P(X_2>X_4)=\int_0^1 dx\tilde{\rho}_2^{(1)}(x)\int_0^x dy\rho_4^{(0)}(y)=\frac{1}{2} . \tag{6.13}$$

Therefore the probability that X_2 will be the maximum among the three quenched variables is

$$p_2=\frac{1}{3}\frac{1}{2}=\frac{1}{6} , \tag{6.14}$$

and, analogously for the two other bonds, we obtain

$$p_3=p_4=\frac{5}{12} . \tag{6.15}$$

We have therefore transformed a process based on quenched random variables into a stochastic (annealed) process. Note that while the first process is deterministic for each realization of the disorder, the second one is stochastic in the sense that individual evolution events are independently selected from a given distribution at each time. The essential idea is that the dynamics in a random environment tests the environment itself, and it provides conditional information for the effective probability distribution corresponding to the future events. This distribution depends, then, on the entire history of the system.

The simple examples we have discussed also clarify how screening effects automatically develop in a random medium. The fact that in the first growth event the variables X_1 prevail over X_2 induces a modification in the future distribution for X_2 that makes it less likely that this bond will be favored with respect to the new ones that appear after the growth process (X_3, X_4).

Once the original quenched problem corresponding to IP has been transformed into a stochastic one, it is possible to apply the FST and to compute the fractal dimension. The first approach that essentially follows the lines of the example discussed above can be found in Pietronero and Schneider (1990). The results are reported in Table II and in Fig. 23. These results should be compared with $D=91/48=1.8958$ for percolation and IP, and $D^{\rm tr}\simeq 1.82$ for IP with trapping (Chandler *et al.*, 1982; Wilkinson and Willemsen, 1983; Feder, 1988; Furnberg and Feder, 1988; Roux and Guyon, 1989). More recently, Marsili (1994) developed and generalized this approach. Following the idea that a quenched dynamics evolves in a cognitive way, that it acquires more and more information on the random environment by testing it, one can consider the problem of the asymptotic distribution for the variables corresponding to the perimeter bonds. This implies writing a self-consistent equation for the asymptotic distribution, and the problem then becomes rather technical. It can be shown, however, that the distribution evolves spontaneously (self-

TABLE II. Fractal dimension of structures generated by dynamical models computed with the FST method. The results are compared with the existing simulations or exact estimate values (for the reference of each result, see text).

Model	D exact	D simulation or series	D FST (best estimate)
Directed percolation ($d=2$)			
Transverse dimension	591/790=0.7481 (conjectured)	0.748	0.7466
Invasion percolation ($d=2$)	91/48=1.8958 (conjectured)		1.8872
IP with trapping		1.82	1.8196
Self-organized criticality ($d=2$)			
Bulk properties of clusters		2.0(0.1)	1.9936

organization) in a step function characterized by the percolation threshold probability, as shown in the lower part of Fig. 27.

In our opinion, invasion percolation represents a very interesting model for various reasons: (i) It shows a self-organized dynamics that evolves spontaneously towards a structure that corresponds to the critical point of standard percolation; (ii) from a theoretical point of view, its treatment requires the combination of the FST with a new concept, the *quenched-stochastic* transformation; and (iii) these two elements appear easily extendible to other problems based on extremal statistics (Bak and Sneppen, 1993).

C. Sandpile models (self-organized criticality)

The sandpile and related models (Bak, Tang, and Wiesenfeld, 1987, 1988; Tang and Bak, 1988; see also Zhang, 1986 and Pietronero, Tartaglia and Zhang, 1991) are nonlinearly coupled cellular automata with random external input which are capable of reaching a steady state with interesting self-similarity properties in both space and time (Erzan and Sinha, 1991). For convenience, only a "height" model (rather than a "slope" model) will be considered here. It is defined by specifying on a two-dimensional lattice the continuous variables $E(r,t)$, which receive random inputs $0<\delta E(r,t)\leq 1$, such that

$$E(r,t+1)=E(r,t)+\delta E(r,t)\ . \tag{6.16}$$

If the value of $E(r,t)$ at any time exceeds a threshold, here chosen to be 1, then one has

$$\begin{aligned} &E(r,t)\rightarrow 0\ , \\ &E(r+\delta r,t)\rightarrow E(r+\delta r,t)+\tfrac{1}{4}E(r,t) \end{aligned} \tag{6.17}$$

at all sites r where $E(r,t)>1$. Here δr are the lattice vectors to the nearest-neighbor sites. After each addition of a packet of energy (6.16), the relaxation is deterministic, and one waits until all the excess energy has been dissipated before adding at another randomly chosen point. The region over which the relaxation events extend, after addition at a particular point, will be termed a "cluster." The boundary conditions adopted here are to set $E=0$ at the boundaries.

It is well known that in the steady state, which can be characterized by an invariant distribution $P(E)$, the clusters defined above reach a power-law distribution of sizes (Bak *et al.*, 1988), for which this state has been termed "self-organized critical" (SOC). However, they are not fractal, but compact.

By using the FST, it is possible to calculate the fractal dimension of the avalanche clusters (Pietronero and Schneider, 1991). In fact, we find for the fractal dimension the strong evidence that it eventually converges to 2:

$$D(\mathrm{I})=1.9353,\quad D(\mathrm{II})=1.9878,\quad D(\mathrm{III})=1.9936\ . \tag{6.18}$$

It is worth mentioning that recently, following a reasoning inspired by the FST framework, we developed a renormalization scheme for the sandpile model (Pietronero *et al.*, 1994; Vespignani *et al.*, 1995). This approach allows us to clarify the SOC nature of the process, to identify the universality classes of several models, and to compute analytically the various critical exponents.

In a recent paper coauthored by one of us (Hüner and Erzan, 1994), the FST was also applied to a system with continuous dynamical variables in discrete time and space, namely, a one-dimensional array of nonlinear maps with Laplacian couplings. Such a set of coupled iterated maps may be regarded as a model for a system described by partial differential equations. It exhibits a transition between an asymptotically turbulent and a laminar state, as a function of several parameters, and spatio-temporal intermittency is observed along the phase boundary. The FST approach has enabled us to compute the fractal dimension of the evolving set of turbulent sites as well as a conditional asymptotic invariant measure on the array.

Table II summarizes the FST results for the simple dynamical models discussed in this section.

VII. FIXED-SCALE TRANSFORMATION FOR DIFFUSION-LIMITED AGGREGATION AND DIELECTRIC BREAKDOWN MODEL

This is the central section of this review, because here we finally approach the problem of the calculation of

fractal dimension for DLA and the DBM. This is the question that has motivated the development of the FST approach and that is problematic to treat with the usual theoretical methods.

In order to compute fractal dimension from the FST fixed point, it is necessary that the FST refer to variables that are coarse grained at a *generic scale* and that the growth rules used be therefore valid at any scale. This problem will be discussed in detail in Sec. VII.A.

In Sec. VII.B we begin by describing the original FST approach with the DBM (bond) rules as originally developed (Pietronero *et al.*, 1988a, 1988b). In Sec. VII.D we shall use instead the renormalized growth rules in which $S^* \neq 1$. We shall see in the end that the results are rather close and lead to a reasonably systematic approach to the fractal properties of DLA and the DBM.

A. Renormalization of the dynamics for diffusion-limited aggregation and the dielectric breakdown model

1. Space of growth rules

We have seen that the asymptotic, scale-invariant-dynamics growth rules are necessary for a complete definition of the FST approach. In addition, the knowledge of this scale-invariant dynamics is one of the key points in the understanding of why growth models give rise to fractal structures. For fractal-growth models like DLA and DBM, this problem is very complex, and a complete and satisfactory understanding has not yet been achieved. This is due to the high number of parameters of the renormalized dynamics of these highly nonlocal models. However, we shall see that (i) increasingly better schemes of renormalization show nontrivial fixed points with similar properties: and (ii) a key parameter for the renormalization of the growth rules is, in our opinion, the effective noise reduction for which we shall present a detailed renormalization study.

TABLE III. Fractal dimension of DLA clusters grown using different types of growth rules (p_s, sticking probability; $o-l$, off-lattice; p_d, diagonal coupling).

Model	D
$P_s=0.25$	1.72±0.06
$o-l$	1.71±0.07
Pd	1.72±0.05

DLA and the DBM are intrinsically critical models in the sense that their dynamics evolves under scale transformation into the asymptotic scale-invariant ones without the tuning of any parameter. The scale-invariant properties of this effective asymptotic dynamics are responsible for the scale-invariant structures generated by these models. The problem is, then, to find the effective dynamics (growth rules) that apply to coarse-grained variables in the scale-invariant, asymptotic regime. In order to address this question, we introduce the *space of growth rules,* in which each point represents a given growth rule (dynamics). In practice, one can consider a subset of these parameters and study their evolution under scale change. The scale-invariant growth rule will be indicated by the fixed point of the RG transformation that acts on the parameters of this space. The existence and nature (stable as well as unstable) of the fixed point is responsible for the universality class of the models. In

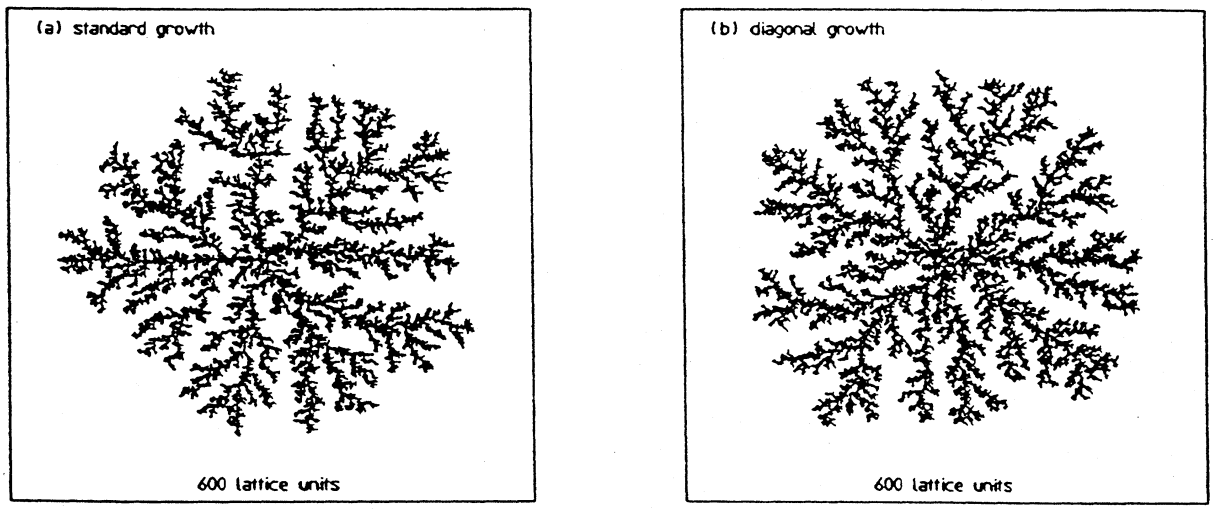

FIG. 28. Example of two clusters generated by the standard DBM (bond) growth rule (left) and by a bond growth rule that also includes diagonal processes. The two structures have the same fractal dimension (1.70); so they give rise to the same effective growth rule for coarse-grained variables at large scale.

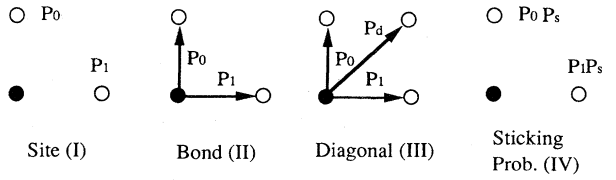

FIG. 29. Four growth rules that give rise to the same asymptotic structures with fractal dimension $D=1.70$ in radial geometry.

addition, the position of the fixed point in this space of growth rules is a nonuniversal element analogous to the value of the critical probability or temperature in percolation or Ising problems. For irreversible-growth phenomena, we can then distinguish between two different aspects of the problem. First, we study the invariant form of the growth rules, which in a certain sense corresponds to the nontrivial part of the Hamiltonian in usual critical phenomena. Then, we restrict our space of growth rules to the parameters describing the relevant invariant form of the dynamics, and we search for the fixed point.

It is useful to illustrate this point by an example. The standard DLA is defined with a site rule, but modified versions of the growth rule can be investigated.

(a) DLA defined per bond: The particles stick when, from a surface site, they move onto a site occupied by the aggregate. In the DBM, the growth probability is associated with each bond.

(b) DLA with *diagonal coupling* (next-nearest-neighbor interactions): In this version the particles stick as soon as they reach a site that is next-nearest neighbor to the aggregate. In the DBM, this corresponds to considering a diagonal bond probability proportional to the electric field.

(c) DLA with sticking probability less than 1: The particles stick to the surface with probability P_s and continue to diffuse with probability $1-P_s$.

The above modifications have been found to be irrelevant from the standpoint of fractal dimensions (see Table III), and the clusters generated by numerical simulations of these different models are identical in their overall behavior, as shown in Fig. 28.

Thus we can say that DLA is universal with respect to the four growth rules of Fig. 29. All these modifications belong to the same universality class, and under scale transformation the dynamics flow automatically in the fixed point that identifies the value of the parameters relative to the asymptotic form of the growth rules. Clearly, the fixed-point parameters could be different from the microscopic ones, even if the form of the microscopic growth rule is the same as that of the asymptotic one.

Our task, then, is to define the asymptotic form of the DBM growth rule and to construct a renormalization scheme for the parameters that allows us to study the essential scale-invariant properties of the model.

2. Asymptotic structure of the dynamics

Let us now consider the growth rules shown in Fig. 29 and try to cast the problem of finding the invariant form of the growth rules in the renormalization-group framework. The model we shall consider is the DBM with $\eta=1$ (equivalent to DLA). If we also consider the diagonal bond, the diagonal growth probability p_d is proportional to the local electric field, given by the gradient of the potential ϕ along this direction,

$$p_d=\frac{|\nabla\phi|_d}{\sqrt{2}} . \tag{7.1}$$

In Fig. 30(a), we show the diagonal growth rule at the minimal scale for a tip configuration. In this case the growth probability is simply proportional to the Laplacian potentials ϕ_i of the corresponding sites, and it is useful to parametrize the growth process by introducing the following variables:

$$\mu_0=1, \quad \mu_1=\frac{\phi_1}{\phi_0}, \quad \mu_d=\frac{\phi_{0'}}{\phi_0} . \tag{7.2}$$

We thus obtain for the growth probabilities of the sites

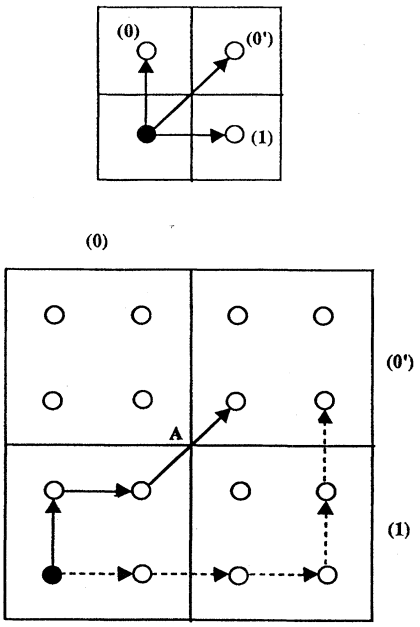

FIG. 30. Renormalization scheme of the growth process for a particular configuration. At the lowest scale (upper figure), the growth probability is simply related to the potentials. At larger scale, the effective growth processes for the coarse-grained variables are composed by many growth processes at the smaller scale (lower figure).

$$P_0=\frac{\mu_0}{\mu_0+\mu_1+\mu_d}\ , \tag{7.3a}$$

$$P_1=\frac{\mu_1}{\mu_0+\mu_1+\mu_d}\ , \tag{7.3b}$$

$$P_d=\frac{\mu_d}{\mu_0+\mu_1+\mu_d}\ . \tag{7.3c}$$

We may then consider analogous variables to characterize the growth process for coarse-grained variables at a larger scale, as shown in Fig. 30(b). In this case the probability of reaching a certain cell corresponds to the sum over all growth processes that lead to the occupation of at least one site of this cell. In this way one can introduce a renormalization transformation

$$\mu_i^{(k+1)}=R(\mu_j^{(k)}) \tag{7.4}$$

that links the growth processes at a scale $(k+1)$ to those at scale (k). The fixed-point vector $\boldsymbol{\mu}$ of the transformation would eventually lead to the characterization of the asymptotic scale-invariant dynamics. The solution of this renormalization problem would imply having to deal with an infinite proliferation of the variables μ_i corresponding to the effective growth probabilities associated with each new type of growth process (or growth cell) induced by the coarse-graining procedure, and the quantitative analysis of the fixed point is very complex. However, we can discuss rather simply the general form of the dynamics. Let us consider the renormalization of the diagonal bond growth rule with a cell-to-bond renormalization scheme and a "corner rule" to define the spanning condition. For the configuration shown in Fig. 30, we can write the RG equation for the diagonal growth probability as

$$\mu_d'=\frac{\sum_\alpha C_\alpha P_{0',\alpha}}{\sum_\alpha C_\alpha P_{0,\alpha}}=R(\mu_i)\ . \tag{7.5}$$

Here the index α identifies the possible configurations of the occupied cell, and C_α is the corresponding statistical weight. The probability $P_{j\alpha}$ represents the sum of the probabilities of the elementary growth paths, each of them given by the product of the elementary growth processes that, starting from the configuration α, lead to the occupation of the coarse-grained cell j (in Fig. 30, $j=0,0',1$).

For the diagonal growth process, the numerator of Eq. (7.5) can be written as

$$\sum_\alpha C_\alpha P_{0',\alpha}=\mu_d A(\mu_0,\mu_d,\ldots+\cdots)+\mu_d^2 B(\mu_0,\mu_d,\ldots,\ldots)\ . \tag{7.6}$$

In fact, the growth paths that correspond to a diagonal growth process for the coarse-grained dynamics can only contain one or two diagonal growth processes at the lower scale. The terms A and B are complex expressions given by the sum over the possible growth processes. The term in the denominator of Eq. (7.5) can be written as

$$\sum_\alpha C_\alpha P_{0',\alpha}=A(\mu_0,\mu_d,\ldots)+\mu_d B(\mu_0,\mu_d,\ldots,\ldots)+\cdots \tag{7.7}$$

because each process that leads to (0′) can lead to (0), if one replaces the last diagonal growth with weight μ_d with a vertical growth whose weight is 1. In addition, there may be other processes that lead to the occupation of the coarse-grained cell (0). Therefore the iterative renormalization equation for the diagonal bond coupling from scale (k) to scale $(k+1)$ becomes

$$\mu_d^{(k+1)}=\mu_d^{(k)}A'(\cdots)+[\mu_d^{(k)}]^2B'(\cdots)\ , \tag{7.8}$$

where $A'(\cdots)<1$ for every value of the vector $\boldsymbol{\mu}$. This equation has a fixed point at

$$\mu_d^*=0\ . \tag{7.9}$$

This fixed point is clearly stable, because

$$\frac{\partial\mu_d^{(k+1)}}{\partial\mu_d^{(k)}}=\left[\frac{\delta R}{\delta\mu_d}\right]_{\mu_d^*}=A'(\cdots)<1\ . \tag{7.10}$$

This means that the diagonal growth process that is present at the lowest scale *disappears* in asymptotic scale-invariant dynamics. We can also illustrate this point in the following intuitive way. The diagonal bond disappears at large scales because the diagonal process implies the occupation of the cell (0′) in Fig. 30 without going through cells (0) or (1). This corresponds only to the processes that go through point A in Fig. 30, and the phase space of these processes is very small compared to the processes that lead to the occupancy of the other cells. Clearly, in the limit of infinite cell size, the relative weight of these paths leading to the diagonal process goes to zero. This implies that, if one begins with growth rules that also include the diagonal growth process at the minimal scale, these will be transformed into an effective asymptotic growth rule where the diagonal processes have disappeared.

Using similar reasoning, it is easy to show that the asymptotic scale-invariant growth rule must be of *bond* type and not of site type. In fact, using our parametrization of the growth rule, the growth probability of a coarse-grained cell is clearly proportional to the number of paths that lead to its occupation. However, the number of paths is clearly proportional to the number of next-nearest occupied coarse-grained cells. Therefore the growth probability is proportional to the number of next-nearest growth sites, i.e., a bond growth rule. With similar simple renormalization schemes, it is possible to show that the sticking probability P_s renormalizes to the trivial value $P_s=1$ (Vespignani and Pietronero, 1993). Figure 31 shows the renormalization flows for diagonal coupling and the sticking probability.

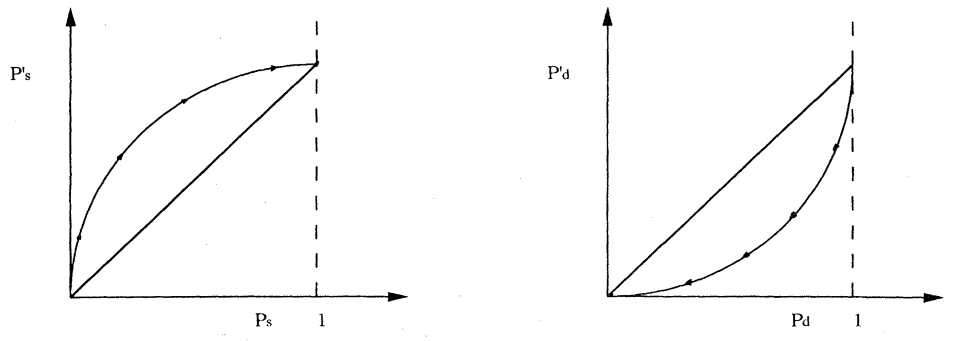

FIG. 31. Renormalization flow of the sticking parameter (a) and the diagonal coupling (b). The stable fixed points are $p_s=1$ and $p_d=0$, respectively.

This naive analysis (for a more rigorous treatment, see De Angelis *et al.*, 1991) shows that only the bond-type growth rule has the correct structure implied by the scale invariance of the dynamics. The other growth rules will flow asymptotically into one of bond type. Of course, this does not imply that the scale-invariant growth rule is identical to the one at the minimal scale.

Recently, similar problems seemed also to arise for percolation. In fact, it has been confirmed (Ziff, 1992) that the probability $R_L(p)$ for a site percolation cluster to span a square lattice of the side L goes to $\frac{1}{2}$ as $L\rightarrow\infty$. This is in agreement with universality and with the fact that, for bond percolation, $R_L(p_c)=1/2$. However, it is in contrast with RG theory defined per site, for which $R_L(p_c)=p_c=0,59$. This could be because site percolation does not possess the correct symmetry from which RG must be defined. On the contrary, bond percolation seems to be completely consistent with RG studies, extensive simulations, and exact results.

3. Parametrization of the growth rules

We have identified the general structure of asymptotic dynamics for growth models like DLA and the DBM, showing that the growth rules renormalize into effective scale-invariant growth rules of simple *bond* type. In this way we have restricted the space of the parameters that characterize the growth dynamics. However, a quantitative analysis of the fixed point $\boldsymbol{\mu}^*$ in this subspace is very complex. The problems are mainly due to a natural proliferation of the relevant parameters. Using the parametrization of Eqs. (7.2) and (7.3), we can try to obtain the renormalization equation for μ_1 to find the fixed point. However, the calculation of this group equation also involves growth process parametrized by a variable μ_2, as shown in Fig. 32. The RG transformation for μ_2 calls for the introduction of the variables μ_3 and μ_4 and so on. At the end, we obtain

$$\mu_1^{k+1}=R_1(\mu_1^k,\mu_2^k)\ ,$$
$$\mu_2^{k+1}=R_2(\mu_1^k,\mu_2^k,\mu_3^k,\mu_4^k)\ , \qquad (7.11)$$
etc.

Therefore this is a problem that leads to an infinite proliferation. Unfortunately, it would be difficult to truncate the set of equations by setting $\mu_i=0$ for $i\geq n$, as is usually done with proliferation problems. This is because we know that all the parameters are, in principle, different from zero. However, it is possible to use this approach to test the consistency of asymptotic growth rules for the fixed-point solution of Eq. (7.11). This can be done by setting $\mu_i=\phi_i/\phi_0$ for $i>n$ (this implies setting its value to the probability corresponding to the original growth rule) and studying the stability of the fixed point with respect to n.

The interesting approach of Nagatani (1987a, 1987b) actually represents an attempt to deal with the renormalization of growth rules. However, it is quite different from the one we have just discussed. In fact, this approach is based on the introduction of a single new parameter σ that represents the dielectric constant for the interface bond. Using a RG procedure, one obtains a fixed-point value σ^* which should represent scale-invariant growth rules. The problem with this approach is that the introduction of a growth rule phase space defined by σ does not necessarily correspond to the natural proliferation of the problem, nor is it clear why this should be a specially relevant parameter. In fact, the use of growth rules with the value σ^* in a computer simulation should lead to asymptotic structures identical to those of the standard growth ($\sigma=1$) but with a faster convergency. We have performed computer simulations

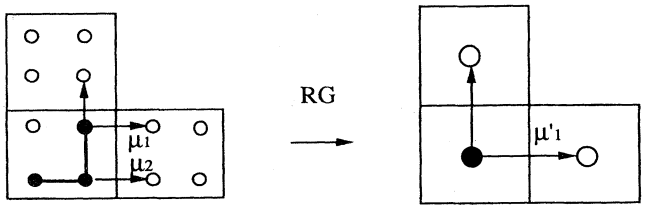

FIG. 32. Example of renormalization transformation for the growth rules characterized by the parameters μ_i. It is possible to see that the calculation of the renormalization equation for μ_1 also involves growth processes characterized by μ_2. This problem leads to an infinite proliferation that cannot be truncated.

in order to check this point (De Angelis *et al.*, 1991), and the result is, instead, that the fractal dimension depends explicitly on the value of σ. In cylinder geometry we obtain $D=1.67$ for $\sigma^*=1$ (standard model), while $D=1.61$ for $\sigma^*=3.11$. This implies that the generalization of the dynamics along the σ line seems to bring the problem out of its natural basin of attraction and universality class. Therefore σ does not seem to be the right parameter for asymptotic growth rules.

In this respect one may speculate that renormalization of the dielectric constant via σ refers only to the static properties. The different probabilities defined by $\sigma \neq 1$ are only used to assign the various weights of each configuration. However, the renormalization process does not refer to the growth probabilities, while it only refers to the static properties.

4. Scale-invariant screening and noise-reduction parameters

Let us focus our attention on the essential features of growth rules that are crucial in order to generate fractal structures. In this sense the FST framework points out the basic concept that can be studied: fractals can be generated only if *screening* persists at the asymptotic scale (see Sec. IV.B). Note that the presence of screening due to the Laplace equation in the original growth rule does not guarantee that a similar effect will persist for coarse-grained variables. In fact, if one studies the growth rules for a coarse-grained cell, a problem of noise reduction (Kertesz and Vicsek, 1986; Nittman and Stanley, 1986) naturally appears. Naively, therefore, one could expect that, asymptotically, the effective noise-reduction parameter (S) could diverge. This would then eliminate screening effects and lead to compact structures. Therefore the key feature of asymptotic growth rules is in the identification of the *fixed-point noise-reduction parameter.*

In the noise-reduction generalization of the DLA and DBM growth rules, a bond is grown only after having been hit by S particles (Kertesz and Vicsek, 1986). A counter is raised by 1 each time a particle hits the respective bond. When a counter reaches the value S, the corresponding bond is occupied and the new bonds near this one have their counters set to zero. The effect of this procedure is a systematic reduction of noise; in fact, the introduction of the parameters S corresponds to averaging over several realizations of the same stochastic process. This reduces fluctuations and introduces, through the counters, a memory effect. For a finite value of S, the branches of DLA patterns acquire a finite thickness, while for $S \to \infty$, screening is suppressed and the structure is compact. It is interesting to note that aggregates grown with noise-reduction parameters greater than 1 seem to cross over to a larger value of the fractal dimension. However, for larger clusters (asymptotic growth), the fractal dimension does not depend on S and equals the one measured for standard clusters. This implies that the universality class of the noise-reduced growth rules is the same for all finite values of S. Therefore the parametrization of the growth rules by this parameter does not change the basin of attraction in the space of growth rules.

The parametrization of the growth rules by the noise-reduction parameter S is rather simple. For example, let us consider the right configuration in Fig. 34, where we have a competition between the two bonds 1 and 2. If the parameter S is equal to 1 (standard growth), the probability P_1 and P_2 of growing, respectively, either bond 1 or 2 is given by the corresponding Laplacian potentials ϕ_1 and ϕ_2. For a generic value of S, the probability $P_1(S)$ that bond 1 will grow before bond 2 can instead be written as

$$P_1(S)=\frac{1}{N}\sum_{k=0}^{S-1}\begin{bmatrix} S+k-1 \\ k \end{bmatrix}\left[\frac{\phi_1}{\phi_1+\phi_2}\right]^S\left[\frac{\phi_2}{\phi_1+\phi_2}\right]^k , \tag{7.12}$$

where N is a normalization factor.

This expression corresponds to the probability that $S-1$ particles arrive at bond 1, while any number between 0 and $S-1$ arrive at bond 2, and, finally, the last particle reaches bond 1. It is then straightforward to obtain $P_2(S)$ by changing in Eq. (7.12) subscript 1 with subscript 2 and vice versa.

This scheme can be naturally generalized to more complex structures that involve more than two growing bonds by using a multinomial generalization. It is also possible to extend the results to noninteger values of S by analytical continuation.

This formalism allows us to obtain the elementary growth probability as a function of the parameter S and to develop an analytical RSRG for the effective noise reduction.

5. Renormalization group for the noise-reduction parameter

We now address the problem of constructing a scheme of renormalization for the noise-reduction parameter S. If one considers the original DLA process with $S=1$ at the minimal scale, it is clear that a nontrivial noise-reduction parameter appears for a coarse-grained cell, because many bonds are needed to span the coarse-grained cells. The problem is therefore to study the evolution of the effective noise-reduction parameter as a function of the scale transformation. We start with the arrival of each particle on a given bond that actually corresponds to a Poisson process. If S particles must arrive on a bond in order for it to grow, the probability distribution of the time t needed to occupy a bond is

$$W(S,t)dt=\frac{e^{-\lambda t}(\lambda t)^{S-1}}{(S-1)!}\lambda dt , \tag{7.13}$$

where λ is a parameter related to the single occupation probability.

It is then possible to show that (Barker and Ball, 1990)

$$\frac{1}{S}=\frac{\langle \delta t^2\rangle}{\langle t\rangle^2}\ , \tag{7.14}$$

where λ has disappeared. For a coarse-grained bond, one also has to consider its internal structure. In this case the growth of the coarse-grained bond will be the superposition of different Poisson processes, each with an associate probability and a certain number of particles $N(S)$ which are functions of the small-scale noise-reduction parameters. One can then define the renormalized noise-reduction parameter via the relative fluctuations of the growth time for this convoluted distribution (see Fig. 33). In practice, this is done via the ansatz that the rescaled distribution still has a Poisson structure.

Describing the relative growth time fluctuations as a function of the number of particles arrived (Barker and Ball, 1990), we obtain

$$\frac{1}{S'}=\frac{1}{\langle N(S)\rangle}+\frac{\langle N(S)^2\rangle-\langle N(S)\rangle^2}{\langle N(S)\rangle^2}\ . \tag{7.15}$$

Our aim is therefore to define the appropriate renormalization scheme in order to compute the averages that appear in Eq. (7.15).

In order to do this analytically, we used the cell-to-bond renormalization of Fig. 34. The transformation is defined by the following renormalization rules: (a) The cell not spanned vertically by grown (thick) bonds is renormalized to a vertical perimeter (thin) bond; and (b) the cell spanned by grown bonds is renormalized to a vertical grown bond.

To obtain the RG transformation, it is convenient, in practice, to consider the renormalization of a single bond along the vertical direction. In this case the renormalization equation is exactly that of Eq. (7.15). It is possible to develop more complex RG schemes (Cafiero *et al.*, 1993) that take into account the coupling between the vertical and the horizontal growth directions with the corresponding proliferation effects, but this leads to a nontrivial complication of the RG equations. However, these improved schemes essentially confirm the results of the simplest one that we present here.

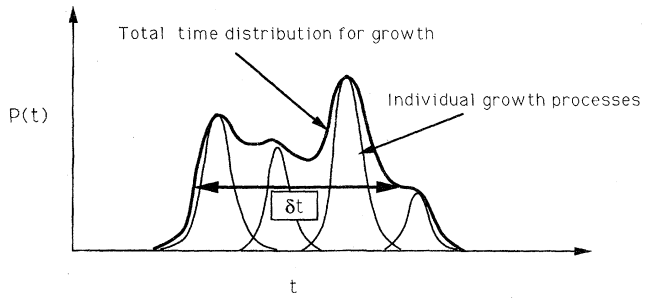

FIG. 33. Schematic of the probability distribution of the time t needed to occupy a rescaled bond. The growth of the coarse-grained bond will be the superposition of different processes. The renormalized noise-reduction parameter is defined via the relative fluctuations of the convoluted distribution.

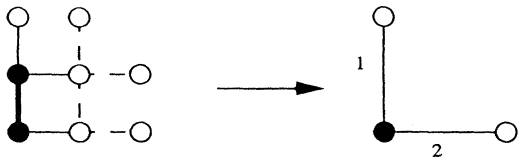

FIG. 34. Cell-bond renormalization scheme. The thick line denotes the growing bonds.

Thus, as a starting point, we have to consider all the configurations renormalized in a perimeter bond (Fig. 35). The next step is to compute the quantities $\langle N(S)\rangle$ and $\langle N(S)^2\rangle$ needed to span each configuration. One must therefore consider all the paths that span the cell for a given starting configuration, weighting them with the probabilities of the corresponding growth process. Note that all the possible configurations of the small-scale counters have to be considered (memory effect). Finally, this process must be repeated for all the possible starting configurations of the considered cell. These configurations, shown in Fig. 35, are related to each other by the growth process. This scheme has technical similarities with those of Wang *et al.* (1989a, 1989b); however, it is now used for different purposes. The weight $W(\alpha)$ of each starting configuration (α) can therefore be related to the probabilities of the elementary growth processes.

Thus we can finally write

$$\langle N(S)\rangle=\sum_{\alpha} W^{(\alpha)}(S)\sum_{i} P_i^{(\alpha)}(S)N_i^{(\alpha)}(S) \tag{7.16}$$

in which the index i refers to a particular path of the starting configuration (α), whose total probability is given by $P_i^{(\alpha)}$, and $N_i^{(\alpha)}$ is the corresponding total number of particles. A similar equation can be written for $\langle N^2(S)\rangle$. Each path probability $P_i^{(\alpha)}(S)$ is given by a sequence of elementary growth process probabilities $P_j(S)$ that depend on the particular configuration (j). One can evaluate these probabilities using the parametrization previously shown, for which Eq. (7.12) is an example.

Within the above scheme it is possible to compute analytically the RG transformation given by Eq. (7.15). The approach we have shown is quite simple; however, there are many technical details to be managed (Cafiero *et al.*, 1993). Here we show only the results which are essentially contained in Fig. 36. In this figure we plot the RG equation $S'=R(S)$ that describes the change of the noise-reduction parameter under scale transformation. These are the essential results:

(a) The fixed point for the noise-reduction parameter is attractive, reflecting the self-critical nature of DLA and DBM.

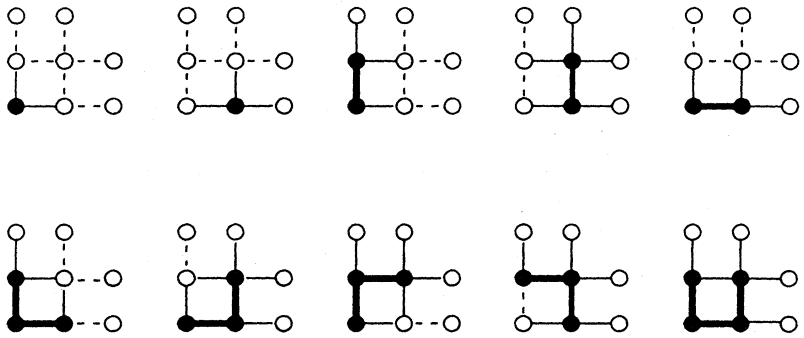

FIG. 35. Ten different occupation configurations for a 2×2 cell. They are related to each other by the growth processes. The thick black lines correspond to occupied bonds, while the thin lines represent the bonds on which growth can occur.

(b) The fixed-point value $S^* \simeq 2.4$ is therefore of the order of unity. Thus the scale-invariant dynamics is rather close to the microscopic one from which the models are defined. Furthermore, this guarantees that effective screening is preserved to all scales in the asymptotic regime.

These results imply that noise-reduced microscopic growth rules flow essentially in the standard microscopic growth rules. This is in contrast to the usual belief that noise reduction accelerates the approach to the asymptotic behavior, but it is in agreement with recent studies (Moukarzel, 1992). In addition, it is important to note that the behavior of the noise-reduction parameter has been studied up to now with respect to the overall shape or anisotropy of the cluster (Barker and Ball, 1980; Eckmann *et al.*, 1989), while our analysis is focused directly on the intrinsic fractal properties that hold for both lattice and off-lattice growth.

The small value of S^* implies that the minimal-scale growth rule is already rather close to the asymptotic one, allowing us to understand why the initial FST studies of DLA, in which minimal-scale growth rules were used, gave, indeed, reasonable results for the fractal dimension. This also ensures the persistence of screening in the scale-invariant dynamics of the growth process, explaining why the DLA process actually leads to a fractal structure. These results also elucidate the self-critical nature of DLA patterns. This is because, under scale change, noise is automatically generated by the dynamics of the system, even if one starts from the quasideterministic case $S=\infty$. This effect can be understood in the following way. Let us consider a growth rule with a large value of S (very small noise) acting at the microscopic scale. We want to estimate how this value changes under scale transformation by evaluating the probability distribution to span a cell and occupy a coarse-grained bond in a time t. The starting configurations of the cell (Fig. 35) lead to various possible paths of lengths between 1 and 4. For simplicity, let us consider only the case of path length equal to two and three steps, with corresponding probabilities p and $(1-p)$. The probability distribution will be given by the superposition of two functions with narrow peaks (small noise limit) at the positions $2S$ and $3S$, respectively:

$$\tilde{W}(S',t)=PW(2S,t)+(1-P)W(3S,t)\ . \tag{7.17}$$

The fact that $\tilde{W}(S',t)$ is a convolution of two peaks naturally introduces fluctuations (noise) that are larger than the intrinsic fluctuations of $W(2S,t)$ and $W(3S,t)$. If p is different from zero (this is certainly the case if different configurations are involved), we can treat these distributions as delta functions, obtaining via Eq. (7.15) the following upper limit for the renormalized S:

$$S'=\frac{\langle t^2\rangle}{\langle \delta t^2\rangle}\le\frac{(3-P)^2}{P(1-P)}\ . \tag{7.18}$$

Therefore the value of S' becomes of the order of unity after few iterations. This reflects the fact that the presence of different paths leads to fluctuations of the order of the path length, and it implies that $\langle \delta t^2\rangle$ and $\langle t\rangle^2$ are of the same order independently of the microscopic value of S. In a certain sense we can look upon this

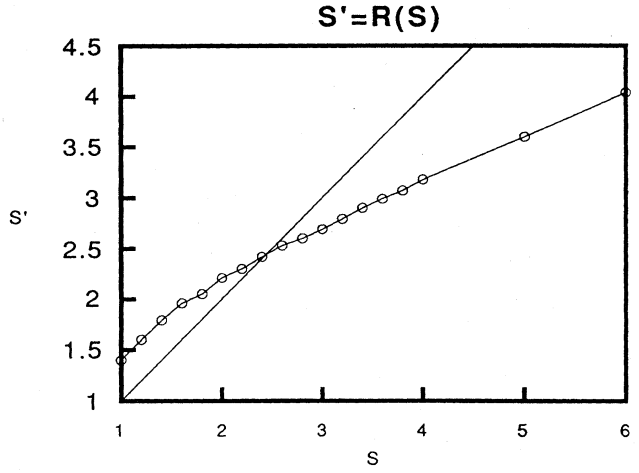

FIG. 36. Renormalization equation for the noise-reduction parameter S' at the coarse-grained scale as a function of the noise-reduction parameter S of the finer scale. One can see that the fixed point is attractive and that the value of S^* is of the order of unity, implying that screening is preserved to the asymptotic scale.

phenomenon as geometrical noise generation. In this way it is possible to understand why DLA dynamics intrinsically generates large noise asymptotically and does not become deterministic.

B. Fixed-scale transformation for diffusion-limited aggregation and dielectric breakdown model with the standard growth rules

This section contains a summary of the original FST approach to DLA and the DBM (Pietronero *et al.*, 1988a, 1988b) in which the standard DBM growth rules are used. However, given the analysis of the scale-invariant growth rules of Sec. VII.A, we are now able to understand *why* the use of the standard growth rules corresponds to a good approximation with respect to the scale-invariant ones.

1. Simplest method for computing the fractal dimension of diffusion-limited aggregation and dielectric breakdown model

We start with the case of closed boundary conditions (see Sec. IV.B) by assuming that the configurations and the growth processes that occur in the central column are identical to those that occur in the adjacent columns. In practice, therefore, this situation corresponds to periodic boundary conditions. Figure 37 shows the scheme for the calculation of the FST matrix elements, starting from a configuration of type 1. We are reminded that these matrix elements are conditional to the existence of a certain starting configuration; so we do not have to consider growth processes inside the initial configuration (within boxes in Fig. 37).

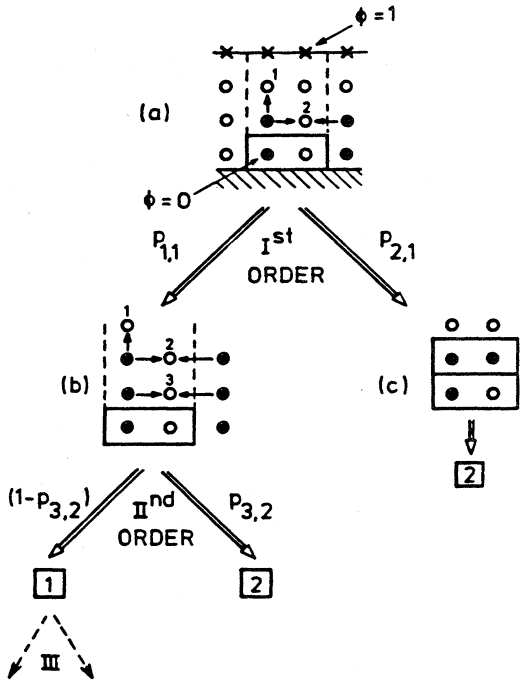

FIG. 37. Starting from a frozen cell of type 1 (boxed), we consider the growth processes that define the asymptotic probability for the next cell in the growth direction to be of type 1 or 2. Periodic boundary conditions are used with the period defined by the dashed lines. The probability of each process is simply related to the Laplacian potential of the configuration.

The first site to be occupied will be necessarily the one above the occupied site of the initial cell; therefore the first nontrivial growth processes are those indicated by the arrows in Fig. 37(a). In order to compute their probabilities, we have to specify the properties of the growth process. Here we use the standard DBM (bond) growth process, so these probabilities are just related to the potentials of sites 1 and 2 in Fig. 37(a). These potentials are given by the solutions of the Laplace equation that for this simple configuration can be computed analytically,

$$\phi_1=\tfrac{43}{82}=0.5244\ ,$$
$$\phi_2=\tfrac{6}{41}=0.1463\ . \tag{7.19}$$

The probabilities corresponding to these growth processes are indicated by $p_{i,j}$, where the first index (i) refers to the site that is going to be occupied and the second one (j) to the order of the process that is given by the number of particles that have been added to the structure (except the first trivial one). Note that these site probabilities correspond to the sum of the various bond probabilities leading to the considered site. The first-order growth probabilities are then

$$p_{2,1}(\eta)=\frac{2\phi_2^\eta}{\phi_1^\eta+1\phi_2^\eta}\ ,$$
$$p_{1,1}(\eta)=1-p_{2,1}(\eta)\ , \tag{7.20}$$

where η is the usual DBM parameter.

If the event corresponding to $p_{2,1}(\eta)$ takes place, site 2 of Fig. 37(a) gets occupied at first order, and the cell following the initial one will be of type 2 asymptotically [Fig. 37(c)].

If, instead, $p_{1,1}(\eta)$ occurs, this cell remains of type 1, but higher-order processes may still lead to the occupation of its second site. For the second-order process, we have

$$p_{3,2}=\frac{2\phi_3^\eta}{\phi_1^\eta+2\phi_2^\eta+2\phi_3^\eta}\ , \tag{7.21}$$

where the potentials refer now to Fig. 37(b) and their values are (Pietronero *et al.*, 1988a, 1988b)

$$\phi_1=0.5245\ ,$$
$$\phi_2=0.1471\ , \tag{7.22}$$
$$\phi_3=0.0392\ .$$

Therefore the probability that the configuration above the starting one will be of type 2, *after infinite growth*, gives the FST matrix element $M_{1,2}$. This can be written

as

$$M_{1,2}(\eta)=p_{2,1}(\eta)+[1-p_{2,1}(\eta)]p_{3,2}(\eta)+\cdots , \quad (7.23)$$

and, in principle, the series should be continued until the probability of occupation of site 2 in Fig. 37(a) is virtually saturated (freezing condition). It is important to note, however, that higher-order terms in this series correspond to configurations in which this site is exponentially screened by growth that has occurred at other sites [see Fig. 37(b), in which site 3 is the original site 2 of Fig. 37(a)].

This screening effect is crucial because it allows rapid convergence of the series given by Eq. (7.23) to a number *smaller than 1.* This is the key point for the formation of *fractal structures.* In fact, if asymptotically

$$M_{1,1}(\eta)=1-M_{1,2}(\eta)>0 , \quad (7.24)$$

there is a finite probability that growth will leave empty sites. From studies of scale-invariant growth rules, we have seen that screening persists in asymptotic behavior. Therefore Eq. (7.24), together with scale-invariant dynamics, implies that holes will be generated at all scales with a finite probability, which is a characteristic of fractal structures.

This conclusion holds for any finite value of η. In the Eden limit ($\eta=0$), we saw instead (Sec. IV.C) that the terms of the series decay only as power laws with respect to the order. This fact is due to the suppression of screening, and it leads asymptotically to a compact structure. The possibility of distinguishing between fractal and nonfractal structures is one of the main results of the FST approach.

For the DLA case ($\eta=1$), we obtain

$$M_{1,1}(\mathrm{I})=0.3581 , \quad (7.25)$$

$$M_{1,2}(\mathrm{II})=0.4142 , \quad (7.26)$$

respectively, at first and second order.

We then have to compute the other matrix elements that correspond to a starting configuration of type 2. The calculation is analogous to the one we have discussed (Pietronero *et al.*, 1988b), and the results are

$$M_{2,1}(\mathrm{I})=1-M_{2,2}(\mathrm{I})=0.5609 , \quad (7.27)$$

$$M_{2,1}(\mathrm{II})=1-M_{2,2}(\mathrm{II})=0.4944 . \quad (7.28)$$

The fixed point is then given by Eq. (4.16), and the corresponding values of the fractal dimensions are

$$D(\mathrm{I})=1.4747 , \quad (7.29)$$

$$D(\mathrm{II})=1.5418 . \quad (7.30)$$

It is not difficult to proceed along the lines indicated and also compute higher-order terms. By going up to fifth order, one observes a rapid convergence towards $D=1.55$. This value can be considered essentially as a lower bound because of two reasons:

(a) The use of closed (periodic) boundary conditions enhances the screening effects and tends to reduce the value of the fractal dimension.

(b) The use of minimal-scale growth rules gives rise to a similar effect. In fact, the asymptotic scale-invariant growth rules show the asymptotic persistence of screening. However, screening effects are slightly reduced with respect to those corresponding to the direct use of the Laplace equation.

We can easily improve with respect to the first point by considering the possibility of fluctuations in the boundary conditions for the growing structure. This is the point that makes the FST more accurate with respect to the usual real-space methods. We can include this effect in the open-closed approximation, as discussed in Sec. IV.D and which we have already used extensively in the previous models. This requires the calculation of FST matrix elements also for "open" configurations. The details of these calculations can be found in Pietronero *et al.* (1988b). The results of the open-closed approximation for second and third order are

$$D(\mathrm{II})=1.6080 , \quad (7.31)$$

$$D(\mathrm{III})=1.6406 . \quad (7.32)$$

By comparing these results with the value $D=1.5$ corresponding to the asymptotic (with respect to order) result of the calculation with only closed configurations, we can see that the self-consistent treatment of boundary-condition fluctuations produces a substantial improvement in the results.

The calculations can be easily generalized to values of $\eta\neq 1$ as shown in Pietronero *et al.* (1988b). The case of $\eta=0$ (Eden) requires particular care, because the convergence of the series becomes slow. It is easy to show, however (Sec. IV.D), that this case leads to a compact nonfractal structure ($D=2$).

2. Empty configurations

The calculation of fractal dimension for DLA and the DBM in $2-d$ that we have discussed is based on a simplified FST scheme. It is important to remark, however, that each of these simplifications can be tested in detail, and eventually the theory can be extended correspondingly. For example, in Sec. IV.E, we have seen that the restriction of the FST to only two configurations is actually an approximation, but it is possible to improve the situation by also including explicitly the empty configurations. The problem arises when one tries to compute the relative probabilities of occurrence via a dynamical evolution as we do in the FST scheme. In fact, strictly speaking, any configuration will eventually evolve into an empty one. This reflects the fact that, asymptotically, a fractal has zero density. In the simple scheme we usually adopt, the empty configurations are eliminated by requiring a condition of connectivity within a single column. However, empty configurations can be included explicitly in the dynamics, and only at

the end are the relative probabilities for nonempty configurations computed. In this way it is possible, for example, to compute the effect of over-hangs on these relative probabilities. The corresponding result, including the empty configurations, is (Vespignani and Pietronero, 1990)

$$D=1.6242\ . \tag{7.33}$$

This leads therefore to the following conclusions: (a) The effect of empty configurations in the FST scheme is small, and the simplified scheme is already rather good; and (b) for DLA in 2-d, the explicit inclusion of empty configurations decreases fractal dimension by about 1%.

3. Multifractal properties of the growth probability

Since the introduction of multifractality, there has been a large amount of work aimed at the characterization of the growth probability distribution for DLA in terms of a multifractal spectrum. The situation turned out to be more complex than expected because, even though some multifractal features are present, there is also evidence that a simple multifractal scheme is not suitable for reproducing all the scaling properties, and the situation is still rather controversial, as we discussed in Sec. II.

From the standpoint of the FST, the growth probabilities are used to compute the matrix elements directly without the need for introducing a multifractal spectrum explicitly. It is possible, however, to compute the regular part of the multifractal spectrum corresponding to these probabilities as a by-product of the FST method. For a given order of the FST calculation, one is left with a frozen portion of the structure above which there is a configuration that represents the growing interface. The various sets of the growth probabilities that appear in these configurations can be considered the nucleus of the multiplicative process from which the multifractal properties can be extracted (Marsili and Pietronero, 1991).

Several questions remain, however, because the usual multifractal scheme does not appear to describe the properties of the growth probability in a complete way. Features like the self-affinity of the support and the anisotropy of correlations probably give rise to a situation that is more complex than the usual multifractal scheme.

C. Diffusion-limited aggregation and dielectric breakdown model in three dimensions

The FST approach for DLA and the DBM can be naturally extended to three dimensions (Vespignani and Pietronero, 1990). The differences are essentially technical:

(a) In three dimensions the intersection is done with a plane, and the basic configurations are five instead of two. This leads to a 5×5 FST matrix.

(b) In the explicit calculation of FST matrix elements, it is necessary to consider growth processes up to a relatively high order to achieve an accuracy comparable to the two-dimensional calculations. The corresponding probability tree is therefore rather complex, and it is necessary to develop a computer algorithm for the calculation of these matrix elements.

(c) The analysis of the boundary-condition fluctuations is also more complex.

Our best scheme of calculation gives the following results for the DBM in three dimensions (Vespignani and Pietronero, 1991),

$$\eta=1 \quad D=2.54 \quad [2.50]\ , \tag{7.34}$$

$$\eta=2 \quad D=2.17 \quad [2.13]\ , \tag{7.35}$$

$$\eta=3 \quad D=1.91 \quad [1.89]\ , \tag{7.36}$$

where in brackets we report the values obtained with computer simulations.

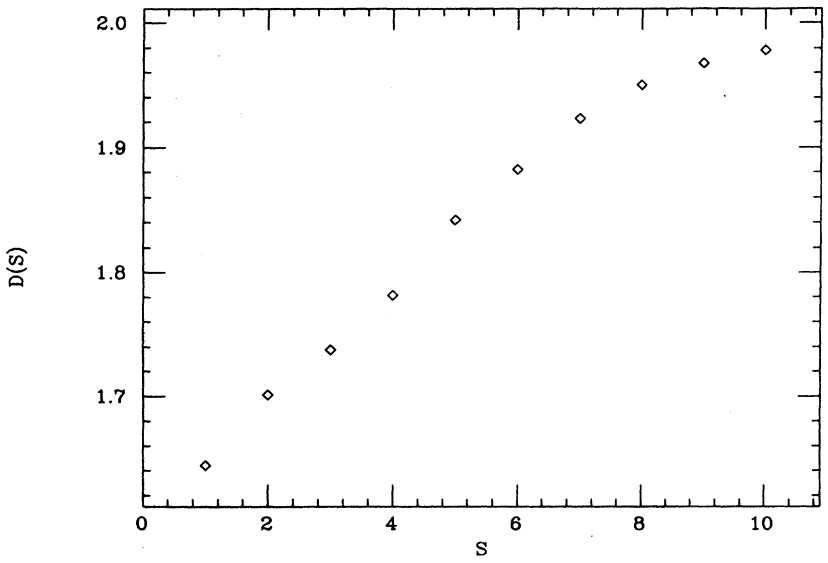

FIG. 38. Values of the fractal dimension obtained with the FST method by using growth rules with noise-reduction parameter other than 1.

D. Fixed-scale transformation for diffusion-limited aggregation and dielectric breakdown model with renormalized growth rules

We have seen that, in order to relate the FST to the fractal dimension, it is necessary to use scale-invariant growth rules. We have studied this question in Sec. VII.A, and the main result is that the crucial parameter that appears in the renormalization of the growth rules is an effective noise reduction. This point can be improved by considering the FST with growth rules in which S^* is different from 1.

In practice, this implies that the growth probabilities are not computed directly by the solutions of the Laplace equation, but instead they are given by the multinomial distribution of Eq. (7.12).

The calculation proceeds, otherwise, along the previous lines. The results for the fractal dimension for different values of S^* are shown in Fig. 38. Since in Sec. VII.A we derived $S^* \simeq 2.4$, the corresponding fractal dimension is $D \simeq 1.70$, which should be compared with the value $D = 1.64$ derived with small-scale growth rules.

We summarize with the following scheme of increasing completeness for the fractal dimension of DLA in 2-d derived with the FST method (Table IV).

(a) The use of small-scale growth rules and only closed (periodic) boundary conditions gives $D = 1.55$.

(b) The inclusion of the fluctuations of boundary conditions in the open-closed scheme up to third order gives $D = 1.64$.

(c) The explicit inclusion of empty configurations decreases this value by about 1%.

(d) The use of renormalized growth rules with $S^* \simeq 2.4$ instead of the small-scale ones ($S = 1$) leads to an enhancement of about $D = 1.70$.

It is important to notice that, even though the FST scheme is not strictly systematic in a mathematical sense, the various effects can be analyzed explicitly and estimated quantitatively. In order to proceed along this line of increasing sophistication, it is important to clarify the origin of the discrepancies that appear in the computer simulations.

E. Topological properties: Backbone

As for the case of the percolating cluster (Sec. V), so for the DLA/DBM clusters it is possible to define substructures selected by their topological properties. In view of the fact that the growth probability is governed by the Laplace equation, it is not possible to have closed loops in a DLA/DBM cluster. Therefore the backbone and the chemical distance coincide for these clusters.

Simulations studies of the properties of the backbone indicate that its dimension is $D_b \simeq 1$ in any Euclidean dimension. This is an important result: It identifies a qual-

TABLE IV. Detailed FST analysis for DLA/DBM in two dimensions. Fractal dimensions computed with FST schemes of increasing complexity are reported (for references, see text).

Method	Fractal dimension
Computer simulations	
Circular geometry:	
Mass-length relation	1.715
Density-density correlation	1.67(0.01)
Box counting	1.60–1.65
Cylinder geometry:	
Box counting	1.60–1.65
FST with small-scale growth dynamics:	
Closed boundary conditions	1.55 (lower bound)
Open-closed scheme	1.6406 (reference value for further improvements)
Inclusion of empty configurations	1.6242
Scale-invariant dynamics	Self-organization: attractive fixed point
(Spontaneous proliferation with respect to the renormalization of noise reduction S)	Fixed-point value: $S^* = 2.4$ [The corresponding growth probabilities are close to those of the small-scale dynamics ($S = 1$).]
FST with scale-invariant dynamics ($S = 2.4$)	
Open-closed scheme	1.70[a]

[a]Should be considered with respect to the open-closed scheme.

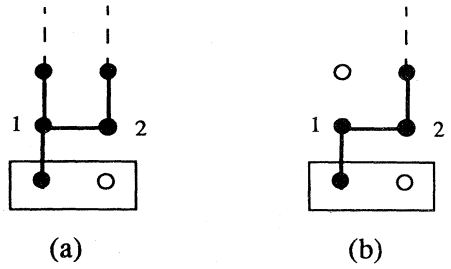

FIG. 39. Configurations involved in the calculation of the fractal dimension of the DLA backbone. Configuration (a) contributes to the matrix element $M_{1,1}$ because only site 1 belongs to the backbone. In configuration (b), instead, sites 1 and 2 both belong to the backbone, giving a matrix element of type $M_{1,2}$.

itative difference between DLA/DBM clusters and the percolating cluster. Furthermore, the fact that D_b never approaches the value of a random walk ($D_w=2$) for high space dimensions can be related to the absence of an upper critical dimension for these growth models. From the standpoint of the FST method, it is easy to consider the problem of the calculation of the fractal dimension of the backbone. The basic point is that one must define the essential configurations and the corresponding probabilities (C_1, C_2) only for the sites or bonds belonging to the backbone. In practice, for each growth configuration, one must first define the backbone and then identify the corresponding configurations. Figure 39(a) shows a configuration of type 1 being followed, in the growth direction, by a configuration of type 1. This is because only site 1 belongs to the backbone, while site 2 does not. In Fig. 39(b), instead, points 1 and 2 both belong to the backbone.

In this way one can easily generalize all the previous calculations to the fractal dimension of the backbone, too. Up to third order, we obtain

$$D_d \simeq 1.04 \ . \tag{7.37}$$

This value is substantially smaller than the chemical distance of the percolating cluster ($D=1.17$), and it represents a reasonable indication that the real value could be exactly 1. In order to check the eventual convergence to this value, it is necessary to consider configurations with more than two sites.

VIII. FRACTAL-GROWTH PHENOMENA

In this section we show the application of the FST method to other nonlocal growth models of general interest. These models are nonlocal in the sense that they are governed by a growth probability distribution which is influenced by the distant points of the structure and, for this reason, they exhibit the same theoretical problems as DLA. In addition, they present some further complications which make them particularly interesting from a theoretical point of view. For instance, the CCA model is strictly related to the diffusive nature of DLA. However, the clustering process is due to aggregates of different sizes; so different scale dynamics are necessary to describe the system. This makes it very difficult even to formulate the problem from the standpoint of the renormalization-group method.

The Born model for fracture is a natural extension of the DBM. In fact, this model is defined in the same spirit as the DBM, by replacing the Laplace equation with the Born elastic equation in order to define the growth probability field. This introduces in the growth model the tensorial nature of elasticity, which is very challenging for an analytical treatment.

The particle-cluster aggregation with Levy flight particle walks has been introduced to explore the effect of fractal trajectories on aggregation. This model enhances the long-range effects contained in DLA in view of the long-range correlations present in the Levy flight. We shall see that the FST method can be extended in a natural way to all these other models. This seems to indicate that in this field the conceptual problems posed by DLA and the DBM are really the central ones. In addition, the fact that the FST can easily be generalized to other models indicates that this method introduces the appropriate theoretical perspective in this field.

A. Cluster-cluster aggregation model

The cluster-cluster aggregation model (CCA; Kolb *et al.*, 1983; Meakin, 1983) is one of the most studied problems of fractal growth because it describes a large amount of interesting physical phenomena in the field of colloids, polymer solutions, and gels (Jullien and Botet, 1987; Vicsek, 1992). The CCA model is usually defined on a square lattice with periodic boundary conditions in which N initial particles are distributed randomly. These particles diffuse by performing a Brownian motion on the lattice and, if they occupy adjacent sites at a given time, they will stick together irreversibly and give rise to larger clusters. These clusters move with a probability of motion proportional to the diffusion coefficient (ρ_d) that is linked to their mass s by the relation

$$\rho_d = c s^{\gamma} \ , \tag{8.1}$$

where the exponent γ depends on the physical process that one intends to describe (Vicsek, 1992). The asymptotic properties of the cluster usually depend on the value of γ. The classical understanding of CCA focuses on the mean distribution as given by the mean-field Smoluchowski equation (Smoluchowski, 1916; Jullien and Botet, 1987). In this equation the approximation used is to neglect the space dependence of all physical quantities, so it cannot provide any information about the geometrical characteristics of clusters, i.e., the fractal dimension. For $\gamma \leq 0$, the aggregation process is homogeneous in space, and the mean-field assumption of the Smolu-

chowski equation is satisfied. In this situation, which is also the most relevant physically, the value of the fractal dimension of clusters obtained from computer simulation is

$$D \simeq 1.45 \pm 0.05 \quad (d=2) , \qquad D \simeq 1.8 \pm 0.05 \quad (d=3) , \tag{8.2}$$

and it is independent of the value of γ. We refer here to the so-called steady state in which asymptotic behavior is well defined (Vicsek *et al.*, 1985). If, instead, $\gamma > 0$, the model will correspond to the unusual situation in which large aggregates move faster than small ones. In this case, the aggregation process is not homogeneous in space, and the fractal dimension increases continuously from $D \simeq 1.45$ to the DLA value, $D \simeq 1.7$, that is reached for $\gamma \geq 2$. An important amount of information on the CCA process is given by the knowledge of the mass distribution of the aggregates n_s, both as a function of time and in the steady-state regime. The $n_s(t)$ curves, obtained from simulations at different times (Vicsek and Family, 1984; Vicsek, Meakin, and Family, 1985), show either a bell-shaped behavior or a power law with exponent $\alpha \leq 2$:

$$n_s(t) \cong t^{-w} s^{-\alpha} g(s/t^z) , \tag{8.3}$$

depending on the range of values of the exponent γ. However, it is necessary to distinguish clearly between some aspects of the $n_s(t)$ due to finite-size effects and the properties we are interested in, i.e., the properties around the s value where at fixed time the aggregation is especially occurring. In fact, the simulations with fixed number of particles unavoidably introduce at long times a finite-size effect in the $n_s(t)$ distribution, due to the disappearance of small aggregates in favor of large ones. This is the origin of the deviation from a power law in the $n_s(t)$ distribution. By the way, around the value $s \simeq t^z$, that is, the typical mass of clusters at time t, the $n_s(t)$ is a power law in s with exponent $\alpha = 2.0$ (Leyvraz, 1986; Jullien and Botet, 1987; Vicsek, 1992). In order to avoid this complication, it is better to study this distribution for a stationary state. To achieve the CCA steady-state regime, one introduces a "source and sinks" technique, corresponding to having an upper cutoff in the cluster's mass and a seed of k particles added each unitary time increment. In this condition, after long enough time, the time dependence of $n_s(t)$ disappears and we observe a power-law behavior

$$n(s) \sim s^{-\alpha} \tag{8.4}$$

with $\alpha = 2$ (Vicsek, Meakin, and Family, 1985). This is actually the behavior predicted by the Smoluchowski theory (Leyvraz, 1986). The properties of $n(s)$ are fundamental for the discussion of the CCA phenomenon. In fact, the growth process can be due to incoming aggregates of different sizes, and the mass distribution is a basic element for the characterization of the dynamical aggregation processes. As we shall see later, this is the key point that differentiates CCA from DLA. For instance, let us consider the dynamics of the growth process at a generic scale of size r_n. We can distinguish between three possibilities. The first one is that the growth process is due to clusters of size $r > r_n$. The second possibility is that $r \simeq r_n$, and in the third case $r < r_n$. Clearly, the relevant contribution to the growth process is given by the clusters of size comparable to or larger than the resolution scale r_n. In fact, a large number of small clusters will be necessary in order to give an appreciable contribution to growth at scale r_n and, at a low order of approximation, they can be neglected. Therefore the basic element for the dynamical process is the relative probability K_n that the growth process will be due to an incoming particle with size r of the order of r_n ($r_{n-1} < r < r_n$) or to a cluster of larger size ($r > r_n$). Considering that, in the steady-state regime, the mass s and the size r are related by $S \sim r^D$, we can compute this ratio as

$$K_n = \frac{P(r_n)}{P(r_n)+P(r>r_n)} = \frac{\int_{r_{n-1}}^{r_n} n(r) r^{D-1} dr}{\int_{r_{n-1}}^{\infty} n(r) r^{D-1} dr} = 1 - \left[\frac{r_n}{r_{n-1}} \right]^{(1-\alpha)D} , \tag{8.5}$$

where $n(r)$ is the cluster size distribution obtained from Eq. (9.4). However, the fractal dimension cannot be computed from this equation that is derived in a mean-field approximation. By the way, since K_n is a power law, it is scale invariant, and we can use Eq. (4.5) as the starting point of our FST approach to CCA.

B. Analytical calculation of cluster-cluster aggregation fractal dimension with the fixed-scale transformation approach

Our discussion of the explicit calculation of fractal dimension is based on a scheme similar to the one originally introduced for DLA, and here we focus mainly on the differences introduced by the CCA process. The starting point consists in the calculation of the matrix elements $M_{i,j}$ using scale-invariant dynamics. In the CCA model, the problem is, in a certain sense, simpler than for DLA. In fact, the relevant contributions to the growth process are given by the clusters of size r_n or larger, for which the probability of aggregation is given by the Laplace equation valid at each scale. This is because at all scales the clusters of size of the order r_n can be considered as single particles whose dynamics is the microscopic one. The renormalization of the aggregation of small clusters, or single particles, which is the main problem for DLA dynamics, can instead be neglected in CCA. In this sense the use of the microscopic dynamics as the scale-invariant one corresponds to neglecting the contributions of particles smaller than the coarse-graining size.

We are now in a position to compute explicitly the FST matrix elements. The aggregation is characterized

by the aggregation process of clusters of size r_n or larger, with the corresponding relative probabilities given by Eq. (8.5). These can be expressed self-consistently as a function of C_i; and for the $d=2$ case, we obtain

$$K_n = 1 - 2^{(1-\alpha)[1+\ln(C_1+2C_2)/\ln(2)]} . \tag{8.6}$$

As an example of the calculation of matrix elements, we can consider the growth processes that originate from a frozen configuration of type 1. With probability K, the next cluster that comes in contact with our starting configuration is of size r_n (the same as the coarse-graining level considered). In this case the cluster is represented by a single site, and it will occupy the site above the occupied one of the starting cell. This corresponds to the zero-order growth process in the DLA scheme. With probability $1-K$, a larger cluster ($r > r_n$) arrives. This gives rise to two possibilities, as shown in Fig. 40. The larger aggregate (shaded region) can occupy a single site (above the starting cell) with probability C_1, or both sites with probability C_2. This is because we assume that in the steady-state regime the arriving aggregates will have the same fractal dimension that we will compute in the end, characterized by the same distribution (C_1, C_2). After the arrival of a large aggregate, the probability tree is stopped because the eventual empty site above the starting cell is considered fully screened. At zero order we have therefore

$$M_{11} = K + (1-K)C_1, \quad M_{12} = (1-K)C_2 . \tag{8.7}$$

When a single particle arrives (of size $r \simeq r_n$), the growth process should instead be continued. Again with probability $1-K$, a large aggregate arrives, but in this case it will stick to the tip of the growing cluster that is now one step higher. The probability that the incoming aggregate will penetrate to occupy the empty site above the starting cell is now of higher order, and (for the moment) we neglect it. With probability K, the incoming aggregate has the size of a single cell, and the process is analogous to DLA. It is possible to extend the construction of the probability tree to higher orders, and the general expression for the matrix element at order l is (Sidoretti and Vespignani, 1992; Pietronero *et al.*, 1993)

$$M_{1,1}(l) = (1-K)C_1 + (1-K)K + \sum_{n=1}^{l-1} K^{n+1}(1-K)M_{1,1}^{\mathrm{DLA}}(n) + K^{l+1}M_{1,1}^{\mathrm{DLA}}(l) , \tag{8.8}$$

where $M_{1,1}^{\mathrm{DLA}}(n)$ corresponds to the DLA matrix element of order n, as discussed in Sec. VII.B.

It is important to notice that the incoming of large clusters produces a faster freezing effect, which is reflected in the fact that the matrix elements consist of power series in K and therefore the convergence is faster than in DLA. For this reason we can draw the general conclusion that

$$D_{\mathrm{CCA}} \leq D_{\mathrm{DLA}} . \tag{8.9}$$

In analogy with the DLA model and the DBM, we have used, in the explicit calculation of the matrix elements, the simplest nontrivial scheme to include self-consistently the fluctuations of the boundary conditions. This is the open-closed approximation, and it is possible in this case to derive analytically the fixed-point distribution (C_1, C_2). In Table V the results obtained for fractal dimension up to third order of calculation are compared with the best simulation results actually available. The result $D=1.39$ obtained for the cluster-cluster model at third order can be compared with the DLA result at the same order, $D=1.64$. Actually, we are making an approximation in the calculus considering the starting cell fully screened as soon as a large cluster reaches the tip of the growing cluster. This is not completely true for the case of open boundary conditions, because of the possibility of lateral growths. Anyway, this correlation can be evaluated (Sidoretti and Vespignani, 1992), and it gives small contributions that increase by about 2% the value of D.

The approach can be naturally extended to the three-dimensional CCA. Even in this case the $n_s(t)$ is a power law with exponent $\alpha=2$. The development of the method is the same as in two dimensions; nevertheless, several technical complications occur in the practical calculation of the matrix elements. This is because, as in the three-dimensional DLA, higher Euclidean dimensions increase the complications of the proper treatment for the boundary conditions. In Table V we also show the result obtained for the $3-d$ CCA fractal dimension. That is also in good agreement with the simulations. The FST application to the CCA model is particularly relevant, because it allows the first analytical treatment of a problem which cannot even be formulated with the usual theoretical methods, as, for example, the RSRG method. On the contrary, the FST can be easily extended to study quantitatively the fractal features of the CCA model.

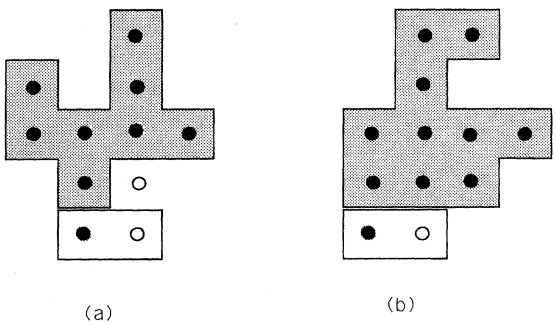

FIG. 40. We consider the growth process conditional to a starting configuration of given type. With probability $1-k$, a large aggregate arrives (shaded region), and this can lead to two possibilities: the occupation of either a single site (a) or both sites (b) above the starting configuration.

This shows the systematicity and the high suitability of this method for treating fractal-growth models.

C. Born model for fracture

A wide variety of models based on deterministic or probabilistic growth processes has been introduced in order to characterize the fractal properties of fracture patterns. Two of the most extensively studied models are the central force model (Luis and Guinea, 1987) and its improvement (Yan *et al.*, 1989), which introduces noncentral forces by using the Born model for the elastic energy. The latter model is the analogous of the DBM Laplacian growth for fracture propagation, describing very simply the fracture propagation controlled by growth instabilities (probabilistic mechanism) and allowing us to take into account the vectorial nature of the problem. The Born model represents the elastic potential of a network of elastic springs with two terms, corresponding to the central and noncentral force contribution,

$$V=\frac{1}{2}(\alpha-\beta)\sum_{i,j}[(\mathbf{u}_i-\mathbf{u}_j)\cdot\mathbf{r}_{ij}]^2+\frac{1}{2}\beta\sum_{ij}[\mathbf{u}_i-\mathbf{u}_j]^2 , \tag{8.10}$$

where $\mathbf{u}_i$ is the displacement vector, r_{ij} is the unit vector, and α and β are force constants. The patterns generated with this model have a well-defined fractal dimension

TABLE V. Fractal dimension for the most-studied fractal-growth models computed with the FST method. The results are compared with the simulation best estimates (for references, see text).

Model	D simulation	D FST (best estimate)
Eden model ($d=2$) (bulk dimension)	2.0(0.1)	2.0 (extrapolation, slow convergency)
DLA/DBM ($d=2$)		
Cluster:		
DLA (DBM, $\eta=1$)	1.60–1.71 (for details, see Table III)	1.64–1.71 (for details, see Table IV)
DBM, $\eta=2$	1.40–1.45	1.43
DBM, $\eta=0.5$	1.85–1.90	1.78 (slow convergency, close to Eden limit)
Backbone	1.00(0.05)	1.04
DLA/DBM ($d=3$)		
Cluster:		
DLA (DBM, $\eta=1$)	2.5(0.1)	2.54
DBM, $\eta=2$	2.13(0.1)	2.17
DBM, $\eta=3$	1.89(0.1)	1.91
Cluster-cluster aggregation		
$d=2$	1.45(0.05)	1.39
$d=3$	1.80(0.05)	1.90
Born model for fracture ($d=2$)		
$\alpha=1;\ \beta=0$	1.52(0.04)	1.56
$\alpha=1;\ \beta=0,1$	1.68(0.03)	1.65
Fractal aggregation with levy flight trajectories		
$f=1.33$	1.88	1.85
$f=1.66$	1.80	1.82
$f=2.0$	1.75	1.76

that depends upon the internal parameter of the model (see Table V). In particular, numerical results (Caldarelli *et al.*, 1994) show that the fractal dimension changes continuously with the ratio (β/α), reaching an asymptotic value for $\beta/\alpha \to 0$. This numerical evidence is also supported by renormalization arguments (Caldarelli *et al.*, 1995).

The FST approach to this model can be developed along the usual lines, considering, however, the tensorial nature of the problem. This is reflected in the fact that the model is intrinsically defined as a bond problem on a triangular lattice. The main differences from DLA are (a) the probability field is given by the tensorial equation (8.10); and (b) bonds between occupied sites can still crack in the future. This leads, for technical reasons, to a different definition of the fine-graining configurations that are now characterized with respect to the broken bonds. In addition, the definition of "growth" column is slightly modified (Caldarelli *et al.*, 1995). After these changes have been made, the calculations are performed in the usual ways; the results are reported in Table V. It is important to note that we have to go to high orders in the calculus of the matrix elements (VI order for $\beta=0$, VII order for $\beta=0,01$) in order to obtain reliable results. The reason for this is that screening is reduced by the tensorial nature of the problem.

The agreement with simulations is rather good, particularly for the case $\beta=0$. For values of β other than zero, the convergence of the matrix elements is slower, and that is why the value of the fractal dimension is lower than the simulations values.

D. Levy flight clusters

In particle-cluster aggregation, the particle trajectory plays a crucial role. In fact, it is the trajectory that determines the density of the structure (i.e., the fractal dimension). For instance, a Brownian motion with dimensionality $D_t=2$ is more effective than a linear trajectory $D_t=1$ in preventing particles from penetrating into the voids of the structure, and such notion leads to structures with a lower fractal dimension. For this reason, it is interesting to consider the relationship between the dimensionality of the particle's walk and the fractal dimension of the aggregates.

To construct a particle trajectory with a well-defined fractal dimension, it is possible to use a generalization of the random walk in which the length of the step x follows a random distribution, satisfying the conditions

$$P(x \geq \lambda)=\lambda^{-f}, \tag{8.11}$$

$$P(x<1)=0. \tag{8.12}$$

Here, the probability $P(x \geq \lambda)$ is the probability that the length of the step will be greater than or equal to λ. This type of trajectory with $1<f<2$ is called Levy flight and has a dimensionality $D_t=f$. Clearly, the Levy flight has, by definition, long-range, power-law correlations into the paths followed by the particles, which affect strongly the fractal dimension of the resulting aggregates. Simulations have been carried out on this model using both lattice and off-lattice techniques (Meakin *et al.*, 1984). The fractal dimension depends on the values of the parameter f, which describes the Levy flight trajectory, and the results show a continuous variation between the limits given by the DLA model (corresponding to $f \to \infty$) and the Vold-Sutherland model (corresponding to $f \to 0$) that gives rise to compact structures. If the parameter f is in the range 1.0–2.0, the fractal dimension of the aggregate will decrease continuously as the dimensionality of the trajectories D_t increases. For f larger than 2, $D_t=2$; but the fractal dimension of the aggregates seems take on a range of values (Meakin, 1984). This last point seems quite strange, because the particle trajectories are Brownian for any $f>2$. However, the interplay between the particle trajectories and the aggregation process might be the origin of this effect. In Table V are reported the values of fractal dimension obtained for circular geometry and several values of f.

The extension of the FST approach to this model is conceptually straightforward and can be done along the lines of the two-dimensional DLA calculations (see Sec. VII). However, the calculation of the matrix elements is substantially more complex. In fact, in these cases the evaluation of the elementary growth processes to be used in the matrix elements cannot be done analytically. For ordinary DLA ($f \to \infty$), the growth probabilities were evaluated, solving the discretized Laplace equation in the growth columns. This is not possible for Levy flight, where the probability of finding a diffusing particle at a given point is not defined by a differential equation, but from the still unclear fractional differential calculus, which is very difficult to use for quantitative calculations.

For this reason, a simple Monte Carlo method has been used to evaluate the matrix elements. This consists in finding the elementary growth processes by using a Monte Carlo procedure in which particles diffuse and perform a Levy flight in the columns of growth. After enough time steps, the probability of each site's being visited becomes stable and defines the matrix elements. Clearly, we must need the boundary conditions inside (adsorbing condition on the grown sites) and outside (closed and open boundary conditions) the growth columns. This procedure must be repeated for all the growth configurations involved in the calculation of the matrix elements. Apart from the calculation of the quantitative values of the growth probability, we use the same schemes as those used for standard DLA. Table V reports the values obtained for different values of the Levy exponent f. Clearly, the closer f is to zero, the more penetrating is the walk of the diffusing particles inside the structure. This corresponds to increasing fractal dimensions, which are well recovered with the FST calculation. In addition, Table V shows that the FST method is able to obtain reliable results for the fractal dimension in the full range of the exponents f. In this respect, it is im-

portant to notice that the freezing condition is slowly reached for small values of f, and the calculation has been extended up to fifth order to achieve a good convergence (Zaratti *et al.*, 1995).

IX. RELATIONSHIP TO PATH INTEGRALS AND OTHER METHODS OF DYNAMICAL CRITICAL PHENOMENA

A. Dynamical critical phenomena and fractal growth

Second-order phase transitions are distinguished by diverging relaxation times (τ) as well as diverging correlation lengths (ξ), and the dynamical critical exponent z can be defined via

$$\tau \sim \xi^z . \tag{9.1}$$

For fractal growth, at the microscopic level, time can be directly measured by the number of aggregated particles. Identifying the correlation length with, say, the radius of gyration of the cluster, one sees from $N \sim R^D$ that the fractal dimension D can be thought of as a dynamical critical exponent. Under a coarse graining of the lengths, $R \to R' = R/b$, then, time should rescale in the same way as the mass, namely, $t' \sim N' \sim N/b^D$. This is indeed the case, since, as shown in Sec. VII, the noise-reduction parameters stays finite under successive coarse-graining operations.

With this analogy in mind, we may recall the mode-coupling theory of critical phenomena (Gunton, 1979). The first step is to identify the relevant "slow" modes for which, at the critical point, the correlation lengths, susceptibilities, and transport coefficients are likely to diverge. Within the FST approach, we identified (see Secs. III and IV) two modes, the uniform and symmetry-breaking cell states of *type* 1 and 2, within a hierarchical ansatz for the projections of the fractal onto transverse subsets. Then we were able to write equations of motion for the C_i, the amplitudes of these modes, under a translation in the growth direction. This is the fixed-scale transformation, and it is in complete analogy with the equations of motion *with respect to time* in the mode-coupling approach. Note that the amplitude of one of the modes we chose, the symmetry-breaking one, can be thought of as a sort of order parameter for fractal (as opposed to compact) growth.

In mode-coupling theory, projection of the microstates onto the slow varying modes introduces memory effects into the equations of motion. In our case, these come about because the equations of motion connect projections of the "frozen" fractal cluster onto successive transverse subsets. As will be discussed at length below, at the expense of enlarging our phase space and integrating over intermediate states, we are once more able to cast the problem in Markovian form.

To extract the scaling behavior, in mode-coupling theory one converts (Gunton, 1979) the equation of motion into equations for the propagator or two-point equal time correlation function (in the simplest case, there will be only one independent correlation function in the problem), and finds $\Gamma(q) \sim q^z$, where q is the wave number.

The route we follow is quite similar. The "equations of motion" solved for the steady state yield the amplitudes C_i in terms of the "kinetic coefficients" M_{ij}. In two dimensions, the expectation value of the total occupation number of the two site states $\langle n_1 + n_2 \rangle = C_1 + 2C_2$ [Eq. (4.2)] can be seen as a two-point correlation function, or a Green's function in the transverse subspace, since it is the probability that, given the first site's being occupied, the second site will also be occupied, normalized by the total possible occupation number. One then reads off the fractal dimension from $\langle n_1 + n_2 \rangle = 2^D$.

The most important accomplishment of both approaches is the derivation of the approximate equations of motion for a set of "gross variables" from the microscopic Liouville equations in one case and the growth rules in the other. As discussed by Gunton (1979), these "semi-phenomenological" equations in the context of critical dynamics in fact form the basis of both the mode-coupling theory and the renormalization-group equations, and in what follows we shall find that the same is true for the fixed-point equations for the FST, in the case of fractal growth.

B. Path-integral approaches to fractal growth

Field-theoretic methods based on a path-integral formulation of stochastic dynamics have been brought to bear on dynamical critical phenomena (De Dominicis, 1975; De Dominicis *et al.*, 1975) and other more general Markovian processes (De Dominicis, 1976; see Janssen, 1979, and references therein). The dynamical renormalization group (Halperin *et al.*, 1972; De Dominicis and Peliti, 1977, 1978; Hohenberg and Halperin, 1977) gives us a complete theory of critical dynamics. The path-integral approach has recently been extended to fractal-growth models by Parisi and Zhang (1985), Shapir and Zhang (1986), and Peliti (1985), among others (Grassberger and de la Torre, 1979; Cardy and Sugar, 1980; Grassberger, 1982; Elderfield, 1985a, 1985b). Path-integral formalism, in principle, provides us with a systematic way to generate all possible histories, together with their weights, along which irreversible aggregation clusters might evolve. However, due to the nonlocality of the resulting field theories, no perturbative computations have been possible, and no general renormalization-group results are available.

In what follows we shall briefly remind the reader of the Fock-space formalism (Peliti, 1985) used in these approaches, and then use this formalism to cast the "growth rules" in the form of microscopic Liouville operators. We shall then construct the FST within this framework.

It is common to start from a Fock-space (occupation number) representation, where the macroscopic state at

any time t is represented by

$$|\Phi(t)\rangle=\sum_{\underline{n}}\phi(\underline{n};t)|\underline{n}\rangle\ , \tag{9.2}$$

where $\phi(\underline{n};t)$ are the probabilities of finding the system in the state $|n\rangle$, at time t. The set $\{n_r\}\equiv\underline{n}$ of occupation numbers at the sites r on the lattice specify the microstates (Peliti, 1985). The state space is spanned by $|\underline{n}\rangle$, with the "exclusive" scalar product

$$\langle\underline{m}|\underline{n}\rangle=\prod m_r\delta_{m_r,n_r}\ . \tag{9.3}$$

We shall also need the "standard bra" $\langle|=\sum_{\underline{n}}(1/\prod_r n_r)|)\langle\underline{n}|$ introduced by Peliti (1985).

The probabilities $\phi(\underline{n};t)$ evolve according to the growth rules, and for Markovian processes it is possible to write the differential equation for the time-dependent macrostates,

$$\frac{d|\Phi(t)\rangle}{dt}=L|\Phi(t)\rangle\ , \tag{9.4}$$

where L is the Liouville operator. L can be expressed in terms of creation and annihilation operators (a_r,π_r), with $a_r,\pi_{r'}=\delta_{r,r'}$ and

$$\begin{aligned} a_r|\ldots,n_r,\ldots\rangle&=n_r|\ldots,n_r-1,\ldots\rangle\ ,\\ \pi_r|\ldots,n_r,\ldots\rangle&=|\ldots,n_r+1,\ldots\rangle\ . \end{aligned} \tag{9.5}$$

Note that if we let T denote the one-time step evolution operator, $L=T-1$ where 1 denotes the identity matrix. Peliti (1985) has shown in detail that with the introduction of auxiliary fields, or "bookkeeping variables," it is always possible to represent processes with memory, as in many irreversible aggregation models, also in this Markovian way. Integrating out the auxiliary fields and taking the continuum limit, one recovers the field theories introduced, say, by Parisi and Zhang (1985), which are nonlocal in space or time (Shapir and Zhang, 1986).

The formal solution of the differential equation (9.4) is given by

$$|\Phi(t)\rangle=U_t|\Phi(0)\rangle\ , \tag{9.6}$$

where $U_t=\exp(tL)\equiv\lim_{N\to\infty}[1+(t/N)L]^N$. Note that Eq. (9.6), in principle, contains a complete description of the process. However, the nonlocality of the action in the path-integral representation of U_t (Peliti, 1985) makes any practical computation very problematic.

The usual route to computing scaling exponents within this formalism would involve, at this point, an evaluation of the two-point correlation function $G(r_1,t_1;r_2,t_2)$ using renormalization-group methods. This, for example, is how the fractal dimension for directed percolation is obtained by Cardy and Sugar (1980), using the renormalization-group results of Migdal *et al.* (1974a, 1974b) and Abarbanel *et al.* (1976) for Reggeon field theory (RFT). In the case of growth models, the time-independent correlations in which we are interested would strictly be achieved in the limit of infinite growth, or $t\to\infty$ in Eq. (9.6). In terms of Green's functions, one would therefore have to compute

$$G(r_1,r_2)=\lim_{t_1\to\infty,t_2\to\infty}\langle|\pi_{r_2}a_{r_2}U_{t_2-t_1}\pi_{r_1}a_{r_1}|\Phi(t_1)\rangle\ . \tag{9.7}$$

Thus a detailed ansatz for the crossover behavior in r^D/t, with $r=|r_1-r_2|$ and $t=|t_2-t_1|$, besides the asymptotic scaling behavior, is called for. No such result is available, however, for the RFT-like theories for irreversible aggregation models; even the Eden model has been treated only so far in the mean-field limit, and that only approximately. [Recent work (Ohno, Kikuchi, Yasuhara, 1992) based on numerical integration of a continuous MFT for DLA might be a promising direction.]

C. Towards gross variables: The stationarity condition and the hierarchical ansatz

Let us now try to understand how we are able to extract nontrivial scaling behavior with the FST with a finite amount of labor.

The most important single piece of information we inject into the problem at this point is that in a rectangular geometry (with periodic boundary conditions) the growth models in which we are interested exhibit a "steady state" (see Sec. II) with stable self-similarity properties in the transverse direction up to the overall length scale (Fig. 41) (Evertsz, 1989). Thus we are not interested in the complete dynamical description of the growing aggregate as represented by Eq. (9.6), but in a steady-state solution for the projections of the macrostates $|\Phi(t)\rangle$ on manifolds perpendicular to the growth direction, which we shall label y. We know that in the steady state the integrated growth probability decays exponentially with the distance from the tip (Marsili and Pietronero, 1991), so that for fixed y and large enough t, growth at the height y can be considered as being effectively frozen and the probability weights of the substates confined to y as being independent of time. Let us denote these time-independent transverse states with

$$|\Psi(y)\rangle=\sum_{\underline{m}}\psi(\underline{m};y)|\underline{m}\rangle\ . \tag{9.8}$$

Here $\underline{m}$ has the same meaning as before, except that the sites r now run over a $(d-1)$-dimensional subspace. The stationarity condition with respect to translation in the growth direction can now be expressed symbolically as

$$\frac{d|\Psi(y)\rangle}{dy}=0\ . \tag{9.9}$$

Solving this differential equation (in practice a difference equation) is a much simpler task than solving the fully time-dependent problem, Eq. (9.6).

Let us now cast the generalized cells description of Sec. IV.A in Fock-space language. To keep the discussion simple, we shall confine ourselves to two dimensions,

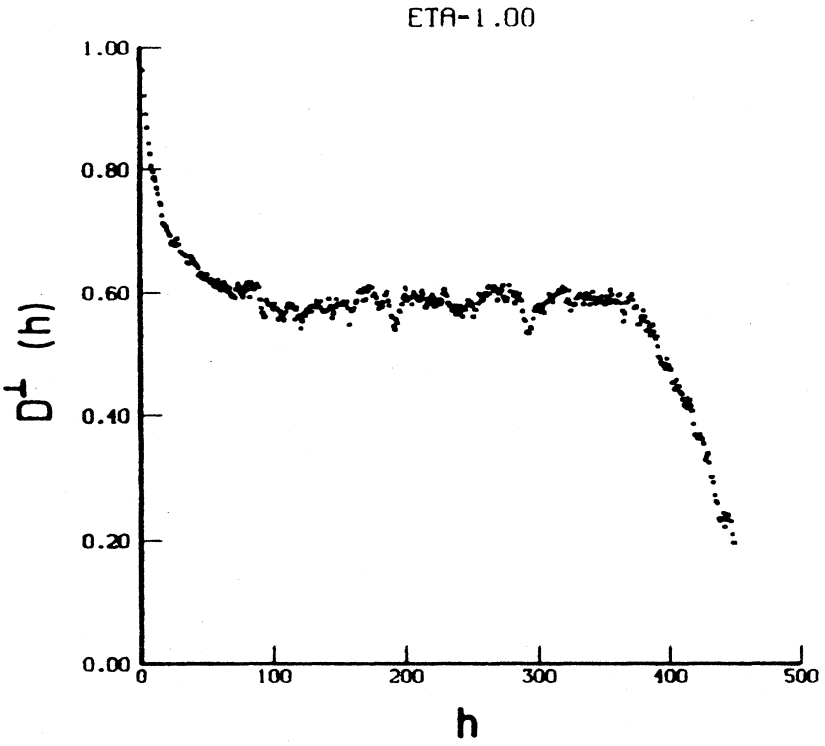

FIG. 41. Box-counting dimension of the intersection sets for $\eta=1$ in a cylinder of circumference $L=256$.

thus to one-dimensional intersection sets. If m_r denotes the occupation number of a site r at a generic length scale, we may group these sites into "cells" containing two sites each, and define the cell occupation numbers $m_{\bar{r}}=m_r+m_{r+1}-m_r m_{r+1}$ with $\bar{r}=(r+1)/2$, r odd. (This, of course, induces an analogous transformation on the creation and annihilation operators, $\pi_{\bar{r}}, a_{\bar{r}}$. Note also that the m_r and $m_{\bar{r}}$ take on only the values 0 or 1.) The cell-state probabilities are then related to the $\psi(\underline{m};y)$ via

$$\psi(m_1,m_2,\ldots,m_r,m_{r+1},\ldots) = \psi(m_{\bar{1}},m_{\bar{2}},\ldots,m_{\bar{r}},\ldots)\prod_{\bar{s}}\psi(m_r,m_{r+1}|m_{\bar{s}}) . \tag{9.10}$$

We have suppressed, for the moment, the explicit dependence of the weight functions on y. The vertical line denotes conditionality as usual, and we define $\psi(\mu,\nu|0)\equiv\delta_{\mu,0}\delta_{\nu,0}$. The probability weights of the internal states, $\psi(\mu,\nu/\cdot)$, are now assumed to be uniform in a given intersection set, as well as being scale invariant. This, together with Eq. (9.10), gives us the possibility of overcoming the closure problem in a way that retains a very high degree of complexity of the solution, unlike any mean-field or effective-medium approach.

With the above assumptions, we can construct the transverse macrostates (9.8) with the weights $\psi(m_1,m_2,\ldots,m_r,m_{r+1},\ldots)$, given $\psi(\mu,\nu|1;y)$ at a generic scale. Therefore we would like to be able to write Eq. (9.9) directly for the reduced cell states

$$|\Psi_2(y)\rangle=\sum_{\mu,\nu}\tilde{\psi}(\mu,\nu;y)|\mu,\nu\rangle , \tag{9.11}$$

where the probabilities $\tilde{\psi}$ have been normalized over the nonempty cell states. Setting

$$\begin{aligned} C_1&=\tilde{\psi}(1,0)+\tilde{\psi}(0,1) ,\\ C_2&=\tilde{\psi}(1,1) , \end{aligned} \tag{9.12}$$

and labeling the cell states by their total occupation number, one has

$$|\Psi_2(y)\rangle=\sum_{i=1,2}C_i(y)|i\rangle . \tag{9.13}$$

The $C_i(y)$ are now our "gross variables," and the fixed-scale transformation is precisely the operator that generates a translation in the y direction in this space. To keep the discussion simple, we shall now present the construction of the FST just for "open" boundary conditions; but it should be easy to see that the effects of the neighboring cells and the void distribution, etc., can all be taken into account.

D. The fixed-scale transformation as a Markovian process

Translation in the y direction in the space of asymptotically frozen transverse states can, in fact, be cast in the form of a Markovian process, even for growth processes with memory. The price to pay for this is having to sum over all growth scenarios originating at some level y and

eventually effecting the occupation of a different level $y+1$. In other words, one again has to sum over auxiliary variables of some kind (Peliti, 1985); in this case, the auxiliary variables are obtained by enlarging the state space from $|\psi(y)\rangle$ to $|\phi(t)\rangle$ [Eqs. (9.2), (9.6)]. Nevertheless, given the hierarchical ansatz, this must be done over a restricted region of space; and for fractal growth, the exponentially fast screening ensures that it has to be done over only a finite number of time steps for any desired degree of accuracy.

The stationarity condition (9.9), together with the subsequent assumptions, directly implies

$$\frac{d|\Psi_2(y)\rangle}{dy}=0 . \tag{9.14}$$

Let us write, in analogy with Eq. (9.4),

$$\frac{d|\Psi_2(y)\rangle}{dy}=Q|\Psi_2(y)\rangle . \tag{9.15}$$

Now,

$$\langle j|Q|i\rangle=M_{ij}-\delta_{i,j} , \tag{9.16}$$

where M_{ij} are the matrix elements of the FST and $C_i(y+1)=\sum_j M_{ij}C_j(y)$. Note that the meaning of the indices here has been reversed to conform with common usage. The M_{ij} are the transition probabilities from the state $|j\rangle$ to the state $|i\rangle$. Let us recall that to compute the M_{ij}, we must consider the effect at level, say, $y+1$, of all the growth processes originating at the level y and proceeding to successive levels $y'\geq y$. Although the intervening growth steps may involve processes with memory, the sum over all such paths clearly depends only on the end states $|j\rangle$ and $|i\rangle$.

It is convenient to express M_{ij} as a Green's function in the larger state space $|\underline{n}\rangle$. Let us embed the transverse cell state $|j\rangle$ in this larger space by taking an empty microstate and acting on it with creation operators at the lattice sites $r_1\equiv(x,y)$ and, if $j=2$, also at $(x+1,y)$. We make the hypothesis that the transverse states at $y'\leq y$ are already frozen. Furthermore, since the initial transverse state will grow with probability 1 (see Sec. IV) to occupy the site $(x,y+1)$, we also create an occupied site there. We thus obtain the initial state

$$|\underline{n}_0^{(j)}\rangle=\pi(x,y)\pi(x+1,y)^{j-1}\pi(x,y+1)|0\rangle . \tag{9.17}$$

Now, setting $r_2\equiv(x+1,y+1)$, for an Nth-order matrix element, we have

$$M_{2,j}^{(N)}=G_j(r_1,t_1;r_2,t_1+N) , \tag{9.18}$$

where, by hypothesis, t_1 is so large that G does not depend on it [see Eq. (9.7)]. Thus

$$\begin{aligned}&G_j(r_1,t_1;r_2,t_1+N)\\&\quad=G_j^{(N)}(r_1,r_2)\\&\quad=\langle|\pi(x+1,y+1)a(x+1,y+1)U_N|\underline{n}_0^{(j)}\rangle .\end{aligned} \tag{9.19}$$

The evolution operator U_N can be written, symbolically, in terms of the one-time step operator T as

$$U_N=T^N . \tag{9.20}$$

It is understood that

$$T^2\equiv\sum_{\underline{n}} T|\underline{n}\rangle\langle\underline{n}|T . \tag{9.21}$$

For Markovian processes, T is state independent and contains only annihilation and creation operators, at sites other than those belonging to the initial frozen transverse cell. For non-Markovian processes, it becomes state dependent. We shall first treat the equilibrium models and directed percolation which can be represented by a Markovian growth process. Then we shall consider the non-Markovian case.

1. Equilibrium models

For equilibrium models such as percolation, Ising, and Potts models, and the like, at the critical values of the parameters (such as temperature, concentration, etc.) the equilibrium distribution of critical fluctuations can be recovered as the *linear size* l of the region under consideration becomes very large—as opposed to the number of particles N added to the cluster. Each configuration extending over a region of linear size l "freezes" instantly, in the sense that each bond is sampled once and only once. Thus the operator U_N should act to generate all configurations confined to a region of size $l(N)$, with the appropriate weights. [In the foregoing (Sec. V), we have taken l to be the order of the operator and equal to the maximum height of the column above the initial cell.]

The Green's function $G^{(l)}(r_1,r_2)$ is given [Sec. V, Pietronero and Stella (1990)] by a sum over contributions from different configurations on the complete graph $S(l)$ (see Fig. 42), each containing connected paths between r_1 and r_2. Since correlations propagate via nearest-neighbor links only, we may simply sum over all paths

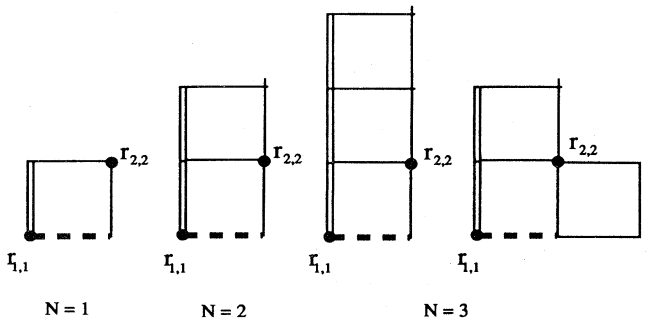

FIG. 42. Complete graphs over which allowed paths will be considered for the various orders (N) of computation. The dashed line may be included as part of a path for G_2, while it is excluded for G_1. The double lines correspond to the backbone.

from r_1 to r_2, irrespective of the rest of the configuration. Thus U_l now has the form

$$U_l = \prod_{\text{paths}\in S(l)} \prod_{r,r'\in\text{path}} T_{r,r'} \tag{9.22}$$

with

$$T_{r,r'} = p_r(\pi(r)-1)\pi(r')a(r')(1-\pi(r)a(r))+1 \ . \tag{9.23}$$

Here p_r is, in general, itself an operator. In terms of the total number of occupied nearest neighbors of r, $N_r \equiv \sum_{\pm\delta}\pi(r+\delta)a(r+\delta)$, where $\{\pm\delta\}$ run over the lattice vectors to the nearest-neighbor sites, one has (Erzan, 1992)

$$p_r = \begin{cases} p_c, & \text{percolation} \\ \dfrac{e^{qN_rK_c}}{e^{qN_rK_c}+q-1}, & \text{Ising}(q=2), \\ \text{Potts}(q=3,4) & \text{clusters} \\ \dfrac{e^{qN_rK_c}-1}{e^{qN_rK_c}+q-1}, & \text{Ising and Potts droplets} \ . \end{cases} \tag{9.24}$$

The prescription of taking a sum over paths may be conveniently expressed in terms of traces over Grassmann variables for the intermediate states (Cardy and Sugar, 1980). For the simplest case of percolation, where the "growth" process is completely uncorrelated, we take a shortcut by normalizing over only the connected configurations by assigning weights of unity to "backbone" bonds; the others will have weights of p_c. To avoid double counting, a factor of -1 is needed for each closed loop.

One introduces (Cardy and Sugar, 1980) the bookkeeping variables $a,\bar{a}$ (not to be confused with our annihilation operator a —) such that

$$\begin{aligned} &\text{Tr}a = 0 \ , \\ &\text{Tr}\bar{a} = 0 \ , \\ &\text{Tr}a_r\overline{a_{r'}} = \delta_{r,r'} \ , \end{aligned} \tag{9.25}$$

with $a^2 = ia, \bar{a}^2 = i\bar{a}$. The Green's functions in Eq. (9.19) may then be written

$$G_1^{(l)}(r_1,r_2) = \text{Tr}a_2 \prod_{r,r'\in b} (\bar{a}_r a_{r'}) \prod_{r,r'\notin b} (1+p_c\bar{a}_r a_{r'})\bar{a}_1 \ , \tag{9.26}$$

with b standing for "backbone," and with the products extending over links on the graph $S(l)$. To get G_2, the only difference is the insertion of a factor $(1+\bar{a}_1 a_{x+1,y})$. Note that each link is a directed object, but the products in this case include links in both senses along any given edge on the graphs shown in Fig. 42. From Eq. (9.25), it follows that $a^3 = -a, a^4 = -ia$, etc., and one obtains, term for term, the expressions for M_{ij} given in Sec. V.

The case of *directed percolation* is obtained if only links in the positive x and y directions are chosen. Then, for an order N computation, the correlations have to be taken between sites removed by N steps (Cardy and Sugar, 1980; Erzan, 1992).

2. Non-Markovian processes

In general, for irreversible aggregation processes where the growth probability at each time step has been normalized to 1, T in Eq. (9.20) will have the form

$$T = \sum_r \pi(r)p_r\Theta_r(s-\pi_r a_r) \tag{9.27}$$

with $r\neq(x+1,y)$ above. We have defined

$$\Theta_r \equiv 1-\prod_{\pm\delta}[1-\pi(r+\delta)a(r+\delta)] \ . \tag{9.28}$$

This operator will have a value of 1 if the site r has one or more nearest neighbors, and zero if it has none. For the parameter value $s=1$, if the site is not already occupied, and if it has at least one nearest neighbor, growth will take place there with probability p_r. Clearly, $s>1$ corresponds to noise reduction.

In the case of Laplacian growth rules, the p_r depend on the spatial correlations between all the sites of the aggregated cluster, through the Green's function for the Laplacian field. Without the inclusion of a further set of auxiliary variables for the Laplacian field (Peliti, 1985), we are unable to write p_r in a state-independent way, solely in terms of the creation and annihilation operators of the aggregated particles. Exhibiting this state dependence explicitly, one has

$$G_i^{(N)}(r_1,r_2) = \sum_{\underline{n}_N} \langle \underline{n}_N|\pi_2 a_2 \prod_{l=1}^{N-1}\left[\sum_{\underline{n}_l} T(\underline{n}_l)|\underline{n}_l\rangle\langle\underline{n}_l|\right] T(\underline{n}_0^{(i)})|\underline{n}_0^{(i)}\rangle \ . \tag{9.29}$$

This is nothing but a compact way of writing down the branching growth scenarios as outlined in Secs. IV and VII for the computation of M_{ij}, where, at each stage, p_r were computed explicitly from the discrete Laplace's equation subject to the boundary conditions (Sec. IV.D). The central factor in Eq. (9.29) is a sum over paths in the space of aggregation clusters, with each path weighted by the growth probabilities.

Clearly, the U_N either in Eqs. (9.19), (9.22) or in (9.29) may be cast, in the continuum limit as $N\to\infty$, in the form of a path integral, and the field-theoretic formulation for these processes (Parisi and Zhang, 1985; Peliti, 1985) will be recovered. In fact, starting from the particle density of the growing cluster and the diffusive field of the random-walking particle encountering the clusters, it is possible to derive the action of the resulting field theory. This is a modified Reggeon field theory with nonlocal interactions with the following action:

$$S=\int d^d x dt \left[\varphi^+\partial_t\varphi+\alpha\nabla\varphi^+\nabla\varphi+\mu^2\varphi^+\varphi+ig(\alpha\nabla\varphi^+\nabla\varphi-\varphi^+\varphi)\int d^d y G(x-y)(\alpha\Delta+\mu^2)\varphi(y)-ig\varphi^+\varphi^+\varphi\right], \quad (9.30)$$

where the field φ is related to the density function of the growing clusters.

One can expand the nonlocal interaction term, obtaining an action with the free part $S_{\text{free}}=\varphi^+\partial_t\varphi+\alpha\nabla\varphi\nabla\varphi^++\mu^2\varphi^+\varphi$ that is similar to those of the random walks with traps problems, plus interacting terms that are nonlocal interactions in the higher powers of φ. One should go beyond the mean-field theory by considering the perturbation terms; but, unfortunately, the usual renormalization treatment is impossible. In fact, the theory is superrenormalizable in the ultraviolet limit in every dimension d, as is easy to show from the dimensional analysis. This means, from a statistical-mechanics standpoint, that there exists no upper critical dimension and the theory is not renormalizable. In this sense, the free action of the random walk is not a good starting point for the perturbative analysis of the problem, and the practical calculations cannot be performed with the usual perturbation methods. In addition, the field theory cannot take into account such variations of the model as the inclusion of the η parameter in the DBM. This last parameter will lead to a nonpolynomial field theory for which it is extremely complicated even to write the corresponding action.

For all these reasons, little progress has been made within the field theory framework in the practical calculation of quantities like $G(r,t;r',t')$. On the other hand, for r,r' chosen on consecutive intersection sets, we are indeed able to compute such Green's functions for finite $N=t'-t$, and they converge rapidly in N. Then these Green's functions play the role of transition probabilities in a Markovian process defined on a set of states dimensionally lower than those describing the whole aggregated cluster. The steady-state solution for this Markovian process gives us the transverse macrostates, from which we are able to compute the fractal dimension of the intersection sets.

E. The fixed-scale transformation and scale-invariant dynamics

Let us now look at the FST method from a field-theory perspective and see how it allows us to overcome at least the most serious difficulties that arise when one tries to cast irreversible fractal growth in a standard theoretical framework. We have seen in the previous section that a Lagrangian approach to DLA leads to a nonrenormalizable, strong-coupling problem. In analogy with other similar situations in field theory, like quantum chromodynamics (QCD), one way to overcome this difficulty is to make a *lattice regularization.* In some sense this corresponds to the original algorithm of growth that is used in the computer simulations. This also seems to imply that the continuum limit for DLA is a delicate problem, and the discreteness of the problem appears to be an essential element.

The point is then how to perform the lattice path integrals analytically and with a finite amount of labor. This brings us back to the problems of the two limits, asymptotic time ($t\to\infty$) and large scale ($r\to\infty$), that we discussed at the beginning. In a standard approach, one would try to do these two limits together, by letting the system evolve and renormalizing its dynamics at the same time. This procedure appears to be extremely complex for DLA-type problems, while it is more feasible for Hamiltonian problems in which ergodicity allows one to simplify the problem by just summing over all the configurations.

Here the FST approach is quite different because it performs these two limits separately. First, one focuses on the short-range correlations generated by asymptotic growth. This is done, in practice, by the intersection and by the transfer matrix along the growth direction. The matrix elements can be defined by suitable lattice path integrals. This represents the original FST scheme, and it represents a novel approach to computing correlations in problems that are *intrinsically dynamical.* Even though the method is in real space, it can be improved systematically by increasing the accuracy of the calculation of the lattice path integrals.

The basic idea of going to large scale does not involve considering larger and larger configurations, but reinterpreting the "sites" for which one is able to compute the short-range correlations as coarse-grained cells. If one is able to do this, then the FST produces the nearest-neighbor correlations for pairs of coarse-grained cells of *any size,* and from these the fractal dimension can be computed analytically. The key point of this second part is the identification of the scale-invariant dynamics for the coarse-grained cells. This implies the formulation of a renormalization procedure that is specific for a given problem. For example, in Ising problems, the scale-invariant dynamics corresponds essentially to the determination of the critical temperature T_c. For percolation, it corresponds to the critical probability p_c. For DLA, the problem is much more complex, as we have seen in Sec. VII. This procedure is able to deal naturally with self-organized processes in which the scale-invariant dynamics corresponds to an attractive fixed point.

The FST consists therefore in a novel approach in which attention is especially focused on the dynamics of the processes, and it should be easily applicable to other problems of this class.

X. CONCLUSIONS

The challenge posed in the Introduction, namely, that of defining a measure on the phase space of far from equilibrium fluctuations, can be restated as formulating a statistical mechanics of spatially extended irreversible dynamical systems. The diversity of models treated in this (by no means exhaustive) review attests to the richness of this domain: we have diffusion-limited, irreversible aggregation of particles and clusters, sandpile, and directed and invasion percolation, as well as equilibrium, or Hamiltonian, models, which we can reformulate in dynamical terms.

Apart from the many technical aspects outlined in the foregoing sections, there are other fundamental issues of spatio-temporal pattern formation, to which we think we have contributed.

These issues are (i) the possibility of computing asymptotic correlations for irreversible growth processes in terms of a suitable lattice path integral; (ii) a method of analysis for identifying the effective scale-invariant dynamics, given the microscopic one, which allows us to understand the self-organized nature of fractal structure in terms of an attractive fixed point for the dynamics; (iii) the combination of the above two points, which allows us to develop an effective language and theoretical framework for the description of fractal growth and for the analytical calculation of fractal dimensions.

The present formulation of the theoretical approach is quite different from the standard renormalization group, even though we have seen that there is a common area, that of equilibrium Hamiltonian models, where both can be applied. In other areas, though, one tends to be more suitable than the other. For example, the FST is designed to work only at the fixed point; so it could not be applied to exponents that characterize the deviations from the critical point, like the magnetic-field exponent $\xi(T) \simeq |T - T_c|^{\beta}$ of the Ising model. On the other hand, the FST is able to deal with self-critical irreversible problems, like DLA growth, for which the standard RG ideas are very problematic.

This is because the RG approach is explicitly designed to compute the exponents that characterize the approach to the critical point. Exponents like ν are, in fact, linked to the derivative of the RG transformation at the critical point. The point is, however, that in fractal growth the dynamical process is self-organized and the corresponding fixed point is attractive. Therefore exponents like ν do not exist, and the derivative of an eventual RG transformation cannot be related to the critical properties.

This situation requires a new way of looking at the problem, and this is what the FST provides. The scale transformation for the dynamics is used only to define the critical parameters, independently of whether the fixed point is repulsive or attractive. Then, from the critical parameter, the FST allows us to derive directly the fractal dimension. This is a new perspective that can also deal naturally with self-organized problems like DLA in which the fixed point is attractive. The FST is then based on various technical points like the separation of the two limits, asymptotic time and large scale. For irreversible-growth problems, these limits must be considered explicitly, because these systems are not ergodic. The method is therefore particularly tuned to focus on the dynamical properties of the system rather than on the equilibrium configurations.

Another intriguing aspect of critical systems is the question of universality. With phase transitions, we are familiar with a strong universality, and the same exponents that describe the onset of magnetization also describe the liquid-vapor transitions. This crucial role of universality is, however, characteristic of equilibrium systems. Self-organized systems, on the other hand, do not exhibit the same degree of universality. It is relatively easy to modify the fractal dimension with some simple change in the growth process, and this seems to be a characteristic of models with irreversible dynamics. This lack of universality is sometimes viewed as a negative element, because one is forced to describe specific systems instead of a single universal model. The truth is probably the opposite. Some theoretical concepts can be considered as general or universal, but the inherent diversity of the various models we have described adds another fascinating dimension to the intellectual search. After all, the fractal structures we observe in nature are quite various and different from each other. In this respect the situation of self-organized fractals is probably more similar to solid-state theory than to equilibrium phase transitions. In solid state there are universal properties like the Bloch theorem, but then one has to make different theories for the various properties of solids.

In this respect the FST represents a general framework that should also be applicable to other problems of the nature. In fact, with these ideas as inspiration, it has recently become possible to describe the properties of the critical state of sandpile models that are a different class of self-organized critical systems (Pietronero *et al.*, 1994). The attractive nature of the fixed point can be properly described, and the various exponents for the avalanche distribution and other properties can be computed analytically. Another important element we have briefly discussed is the transformation of a deterministic problem with quenched variables in a stochastic dynamics with cognitive memory. This brings a vast class of quenched models (like IP) into the area of FST applicability.

ACKNOWLEDGMENTS

During our activity on this subject, we benefited from continuous discussions and collaborations with R. Cafiero, G. Caldarelli, C. Castellano, R. De Angelis, M. Di Stasio, C. Evertsz, M. Hüner, M. Marsili, M. Piccioni, I. Ruiz, W. R. Schneider, S. Sidoretti, A. P. Siebesma, A. Stella, R. R. Tremblay, H. J. Wiesmann, S. Zapperi, and F. Zaratti, and we thank them very warmly.

We also want to thank D. Amit, P. Bak, R. Benzi, E. Caglioti, A. Coniglio, F. Corberi, M. Costantini, A. Crisanti, L. De Arcangelis, D. Dhar, C. Di Castro, J. Feder, M. E. Fischer, P. Grassberger, S. Havlin, L. P. Kadanoff, H. Kaufman, B. B. Mandelbrot, U. Marini Bettolo, A. Maritan, P. Meakin, G. Paladin, G. Parisi, L. Peliti, A. Petri, H. E. Stanley, P. Tartaglia, E. Tosatti, M. Vergassola, T. Vicsek, M. Virasoro, A. Vulpiani, and Y. C. Zhang, who, through various discussions, have contributed to the development of the ideas presented in this review. Finally, we thank S. Pallagrosi for her kind technical support during the preparation of the manuscript.

REFERENCES

Abarbanel, H. D. I., J. B. Bronzan, A. Schwimmer, and R. L. Sugar, 1976, Phys. Rev. D **14**, 632.
Amit, D. J., 1978, *Field Theory, the Renormalization Group and Critical Phenomena* (McGraw-Hill, New York).
Arneodo, A., Y. Couder, G. Grasseau, V. Hakim, and M. Rabard, 1989, Phys. Rev. Lett. **63**, 984.
Arneodo, A., G. Grasseau, and M. Holschneider, 1988, Phys. Rev. Lett. **61**, 2281.
Bak, P., and K. Sneppen, 1993, Phys. Rev. Lett. **71**, 4083.
Bak, P., C. Tang, and K. Wiesenfeld, 1987, Phys. Rev. Lett. **59**, 381.
Bak, P., C. Tang, and K. Wiesenfeld, 1988, Phys. Rev. A **38**, 364.
Ball, R., and T. A. Witten, 1984, Phys. Rev. A **29**, 2966.
Barker, P. W., and R. Ball, 1990, Phys. Rev. A **42**, 6289.
Baxter, R., and A. J. Guttman, 1988, J. Phys. A **21**, 3193.
ben Avraham, D., R. Bidaux, and L. S. Schulman, 1991, Phys. Rev. A **43**, 7093.
Benzi, R., G. Paladin, G. Parisi, and A. Vulpiani, 1984, J. Phys. A **17**, 3521.
Blumenfeld, R., and A. Aharony, 1989, Phys. Rev. Lett. **62**, 2927.
Bohr, T., P. Cvitanovic, and M. H. Jensen, 1988, Europhys. Lett. **6**, 445.
Burkhard, T. W., and J. M. J. Van Leuwen, 1982, *Real Space Renormalization* (Springer, Heidelberg).
Cafiero, R., L. Pietronero, and A. Vespignani, 1993, Phys. Rev. Lett. **70**, 3939.
Caldarelli, G., C. Castellano, and A. Vespignani, 1994, Phys. Rev. E **49**, 2673.
Caldarelli, G., A. Vespignani, and L. Pietronero, 1995, Physica A **215**, 223.
Cardy, J., and R. L. Sugar, 1980, J. Phys. A **13**, L423.
Chayes, J. T., and L. Chayes, 1986, in *Critical Phenomena Random Systems and Gauge Theories,* edited by K. Ostwalder and R. Stora (North-Holland, Amsterdam), p. 1090.
Chendler, R., J. Koplik, K. Lerman, and J. F. Willemsen, 1982, J. Fluid Mech. **119**, 249.
Coleman, P., and L. Pietronero, 1992, Phys. Rep. **213**, 311.
Coniglio, A., 1989, Phys. Rev. Lett. **62**, 3054.
Coniglio, A., C. Amitrano, and F. Di Liberto, 1986, Phys. Rev. Lett. **57**, 1016.
Coniglio, A., and W. Klein, 1980, J. Phys. A **13**, 2775.
Coniglio, A., and F. Peruggi, 1982, J. Phys. A **15**, 1873.
Coniglio, A., and M. Zannetti, 1990, Physica A **163**, 325.
De Angelis, R., M. Marsili, L. Pietronero, A. Vespignani, and H. J. Wiesmann, 1991, Europhys. Lett. **16**, 417.
De Dominicis, C., 1975, Nuovo Cimento Lett. **12**, 567.
De Dominicis, C., 1976, J. Phys. (Paris) Colloq. **37**, C-247.
De Dominicis, C., E. Brezin, and J. Zinn Justin, 1975, Phys. Rev. B **12**, 4945.
De Dominicis, C., and L. Peliti, 1977a, Phys. Rev. Lett. **38**, 505.
De Dominicis, C., and L. Peliti, 1977b, Phys. Rev. B **18**, 353.
de Gennes, P. G., 1979, *Scaling Concepts in Polymers Physics* (Cornell University, Ithaca, New York).
den Nijs, M., 1979, J. Phys. A **12**, 1857.
den Nijs, M., 1983, Phys. Rev. B **27**, 1674.
Derrida, B., and D. Stauffer, 1985, J. Phys. (Paris) **46**, 1623.
Dickmann, R., 1986, Phys. Rev. A **34**, 4246.
Di Stasio, M., L. Pietronero, A. Stella, and A. Vespignani, 1994, J. Phys. A **27**, 317.
Duplantier, B., and H. Saleur, 1989, Phys. Rev. Lett. **63**, 2536.
Eckmann, J. P., P. Meakin, I. Procaccia, and R. Zeitak, 1989, Phys. Rev. A **29**, 3185.
Eckmann, J. P., P. Meakin, I. Procaccia, and R. Zeitak, 1990, Phys. Rev. Lett. **65**, 52.
Eden, M., 1961, in *Proceedings of the Fourth Symposium on Mathematical Statistics and Probability,* edited by F. Neyman (University of California, Berkeley), Vol. IV, p. 223.
Elderfield, D., 1985a, J. Phys. A **18**, L767.
Elderfield, D., 1985b, J. Phys. A **18**, L773.
Elderfield, D., and D. D. Vedensky, 1985, J. Phys. A **18**, 2591.
Erzan, A., 1992, Physica A **185**, 66.
Erzan, A., and L. Pietronero, 1991, J. Phys. A **24**, 1875.
Erzan, A., and L. Pietronero, 1992, Europhys. Lett. **20**, 595.
Erzan, A., and S. Sinha, 1991, Phys. Rev. Lett. **66**, 2750.
Essam, J., A. J. Guttman, and K. De'Bell, 1988, J. Phys. A **21**, 3815.
Evertsz, C., 1989, Ph.D. thesis (University of Groningen).
Evertsz, C., 1990, Phys. Rev. B **41**, 1830.
Feder, J., 1988, *Fractals* (Plenum, New York).
Fisher, M. S., 1967, Rep. Prog. Phys. **30**, 615.
Furnberg, L., and J. Feder, 1988.
Furnberg, L., J. Feder, A. Aharony, and T. Jossang, 1988, Phys. Rev. Lett. **61**, 2117.
Glauber, R. J., 1963, J. Math. Phys. **4**, 294.
Grassberger, P., 1982, Z. Phys. B **47**, 465.
Grassberger, P., 1986, in *Fractals in Physics,* edited by L. Pietronero and E. Tosatti (North-Holland, Amsterdam), p. 273.
Grassberger, P., 1992, J. Phys. A **25**, 5475.
Grassberger, P., and A. de la Torre, 1979, Ann. Phys. **122**, 373.
Gunton, J. D., 1979, in *Dynamical Critical Phenomena and Related Topics,* Lecture Notes in Physics 104, edited by C. P. Enz (Springer-Verlag, Berlin), p. 1.
Guold, H., F. Family, and H. E. Stanley, 1983, Phys. Rev. Lett. **50**, 686.
Halperin, B. I., P. C. Hoenberg, and S. Ma, 1972, Phys. Rev. Lett. **29**, 1548.
Halpin-Healy, T., and Y. C. Zhang, 1955, Phys. Rep. **254**, 215.
Halsey, T. C., 1994, Phys. Rev. Lett. **72**, 1228.
Halsey, T. C., and M. Leibig, 1992, Phys. Rev. A **46**, 7793.
Hohenberg, P. C., and B. I. Halperin, 1977, Rev. Mod. Phys. **49**, 425.
Holschneider, M., 1988, J. Stat. Phys. **50**, 953.
Honda, K., H. Toyoki, and M. Matsushita, 1986, J. Phys. Soc. Jpn. **55**, 707.
Hüner, M., and A. Erzan, 1994, Physica A **212**, 314.
Janssen, H., 1979, in *Dynamical Critical Phenomena and Related Topics,* Lecture Notes in Physics 104, edited by C. P. Enz

(Springer-Verlag, Berlin), p. 26.
Jullien, R., and R. Botet, 1987, *Aggregation and Fractal Aggregates* (World Scientific, Singapore).
Kadanoff, L. P., 1967, Rev. Mod. Phys. **39**, 395.
Kaneko, K., 1985, *Collapse of Tori and Genesis of Chaos in Dissipative Systems* (World Scientific, Singapore).
Kardar, M., G. Parisi, and Y. C. Zhang, 1986, Phys. Rev. Lett. **56**, 889.
Kertesz, J., and T. Vicsek, 1986, J. Phys. A **19**, L257.
Kinzel, W., 1983, in *Percolation Structures and Process,* Annals of the Israel Physical Society Vol. 5, edited by G. Deutcher, R. Zallen, and J. Adler (Adam Hellinger, Bristol), p. 425.
Kirkaldy, J. S., 1992, Rep. Prog. Phys. **55**, 723.
Kolb, M., R. Botet, and R. Jullien, 1983, Phys. Rev. Lett. **51**, 1123.
Leyvraz, F., 1986, in *On Growth and Form,* edited by H. E. Stanley and N. Ostrowsky (Nijhoff, Dordrecht), p. 136.
Ligget, T. M., 1985, *Interacting Particle Systems* (Springer, New York).
Luis, E., and F. Guinea, 1987, Europhys. Lett. **3**, 871.
Mandelbrot, B. B., 1974, J. Fluid Mech. **62**, 331.
Mandelbrot, B. B., 1982, *The Fractal Geometry of Nature* (Freeman, San Francisco).
Mandelbrot, B. B., 1992, Physica A **191**, 95.
Mandelbrot, B. B., and C. J. G. Evertsz, 1990, Nature **348**, 143.
Mandelbrot, B. B., H. Kaufmman, A. Vespignani, I. Yekutieli, and C. H. Lam, 1995, Europhys. Lett. (in press).
Marsili, M., 1994, J. Stat. Phys. **77**, 733.
Marsili, M., and L. Pietronero, 1991, Physica A **175**, 9.
Mazenko, G. F., 1979, in *Dynamical Critical Phenomena and Related Topics,* Lecture Notes in Physics 104, edited by C. P. Enz (Springer-Verlag, Berlin), p. 97.
Meakin, P., 1983, Phys. Rev. Lett. **51**, 1119.
Meakin, P., 1984, Phys. Rev. B **29**, 3722.
Meakin, P., 1988, in *Phase Transitions and Critical Phenomena,* edited by C. Domb and J. L. Lebowitz (Academic, New York), Vol. 12, p. 335.
Meakin, P., and S. Tolman, 1989, in *Fractal's Physical Origin and Properties,* edited by L. Pietronero (Plenum, New York), p. 137.
Meinhardt, M., 1992, Rep. Prog. Phys. **55**, 797.
Migdal, A. A., A. M. Polyakov, and K. A. Ter-Martirosyan, 1974, Phys. Lett. B **48**, 239.
Migdal, A. A., A. M. Polyakov, and K. A. Ter-Martirosyan, 1974b, Zh. Eksp. Teor. Fiz. **67**, 84.
Moukarzel, C., 1992, Physica A **188**, 469.
Muthukumar, M., 1983, Phys. Rev. Lett. **50**, 839.
Nagatani, T., 1987a, J. Phys. A **20**, L381.
Nagatani, T., 1987b, Phys. Rev. A **36**, 5812.
Nicholis, G., and I. Prigogine, 1977, *Self-Organization in Nonequilibrium Systems* (Wiley Interscience, New York).
Niemeyer, L., L. Pietronero, and H. J. Wiesmann, 1984, Phys. Rev. Lett. **52**, 1038.
Nittman, J., and H. E. Stanley, 1986, Nature **321**, 663.
Ohono, K., K. Kakuchi, and H. Yasuhara, 1992, Phys. Rev. A **46**, 3400.
Ossadnik, P., 1992, Phys. Rev. A **45**, 1058.
Paladin, G., and A. Vulpiani, 1987, Phys. Rep. **156**, 145.
Parisi, G., and Y. C. Zhang, 1985, J. Stat. Phys. **41**, 1.
Peliti, L., 1985, J. Phys. (Paris) **46**, 1469.
Piccioni, M., 1995, unpublished.
Pietronero, L., 1993, J. Fractals **1**, 650.
Pietronero, L., A. Erzan, and C. Evertsz, 1988a, Phys. Rev. Lett. **61**, 861.
Pietronero, L., A. Erzan, and C. Evertsz, 1988b, Physica A **151**, 207.
Pietronero, L., and W. R. Schneider, 1990, Physica A **170**, 81.
Pietronero, L., and W. R. Schneider, 1991, Phys. Rev. Lett. **66**, 2336.
Pietronero, L., and W. R. Schneider, 1995, in *Stochastic Processes, Physics and Geometry,* edited by S. Albeverio and D. Merlini (World Scientific, Singapore), p. 581.
Pietronero, L., W. R. Schneider, and A. Stella, 1990, Phys. Rev. A **42**, 7496.
Pietronero, L., W. R. Schneider, and A. Vespignani, 1995, preprint.
Pietronero, L., S. Sidoretti, and A. Vespignani, 1993, Fractals **1**, 41.
Pietronero, L., and A. Stella, 1990, Physica A **170**, 64.
Pietronero, L., P. Tartaglia, and Y. C. Zhang, 1991, Physica A **173**, 22.
Pietronero, L., and E. Tosatti, 1986, Eds., *Fractals in Physics* (North-Holland, Amsterdam).
Pietronero, L., A. Vespignani, and S. Zapperi, 1994, Phys. Rev. Lett. **72**, 1690.
Pietronero, L., and H. J. Wiesmann, 1984, J. Stat. Phys. **36**, 811.
Rintoul, M. D., and H. Nakanishi, 1992, J. Phys. A **25**, L945.
Roux, S., and E. Guyon, 1989, J. Phys. A **19**, 3693.
Schlogel, F., 1972, Z. Phys. **253**, 147.
Schwarzer, S., J. Lee, A. Bunde, S. Havlin, H. E. Roman, and H. E. Stanley, 1990, Phys. Rev. Lett. **65**, 603.
Shapir, Y., and Y. C. Zhang, 1986, J. Phys. (Paris) Lett. **46**, L529.
Sidoretti, S., and A. Vespignani, 1992, Physica A **185**, 202.
Siebesma, A. P., R. R. Tremblay, A. Erzan, and L. Pietronero, 1988, Physica A **156**, 613.
Smolukowski, M. V., 1916, Phys. Z. **17**, 585.
Stanley, H. E., 1971, *Introduction to Phase Transitions and Critical Phenomena* (Academic, New York).
Stanley, H. E., and N. Ostrowsky, 1986, Eds., *On Growth and Form* (Nijhoff, Dordrecht).
Stanley, H. E., P. J. Reynolds, S. Redner, and F. Family, 1982, in *Real Space Renormalization,* edited by T. W. Burkhard and J. M. J. Van Leuwen (Springer, Heidelberg).
Stauffer, D., 1985, *Introduction to Percolation Theory* (Taylor & Francis, London).
Stell, G., 1987, *Phase Transitions and Critical Phenomena,* edited by C. Domb and J. L. Lebowitz (Academic, New York), p. 205.
Stella, A., and C. Vanderzande, 1989, Phys. Rev. Lett. **62**, 1067.
Stinchcombe,
Suzuki, M., 1979, in *Dynamical Critical Phenomena and Related Topics,* Lecture Notes in Physics 104, edited by C. P. Enz (Springer-Verlag, Berlin), p. 75.
Sykes, M. F., A. J. Guttman, M. G. Watts, and P. D. Roberts, 1972, J. Phys. A **5**, 653.
Tang, C., and P. Bak, 1988, Phys. Rev. Lett. **60**, 2347.
Tremblay, R. R., and A. P. Siebesma, 1989, Phys. Rev. A **40**, 5377.
Turkevic, L. A., and H. Scher, 1985, Phys. Rev. Lett. **55**, 1026.
Vanderzande, C., 1992, Physica A **185**, 235.
Vannimenus, J., B. Nickel, and V. Hakim, 1984, Phys. Rev. B **30**, 391.
Vespignani, A., and L. Pietronero, 1990, Physica A **168**, 723.
Vespignani, A., and L. Pietronero, 1991, Physica A **173**, 1.
Vespignani, A., and L. Pietronero, 1993, Fractals **1**, 1002.
Vespignani, A., S. Zapperi, and L. Pietronero, 1995, Phys. Rev. E **51**, 1711.

Vicsek, T., 1992, *Fractal Growth Phenomena* (World Scientific, Singapore).
Vicsek, T., and F. Family, 1984, Phys. Rev. Lett. **52**, 1669.
Vicsek, T., P. Meakin, and F. Family, 1985, Phys. Rev. A **32**, 1122.
Wang, X. R., Y. Shapir, and M. Rubinstein, 1989a, J. Phys. A **22**, L507.
Wang, X. R., Y. Shapir, and M. Rubinstein, 1989b, Phys. Rev. A **39**, 5974.
Watts, M. G., 1975, J. Phys. A **8**, 61.
White, S. R., and R. M. Noack, 1992, Phys. Rev. Lett. **68**, 3487.
Wilkinson, D., and J. F. Willemsen, 1983, J. Phys. A **16**, 3365.
Wilson, K. G., and J. B. Kogut, 1974, Phys. Rep. **12**, 75.
Witten, T. A., and L. M. Sander, 1981, Phys. Rev. Lett. **47**, 1400.
Witten, T. A., and L. M. Sander, 1983, Phys. Rev. B **27**, 5685.
Wolfram, S., 1983, Rev. Mod. Phys. **55**, 601.
Yan, H., G. Li, and L. M. Sander, 1989, Europhys. Lett. **10**, 7.
Zaratti, F., I. Ruiz, L. Pietronero and A. Vespignani, 1995 (unpublished).
Zhang, Y.C., 1989, Phys. Rev. Lett. **63**, 473.
Ziff, R. M., 1992, Phys. Rev. Lett. **69**, 2670.

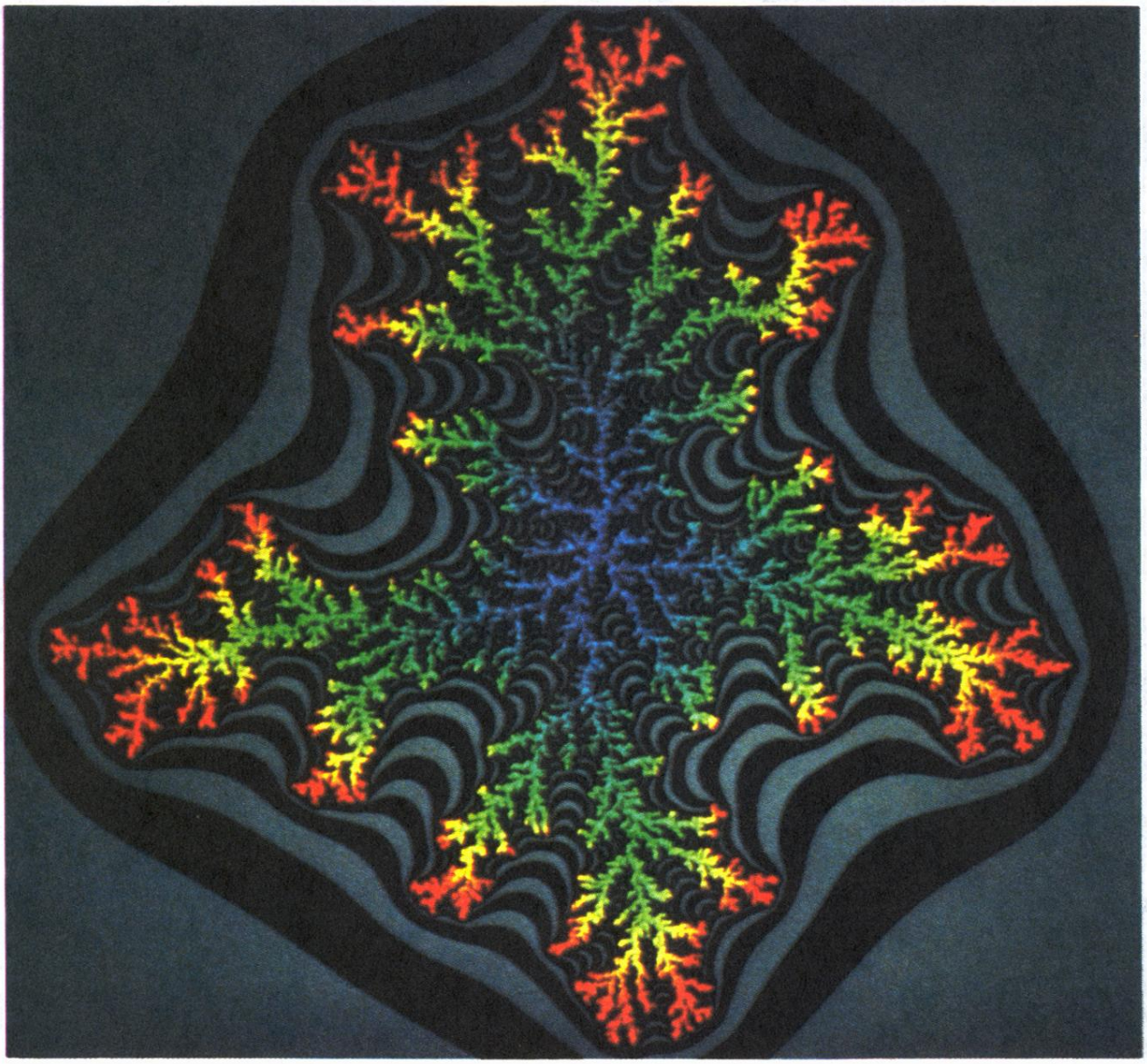

FIG. 1. DLA/DBM cluster (off-lattice) with radial boundary conditions. The colors of the structure refer to the aggregation time of each particle. Note the screening effect: late (red) particles cease modifying the inner blue portion, which therefore can be considered asymptotic. Only for this "frozen" part can fractal properties be properly defined. The contours around the structure represent equipotential lines for the Laplacian field. A pair of black and white stripes corresponds to a change by a factor of 10 of the potential (courtesy of C. J. G. Evertsz and B. B. Mandelbrot).